

The miR-17~92 cluster regulates adult neural stem cell behavior

Inauguraldissertation

zur

Erlangung der Würde eines Doktors der Philosophie

vorgelegt der

Philosophisch-Naturwissenschaftlichen Fakultät

der Universität Basel

Von

Fabrizio Favaloro

aus Italien

2021

Genehmigt von der Philosophisch-Naturwissenschaftlichen Fakultät auf Antrag
von

Prof. Dr. Fiona Doetsch

Prof. Dr. Peter Scheiffele

Basel, den 18. Februar 2020

Prof. Dr. Martin Spiess
Dekan

Abstract

The miR-17~92 cluster regulates adult neural stem cell behavior

Fabrizio Favalaro

In the adult mammalian brain, the ventricular-subventricular zone (V-SVZ) generates neurons and glia throughout life. In this germinal niche, neural stem cells (NSCs) coexist in quiescent and activated states. However, the molecular mechanisms underlying this transition remain elusive. miRNAs have been implicated in stem cell self-renewal and differentiation, but their role in adult NSC activation is unknown. By performing miRNA profiling of FACS-purified quiescent and activated adult V-SVZ NSCs, we identified the miR-17~92 cluster as highly upregulated in activated stem cells in comparison to their quiescent counterparts. Conditional deletion of miR-17~92 in FACS-purified adult NSCs reduced NSC proliferation *in vitro*. *In vivo*, miR-17~92 deletion in NSCs decreased NSC activation, proliferation, and neurogenesis. Unexpectedly, it also led to increased oligodendrogenesis in the V-SVZ, *corpus callosum* and *septum*, due to an expansion of OLIG2⁺ transit-amplifying cells (TACs). Finally, bioinformatic analysis of predicted miR-17~92 targets upregulated in qNSCs versus aNSCs identified *Slpr1* and *Pdgfrβ* as promising potential miR-17~92 targets for stem cell activation. In addition, pathway analysis unveiled a gene category related to oligodendrogenesis among the gene categories enriched for miR-17~92 targets. We validated *Pdgfra*, a key regulator of oligodendrocyte generation, as a miR-17~92 target by luciferase assay and *in vivo* analysis. Together, these data uncover multiple functions of the miR-17~92 cluster in adult NSC activation and proliferation, and in the regulation of the balance between neurogenesis and oligodendrogenesis from TACs.

To my mother, my godmother's family,
my wife-to-be and my daughter,
for always supporting me and helping me become,
each in a different way,
the man I am proud to be today.

TABLE OF CONTENTS

CHAPTER 1: INTRODUCTION

| | |
|---|-----------|
| 1. Adult neural stem cells | 1 |
| 1.1 Brief history of the identification of adult neural stem cells..... | 1 |
| 1.2 Adult V-SVZ neural stem cells and their lineages..... | 2 |
| 1.3 Quiescent and Activated NSCs coexist in the adult V-SVZ niche..... | 5 |
| 1.4 Adult V-SVZ NSCs exhibit extensive heterogeneity at multiple levels..... | 7 |
| 1.4.1 <i>Developmental origin of adult neural stem cells</i> | 8 |
| 1.4.2 <i>Morphology: not all radial NSCs are the same</i> | 8 |
| 1.4.3 <i>The adult V-SVZ is a mosaic of regionally distinct neural stem cells</i> | 8 |
| 1.4.4 <i>Adult NSCs differentially sense and respond to distinct environmental cues</i> | 11 |
| | |
| 2. microRNAs (miRNAs): key sculptors of cell transcriptomes | 12 |
| 2.1 Biogenesis and mechanisms of action of miRNAs..... | 12 |
| 2.2 miRNAs in adult V-SVZ NSCs and their progeny..... | 14 |
| | |
| 3. The miR-17~92 cluster: more than a mere oncogene | 16 |
| | |
| AIMS | 18 |

CHAPTER 2: miR-17~92 REGULATION OF ADULT NEURAL STEM CELLS

| | |
|---|-----------|
| Introduction | 19 |
| Results | 19 |
| qPCR validation of miR-17~92 expression profile in the adult V-SVZ NSC lineage..... | 19 |
| miR-17~92 deletion reduces adult NSC proliferation and colony formation <i>in vitro</i> | 21 |
| Deletion of miR-17~92 in NSCs <i>in vivo</i> decreases stem cell proliferation and expands oligodendrogenic transit amplifying cells at short time points | 23 |
| miR-17~92 deletion <i>in vivo</i> reduces NSC activation and neurogenesis at long time points... | 26 |
| miR-17~92 ablation <i>in vivo</i> promotes oligodendrogenesis at long time points..... | 29 |
| Computational identification of biological pathways regulated by the miR-17~92 cluster ... | 30 |
| <i>Pdgfra</i> is a functional miR-17~92 target in the V-SVZ | 31 |
| Conclusions | 33 |
| Materials and Methods | 35 |

CHAPTER 3: POTENTIAL miR-17~92 TARGETS FOR STEM CELL ACTIVATION:

S1pr1 and *Pdgfr β*

| | |
|---|-----------|
| Introduction | 40 |
| Results | 40 |
| Bioinformatic analysis of miRNA-mRNA interactions in the early V-SVZ NSC lineage | 40 |
| The miR-17~92 cluster regulates the expression of <i>S1pr1</i> , <i>Pdgfrb</i> and <i>Ncam1</i> | 41 |
| Characterization of S1PR1 expression and distribution in the V-SVZ | 43 |
| S1PR1 and PDGFR β are co-expressed in quiescent neural stem cells | 47 |
| Conclusions | 49 |
| Materials and Methods | 49 |

CHAPTER 5: DISCUSSION AND FUTURE DIRECTIONS

| | |
|---|-----------|
| miR-17~92 expression in the V-SVZ NSC lineage..... | 52 |
| miR-17~92 underlies neural stem cell activation and proliferation | 53 |
| miR-17~92 regulates neurogenesis and oligodendrogenesis <i>in vivo</i> | 54 |
| | |
| miR-17~92 targets for neural stem cell activation and fate specification | 56 |
| <i>S1pr1</i> and <i>Pdgfrβ</i> are potential targets of miR-17~92 for stem cell activation | 56 |
| <i>The miR-17~92 target Tbr2 promotes glutamatergic neuronal production</i> | 56 |
| <i>The oligodendrogenesis regulator Pdgfrα is a functional target of miR-17~92</i> | 57 |
| Final conclusions..... | 58 |
| | |
| Acknowledgements | 60 |
| Curriculum vitae | 61 |
| References | 63 |

Abbreviations**4OHT:** hydroxytamoxifen**aNSC:** activated neural stem cell**BrdU:** 5-bromo-2'-deoxyuridine**CC:** *corpus callosum***CDS:** coding sequence**cKO:** conditional knock-out**CSF:** cerebrospinal fluid**Dpi:** days post injection**ECM:** extracellular matrix**ELCS:** envelope-limited chromatin sheets**FACS:** Fluorescence Activated Cell Sorting**GN:** granule neuron**IHC:** immunohistochemistry**LR:** label-retaining**LVCP:** lateral ventricle choroid plexus**miR or miRNA:** microRNA**MVB:** multivesicular bodies**NB:** neuroblast**NE:** neuroepithelial cells**NSC:** neural stem cell**OB:** olfactory bulb**OL:** oligodendrocyte**OPC:** oligodendrocyte progenitor cell**OPP:** O-propargyl-puromycin**PGN:** periglomerular neuron**POMC:** proopiomelanocortin**qNSC:** quiescent neural stem cell**qPCR:** quantitative PCR**RGC:** radial glia cell**RMS:** rostral migratory stream**SC:** stem cell**SG:** stress granules**SGZ:** subgranular zone**TAC:** transit-amplifying cell**TF:** transcription factor**TGN:** trans-Golgi network**Tmx:** tamoxifen**Tom:** Tomato**UTR:** untranslated region**V-SVZ:** ventricular-subventricular zone

Chapter 1: Introduction

1. ADULT NEURAL STEM CELLS

Stem cells (SCs) are a special population of undifferentiated cells that are able to self-renew, that is to make identical copies of themselves over time, and to generate several distinct cell types with characteristic morphologies and specialized functions. Most adult organs retain stem cells from embryonic development. Their primary function is the maintenance of tissue homeostasis by replacing cells that are lost owing to tissue turnover or injury. In most adult tissues, adult stem cells reside within specialized microenvironments, referred to as ‘niches’, that provide support and a continuous source of external cues to both SCs and their progeny. Frequently, SCs give rise to intermediate precursors or progenitors, that undergo several rounds of divisions before differentiating into mature tissue cell types (reviewed in Goodell et al., 2015).

1.1 Brief history of the identification of adult neural stem cells

For a long time the adult brain was considered fixed and incapable of regeneration as no mitosis was convincingly shown in neurons. It was widely assumed that the adult brain only contained progenitors to generate glial cells. The first indication of adult neurogenesis was provided in the 1960s by Joseph Altman who showed the integration of newly-generated cells labeled by radioactive thymidine in the hippocampus, olfactory bulb and cortex of the adult rat brain (Altman and Das, 1965). A decade later, Michael Kaplan demonstrated that these adult-generated cells were neurons by reproducing Altman’s experiments coupling the autoradiographic technique to electron microscopy. Newly-generated neurons are able to functionally integrate into neuronal circuits as shown by studies in songbirds led by the laboratory of Fernando Nottebohm (Paton and Nottebohm, 1984). Despite the increasing number of reports describing the existence of adult neurogenesis in several species including fish, reptiles, birds and rodents (reviewed in Grandel et al., 2013 and Augusto-Oliveira et al., 2019), the precise source of adult-born neurons remained long unknown. In the 1990s, Reynolds and Weiss showed that stem cells could be isolated from the adult mammalian brain and cultured as free-floating clusters named neurospheres (Reynolds and Weiss, 1992). However, it was only a few years later that adult neural stem cells in the ventricular-subventricular zone (V-SVZ) and subgranular zone (SGZ) were surprisingly found to be radial cells displaying astroglial properties (Doetsch et al., 1999a; Seri et al., 2001).

1.2 Adult V-SVZ neural stem cells and their lineages

In the adult mouse brain, the ventricular-subventricular zone (V-SVZ), lining the lateral ventricles, is the largest germinal niche where neural stem cells (NSCs) lie. The V-SVZ consists of a thin layer of dividing cells at the interface between the ventricular surface, composed of multiciliated ependymal cells, and the *striatum*. In the V-SVZ, NSCs, also called B1 cells, display radial-like morphology reminiscent of embryonic radial glia cells (RGCs) and exhibit hallmark ultrastructural and molecular features of astrocytes, including expression of Glial Fibrillary Acidic Protein (GFAP), Glutamate Aspartate Transporter (GLAST), and Brain Lipid-Binding Protein (BLBP). Morphologically, B1 cells span throughout the V-SVZ thickness, contacting the cerebrospinal fluid (CSF) at the center of pinwheel structures made by ependymal cells via a small apical process containing a primary cilium, and extending a long basal process ending on a planar vascular plexus at the interface with the *striatum* (Chaker et al., 2016) (Figure 1.1).

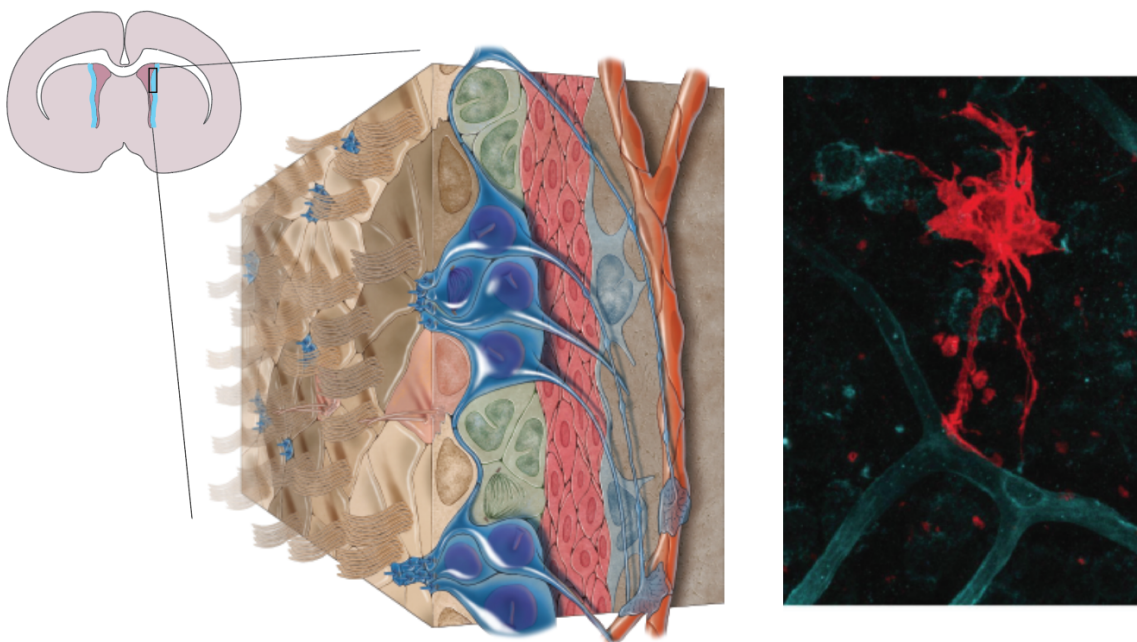


Figure 1.1. [On the left] Schema of mouse brain coronal section showing the lateral V-SVZ in light blue. The blow-up image shows the cytoarchitecture of the V-SVZ niche composed of ependymal cells (beige, brown and peach), B1 cells (blue), transit amplifying cells (green), neuroblasts (red) and blood vessels (orange), among other cell types. [On the right] Radial stem cell (Promininin-mCherry reporter, red) sending a long basal process terminating on blood vessels (laminin, blue). Images adapted from Mirzadeh et al., *Cell Stem Cell* (2008) and Codega et al., *Neuron* (2014).

Adult NSCs enter quiescence (qNSCs) in mid and late embryogenesis and are actively maintained in a dormant state until they become activated postnatally (Fuentealba et al., 2015; Furutachi et al., 2015; Yuzwa et al., 2017). Like a subpopulation of RGCs, qNSCs display a

unique nuclear compartment containing envelope-limited chromatin sheets (ELCS), which are invaginations of the nuclear envelope enriched in heterochromatin domains related to quiescence (Cebrián-Silla et al., 2017). Upon activation, NSCs upregulate epidermal growth factor receptor (EGFR) and Nestin (Doetsch et al., 2002; Pastrana et al., 2009; Codega et al., 2014) and enter cell cycle. Activated NSCs (aNSCs) divide once before giving rise to transit-amplifying cells (TACs, also known as C cells) (Ponti et al., 2013). Recently, Obernier et al. demonstrated that the majority of GFAP⁺ V-SVZ NSCs divide symmetrically, with about 20% of NSCs undergoing symmetric self-renewing divisions to give rise to two stem cells and ~80% symmetric differentiative consuming divisions to generate TACs (Obernier et al., 2018). TACs, in turn, undergo three to four rounds of symmetric divisions to expand the progenitor pool before giving rise to their progeny (Costa et al., 2011; Ponti et al., 2013). TACs do not express *Gfap* and are frequently identified by the expression of *Egfr*, *Ascl1* (Achaete-Scute Family BHLH Transcription Factor 1, also known as *Mash1*) and *Dlx2* (Distal-Less Homeobox 2). Together with dividing NSCs, TACs are tightly apposed to SVZ blood vessels and contact the vasculature at sites that lack astrocyte endfeet and pericyte coverage, a modification of the blood-brain barrier unique to the SVZ (Tavazoie et al., 2008). TACs predominantly give rise to young neurons called neuroblasts (NBs, also known as A cells). NBs retain *Dlx2* expression and exhibit a migratory phenotype. Doublecortin (DCX) (Gleeson et al., 1999; Nacher et al., 2001; Garcia et al., 2004), CD24 (Calaora et al., 1996), PSA-NCAM (Polysialylated-neural cell adhesion molecule) and TuJ1 (also called Beta-III tubulin, Doetsch et al., 1997) are among the markers these cells express. In young adult mice, B1 cells produce ~10,000 neuroblasts every day (Lois et al., 1996). These neuroblasts travel several millimeters towards the olfactory bulb (OB), moving along one another in a particular form of tangential migration known as chain migration. Networks of neuroblast chains, ensheathed by the processes of GFAP⁺ cells (Lois et al., 1996; Wichterle et al., 1997) then converge rostrally, forming the rostral migratory stream (RMS) at the anterior V-SVZ (Doetsch and Alvarez-Buylla, 1996). Once they reach the OB, individual NBs leave the chains and migrate radially to reach different layers of the OB. The vast majority of adult-born neurons differentiate into granule neurons (GNs) (~94%), while the remainder become periglomerular neurons (PGNs) (~4%) or astrocytes (<2%) (reviewed in Lledo and Valley, 2016). However, only a subset of newly generated neurons integrates into already established olfactory circuits and survives (reviewed in Malvaut and Saghatelian, 2016). Adult-born OB neurons are largely GABAergic and immunopositive for the neuronal nuclear antigen NeuN (Mullen et al., 1992). A small subpopulation of glutamatergic juxtglomerular OB neurons is also contributed by adult V-SVZ NSCs (Brill et al., 2009). The

normal function of these newly formed interneurons is eventually to modulate the activity of mitral and tufted cells, thereby optimizing perceptual learning and olfactory memory (Lazarini and Lledo, 2011).

Importantly, B1 cells not only give rise to OB neurons but also generate a small number of glial cells, including GFAP⁺ astrocytes destined for the *corpus callosum* (CC) and RMS, and OLIG2⁺ (Oligodendrocyte Transcription Factor 2), PSA-NCAM⁺ and PDGFR α ⁺ (Platelet Derived Growth Factor Receptor Alpha) oligodendrocyte progenitor cells (OPCs) that migrate into the CC, *striatum* and *fimbria fornix* to differentiate into immature CSPG4⁺ (Chondroitin Sulfate Proteoglycan 4, also known as NG2) cells that continue to divide locally or mature into myelinating cells (Sohn et al. 2015; Menn et al. 2006) (Figure 1.2). However, the precise gliogenic lineage in the V-SVZ has not yet been fully characterized.

Adult neurogenesis occurs in most mammals, including humans. Indeed, GFAP⁺ NSCs are also described in the adult human V-SVZ. However, the lack of intermediate progenitors and migrating cells in this region suggests that the majority of these cells are largely quiescent (Sanai et al., 2004; Sanai et al., 2011; Van Den Berge et al., 2010). Moreover, retrospective determination of cell birth in the adult human brain through carbon dating showed that adult-born neurons are added to the *striatum* but not to OB, establishing that there is no significant postnatal turnover in the adult human OB (reviewed in Bergmann et al., 2015).

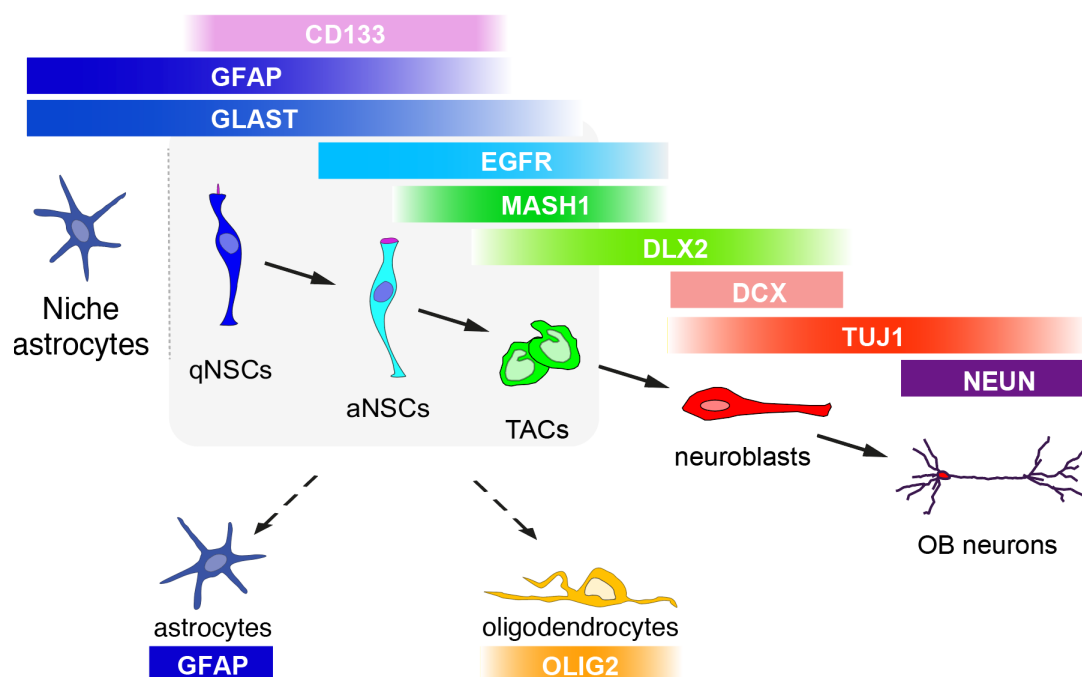


Figure 1.2. Schema depicting V-SVZ lineages and common markers used to identify distinct cell types. Whereas neuroblasts are known to arise from TACs, the precise V-SVZ lineage generating glial cells is still unclear.

1.3 Quiescent and Activated NSCs coexist in the adult V-SVZ niche

Like stem cells in other adult tissues, NSCs in the V-SVZ exist in both quiescent and activated states and can be purified from their *in vivo* niche via Fluorescence Activated Cell Sorting (FACS). Indeed, despite their shared astrocytic nature, qNSCs can be separated from aNSCs and other brain astrocytes based on the expression of EGFR and CD133 (Prominin), respectively (Codega et al., 2014). Several strategies combining different markers or transgenic mice to prospectively identify quiescent stem cells have been proposed, including hGFAP::GFP, CD133, GLAST, Hes5::GFP or LeX (Codega et al., 2014; Khatri et al., 2014; Mich et al., 2014; Giachino et al., 2014; Daynac et al., 2013; Daynac et al., 2016). Although the exact extent of overlap of these qNSC populations is unclear, they do exhibit common functional properties. Indeed, unlike their activated counterparts, *in vivo* qNSCs lack expression of proliferation markers, are label-retaining, survive antimetabolic drug treatment like Ara-C infusion and are able to regenerate the lineage after depletion of actively dividing stem cells and TACs (Codega et al., 2014; Mich et al., 2014; Giachino et al., 2014; Daynac et al., 2013). Moreover, qNSCs do not express Nestin (Codega et al., 2014) and only rarely form neurospheres or give rise to adherent colonies as a consequence of their slowly dividing nature (Codega et al., 2014; Mich et al., 2014; Daynac et al., 2013).

Transcriptionally, qNSCs are enriched in genes associated with cell-cell adhesion, extracellular-matrix-response as well as signaling receptors, transmembrane transporters and ion channels, suggesting that they actively maintain the quiescent state in response to signals from the microenvironment. By contrast, aNSCs are highly enriched in the gene categories of cell cycle and DNA repair (Codega et al., 2014). An increasing number of single cell analyses of V-SVZ cells has confirmed the existence of populations of qNSCs and aNSCs (Llorens-Bobadilla et al., 2015; Dulken et al., 2017; Basak et al., 2017; Leeman et al., 2018, Mizrak et al., 2019). Despite differences in the choice of markers to FACS-purify V-SVZ cells and in the RNA sequencing protocols, these studies unveil a continuum of single cell profiles spanning from quiescence to activation, proliferation and differentiation. In addition to the aforementioned gene categories, qNSCs and aNSCs were also found to differ in their energy metabolism and protein synthesis rate. Indeed, as NSCs transition from quiescence to activation, they switch from glycolysis to oxidative phosphorylation and upregulate genes for protein synthesis and ribosomal biogenesis such as *Rpl32* (Ribosomal Protein L32) (Llorens-Bobadilla et al., 2015). Importantly, the increased levels of protein synthesis occurring upon activation of qNSCs has been functionally validated by incorporation of O-propargyl-puromycin (OPP) into nascent proteins in primary sorted V-SVZ cells (Llorens-Bobadilla et

al., 2015; Baser et al., 2019). Pseudotime analyses revealed that the expression of some transcription factors associated with neuronal differentiation, like *Dlx1* and *Dlx2*, already begins in some mitotic aNSCs suggesting that some neuronal programs might be initiated early in the lineage to prime NSCs for differentiation (Basak et al., 2018). However, unlike cell cycle-related genes, which exhibit a robust coregulation along the pseudotime and are able to clearly separate dividing and non-dividing cell types, changes in differentiation markers occur at different intermediate points, which argue against a single molecular switch of differentiation (Basak et al., 2018). Interestingly, intermediate states or subpopulations of qNSCs and aNSCs along the NSC-to-neuron differentiation axis were also identified (Llorens-Bobadilla et al., 2015; Dulken et al., 2017). For instance, qNSCs were found in deep dormant (q1) and primed (q2) states, with primed qNSCs displaying slightly higher ribosomal activity and lower glial marker expression than dormant stem cells, but still lacking cell cycle markers (Figure 1.3). Interestingly, primed qNSCs were shown to increase their proportion in response to ischemic brain injury (Llorens-Bobadilla et al., 2015). Single cell analyses also identified distinct subpopulations of aNSCs [two aNSCs (Llorens-Bobadilla et al., 2015) and three aNSCs (Dulken et al., 2017)] that, along the NSC-to-neuron differentiation trajectory, progressively down-regulate glial-associated genes and up-regulate mitosis-related genes as well as early markers of neurogenesis.

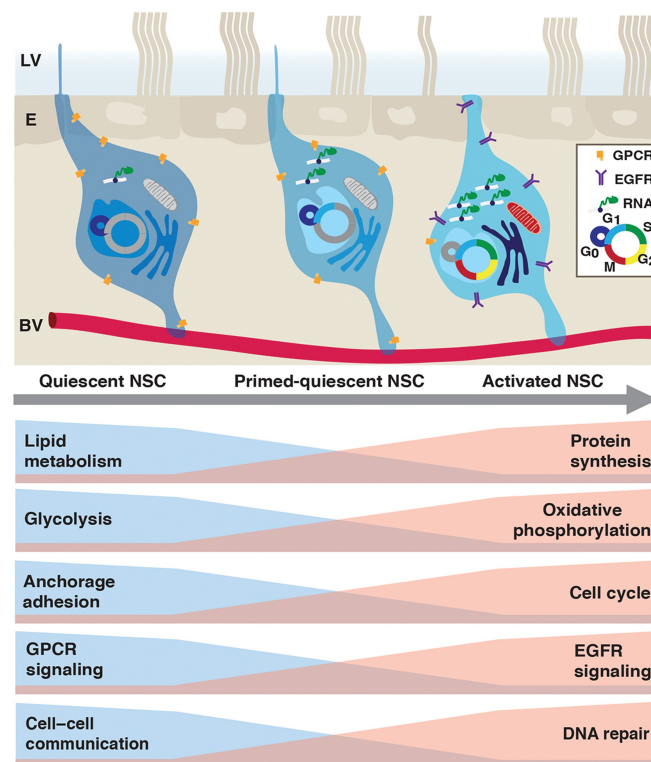


Figure 1.3. Molecular changes upon stem cell activation. Top: Schema of quiescent (left), primed-quiescent (middle), and activated (right) adult V-SVZ NSCs, located between the ependymal cell layer (E) lining the lateral

ventricle (LV), and the vascular plexus (BV). Summary of transcriptome data of purified qNSCs and aNSCs at the population and single cell level. EGFR, epidermal growth factor receptor; GPCR, G-protein coupled receptor; NSC, neural stem cell. From Chaker et al., WIREs Developmental Biology (2016).

Recently, the differential preference of qNSCs and aNSCs for protein metabolism has functionally been investigated. Indeed, whereas aNSCs showed a high proteasome activity, qNSCs accumulated protein aggregates within large lysosomes over time. Interestingly, by enhancing lysosomal activity, qNSCs were shown to ameliorate protein aggregate clearance and to increase their ability to activate. Thus, the decline in NSC activation occurring during aging appears to be related, in part, to a progressively more impaired lysosome activity (Leeman et al., 2018).

1.4 Adult V-SVZ NSCs exhibit extensive heterogeneity at multiple levels

The V-SVZ extends along the lateral ventricles which are delimited by the lateral wall, adjacent to the *striatum*, the septal wall, adjacent to the *septum* and the roof, underlying the *corpus callosum* (Figure 1.4). Recent work has increasingly shown that NSCs in the adult V-SVZ are not a homogeneous population but rather exhibit heterogeneity at multiple levels. In this section, I will focus on the heterogeneity that NSCs display with respect to their developmental origin, morphology, regional position and response to environmental cues.

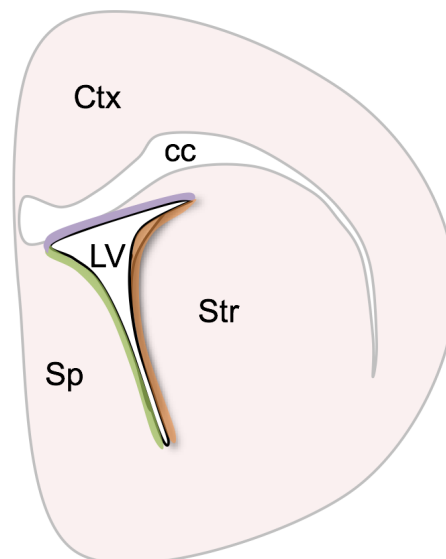


Figure 1.4. Schematic representation of the lateral ventricle walls. Septal wall in green, lateral wall in orange, roof in purple and *corpus callosum* in white. Ctx: cortex, cc: *corpus callosum*, LV: lateral ventricle, Sp: *septum*, Str: *striatum*.

1.4.1 Developmental origin of adult neural stem cells

During embryonic development, neuroepithelial cells (NE), which are the first stem cells appearing in the brain, give rise to radial glial cells (RGCs). Although a linear NSC lineage spanning from NE to RGC to B1 cell astrocyte had been suggested, it remained long unclear whether B1 cells were the end product of such lineage or if they diverged from other RGCs during development. By lineage tracing of individual embryonic progenitors, B1 cells were recently shown to arise from RGC subpopulations that diverged from other RGCs as early as E11.5 (embryonic day 11.5) and entered quiescence during mid-embryonic development (between E13.5 and 15.5) (Fuentelba et al., 2015; Furutachi et al., 2015). These pre-B1 cells upregulated the negative cell cycle regulator $p57^{\text{kip2}}$ (Cdkn1c, Cyclin Dependent Kinase Inhibitor 1C) and remained largely quiescent until they became activated postnatally (Furutachi et al., 2015). More recently, another study based on single cell transcriptional profiling of only cortical forebrain cells identified a subpopulation of GFAP-expressing RGCs acquiring the transcriptomic signature of quiescent B1 cells during late embryogenesis (around E17.5) (Yuzwa et al., 2017). Although it remains unclear whether the RGC subsets identified by these two works are distinct subpopulations, these studies suggest that a first layer of V-SVZ heterogeneity might already be present at the developmental time at which NSCs are generated.

1.4.2 Morphology: not all radial NSCs are the same

Adult V-SVZ NSCs are a special subset of radial astrocytes extending a small apical process to contact the ventricular surface and sending a long basal process frequently ending on blood vessels. Although NSCs share a radial shape, they can be found in different morphologies that allow them to enter in contact with distinct components of the V-SVZ niche. Indeed, radial NSCs with a process either perpendicular or parallel to the ventricle have been described to exist in V-SVZ and to be differentially distributed along the dorso-ventral aspect of the V-SVZ as well as across the lateral and septal walls (Shen et al., 2008; Delgado et al., bioRxiv 2019). However, whether cells with distinct radial morphologies are functionally different is still unknown.

1.4.3 The adult V-SVZ is a mosaic of regionally distinct neural stem cells

It is widely recognized that the adult V-SVZ is highly regionalized, being composed of a mosaic of NSCs located in spatially segregated domains characterized by the expression of specific transcription factors (TFs). Such domains, including microdomains, have been shown to arise from discrete germinal regions in the developing forebrain appearing as early as E11.5

before NSCs are set aside (Fuentelba et al., 2015). Indeed, Cre-loxP fate mapping approaches using the Cre recombinase under the promoter of regionally expressed TFs have revealed that the pallium, lateral/medial ganglionic eminences and *septum* of the embryo give rise to the dorsal, lateral and medial walls of the adult V-SVZ, respectively (Young et al., 2007; Fiorelli et al., 2015).

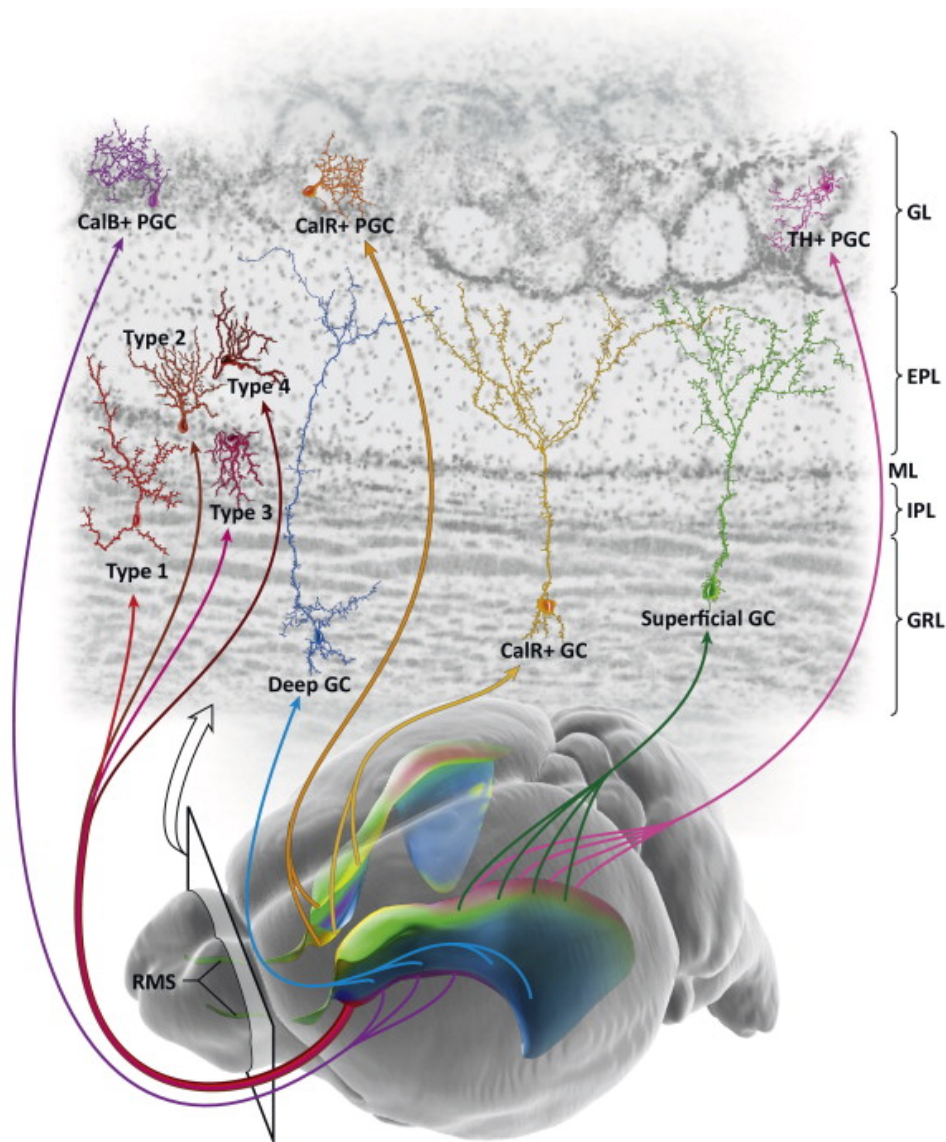


Figure 1.5. Regional organization of V-SVZ NSCs. Oblique view of the adult mouse brain (bottom) with colorized lateral ventricles to indicate the regional organization of this major neurogenic niche. Cells born in different subregions of the adult V-SVZ migrate along the rostral migratory stream (RMS) into the olfactory bulb to give rise to unique types of interneurons. Abbreviations: CalB, calbindin; CalR, calretinin; TH, tyrosine hydroxylase; PGC, periglomerular cell; GC, granule cell; GL, glomerular layer; EPL, external plexiform layer; ML, mitral cell layer; IPL, internal plexiform layer; GRL, granular layer. From Lim and Alvarez-Buylla, *Trends in Neurosciences* (2014)

Some of such regionally expressed TFs in the embryo are maintained by postnatal and adult NSCs. For instance, pallial regulators (like *Emx1*, *Pax6*, *Tbr1/2* and *Neurog2*) are confined to the dorsal-most regions of the V-SVZ, whereas subpallial markers (like *Dlx1/2/5*, *Gsh1/2*, *Ascl1*, *Nkx2.1* and *Nkx6.2*) and the septal markers (like *Zic1/3*) are restricted more ventrally to the lateral and medial regions of the V-SVZ, respectively (reviewed in Azim et al., 2016). Thus, adult NSCs retain their positional information from embryonic development into adulthood likely in a TF code.

Depending on their location along the anterior-posterior and dorsal-ventral axes of the lateral wall, as well as along the most anterior-ventral tip of the medial wall of the lateral ventricles, NSCs give rise to specific subtypes of morphologically and molecularly distinct granule neurons (GNs) and periglomerular neurons (PGNs). Indeed, NSCs in the dorsal V-SVZ of the lateral wall produce mostly superficial GNs and dopaminergic PGNs, whereas ventral NSCs generate deep GNs and calbindin (CalB⁺) PGNs. In contrast, calretinin (CalR⁺) GNs and CalR⁺ PGCs are derived from medial V-SVZ NSCs (Merkle et al., 2007). In addition to these abundant OB subtypes, NSCs located in very restricted subdomains of the anterior V-SVZ have been shown to generate small populations of novel OB interneuron subtypes, including Type 1-4 neurons, that differentiate near the mitral cell layer (Merkle et al., 2014). Finally, some glutamatergic juxtglomerular interneurons are also contributed by dorsal *Tbr2* (also called *Eomes*)- and *Neurog2*-expressing progenitors (Brill et al., 2009). Thus, the adult V-SVZ is divided into subregions that are specialized for the production of distinct types of OB interneurons. Interestingly, this regional specification of NSCs is in large part cell-intrinsic as suggested by heterotopic grafting experiments. Indeed, transplanting ventral NSCs into the dorsal V-SVZ or vice versa is not sufficient to change the OB interneuron subtype they generate probably because of early established epigenetic barriers related to their physical location (Merkle et al., 2007) (Figure 1.5).

Besides OB interneurons, adult V-SVZ NSCs also give rise to OLIG2⁺ and PDGFR α ⁺ OPCs, that differentiate into oligodendrocytes (OLs) in different white matter regions, through *Olig2*-expressing TACs (Menn et al., 2006). Under normal conditions, the production of OLs in the SVZ is modest. However, injury paradigms including demyelinating lesions in the neighboring white matter can significantly increase the numbers of OLs generated by V-SVZ progenitors (Nait-Oumesmar et al., 1999; Picard-Riera et al., 2002; Menn et al., 2006; Samanta et al., 2015). Based on *in vitro* time-lapse imaging, it has been shown that the neurogenic and oligodendrogenic lineages are generated by distinct subsets of NSCs (Ortega et al., 2013). Although the precise identity of these NSC subpopulations *in vivo* remains unknown, several

studies have reported that V-SVZ-derived OLs mostly come from dorsal NSCs in a sonic hedgehog (SHH)- and WNT-dependent fashion, and settle in the *corpus callosum* in both the postnatal (Azim et al., 2014; Tong et al., 2015) and adult brain (Menn et al., 2006; Ortega et al., 2013). Thus, dorsal NSCs represent a distinct source of OLs from the parenchymal OPCs, which are found throughout the brain and generated during development. However, despite the different origin and distribution of parenchymal and SVZ-derived OPCs, with the latter restricted to the dorsal V-SVZ, these progenitors share expression of the same early oligodendrocyte lineage markers, including OLIG2, PDGFR α and NG2. In addition to SHH and WNT- pathways, infusion of EGF ligand at high doses was also shown to exhibit a pro-oligodendrogenesis effect on V-SVZ NSCs both during early postnatal development and adulthood (Aguirre et al., 2005; Gonzalez-Perez et al., 2010). Similarly, selective activation of the PI3K/Akt signaling by intraventricular infusions of pharmacological active compounds resulted in the targeted activation of dorsal NSCs to generate oligodendrocytes *in vivo* (Azim et al., 2017). Interestingly, Delgado et al. recently identified a novel population of V-SVZ-derived intraventricular OPCs bathed by the cerebrospinal fluid (CSF) and in contact with supraependymal axons from distant brain regions. Although their characterization has just begun, their strategic position within the ventricles suggests that signals in cerebrospinal fluid as well as from other brain areas might be dynamically sensed by these cells and modulate their behavior (Delgado et al., bioRxiv 2019).

Finally, under normal conditions, adult NSCs also produce GFAP⁺ astrocytes destined for the CC and RMS (Sohn et al., 2015). However, the precise location of astrogenic NSCs is still unclear. Recently, the septal V-SVZ has been proposed to harbor astrogenic NSCs. Indeed, the release of NSCs from quiescence through deletion of Platelet-Derived Growth Factor Receptor beta (PDGFR β) was found to increase the number of a newly described cell type in the septal wall of the V-SVZ, named ‘gorditas’, characterized by a rounded, plump soma with short small GFAP⁺ processes, that give rise to astrocytes in the *septum* (Delgado et al., bioRxiv 2019).

1.4.4 Adult NSCs differentially sense and respond to distinct environmental cues

NSCs are not isolated but reside within a specialized microenvironment, referred to as ‘niche’, that regulates their behavior. In the V-SVZ, NSCs receive a wide range of extrinsic cues from several sources including cell-extracellular matrix (ECM) and cell–cell interactions as well as signaling molecules coming from immediate NSC neighbors, from the lateral ventricle choroid plexus (LVCP) which produces cerebrospinal fluid (CSF), from the

vasculature, and from local and distant neuronal innervation (reviewed in Obernier and Alvarez-Buylla, 2019). All these cues regionally pattern the V-SVZ niche and dynamically change in response to physiological states. Interestingly, it is emerging that depending on their morphology, location as well as receptor repertoire, NSCs can differentially sense and respond to such signals. For instance, hypothalamic proopiomelanocortin (POMC) neurons, which regulate feeding behavior, selectively modulate the proliferation of a specific subset of NSCs located in the anterior-ventral part of the V-SVZ (Paul et al., 2017). Thus, the heterogeneity existing in the V-SVZ is not only a function of the intrinsically-determined diversity of NSCs but also relies on a fine regulation exerted by niche-derived external cues.

2. MICRORNAs (miRNAs): KEY SCULPTORS OF CELL TRANSCRIPTOMES

miRNAs are a class of small non-coding RNA molecules, around 22 nucleotides in length, that play critical roles in regulating gene expression. Since their serendipitous discovery in nematodes over 20 years ago (Lee et al., 1993; Wightman et al., 1993), thousands of miRNA genes have been documented in nearly all eukaryotic organisms (Griffiths-Jones, 2004; Kozomara and Griffiths-Jones, 2014). miRNAs are essential for normal animal development and are implicated in a variety of biological processes including cell proliferation, differentiation, apoptosis, and immune responses (Tüfekci et al., 2014). Importantly, deregulation of miRNA function is associated with numerous diseases, particularly cancer (Lin et al., 2015; Bracken et al., 2016).

miRNAs localize and function in multiple subcellular compartments such as the nucleus (Miao et al., 2016; Xiao et al., 2017), the rough endoplasmic reticulum (Barman et al., 2015), processing (P)-bodies (Nishi et al., 2015), stress granules (SG) (Detzer et al., 2011), the trans-Golgi network (TGN), early/late endosomes (Bose et al., 2017), multivesicular bodies (MVB), lysosomes (Gibbins et al., 2009) and mitochondria (Barrey et al., 2011; Zhang et al., 2014). However, miRNAs can also be released into extracellular fluids either associated with proteins, especially AGO2 (Gallo et al., 2012; Turchinovic et al., 2011) or within vesicles such as exosomes, microvesicles, and apoptotic bodies (Iftikhar et al., 2016; Gallo et al., 2012). Thus, miRNAs can be delivered and modulate the activity of neighbor or distant target cells, displaying in this regard a hormone-like function.

2.1 Biogenesis and mechanisms of action of miRNAs

The biogenesis of the vast majority of miRNAs begins with the transcription, mediated by RNA polymerase II/III, of a long primary transcript, called ‘pri-miRNA’, able to fold back

into one or several stem-loop structures as in the case of miRNA clusters. Like protein-coding transcripts, the pri-miRNA is capped and polyadenylated. Along its biogenetic pathway, the pri-miRNA undergoes two sequential processing events. First, while in the nucleus, the pri-miRNA is cropped into a short hairpin, known as ‘pre-miRNA’, by the microprocessor complex containing the RNase III Droscha and the RNA binding protein DiGeorge Syndrome Critical Region 8 (DGCR8) among other factors. Second, once exported into the cytoplasm, mostly through Exportin 5, the pre-miRNA is cleaved by the RNase III Dicer that removes the terminal loop to generate the mature miRNA duplex.

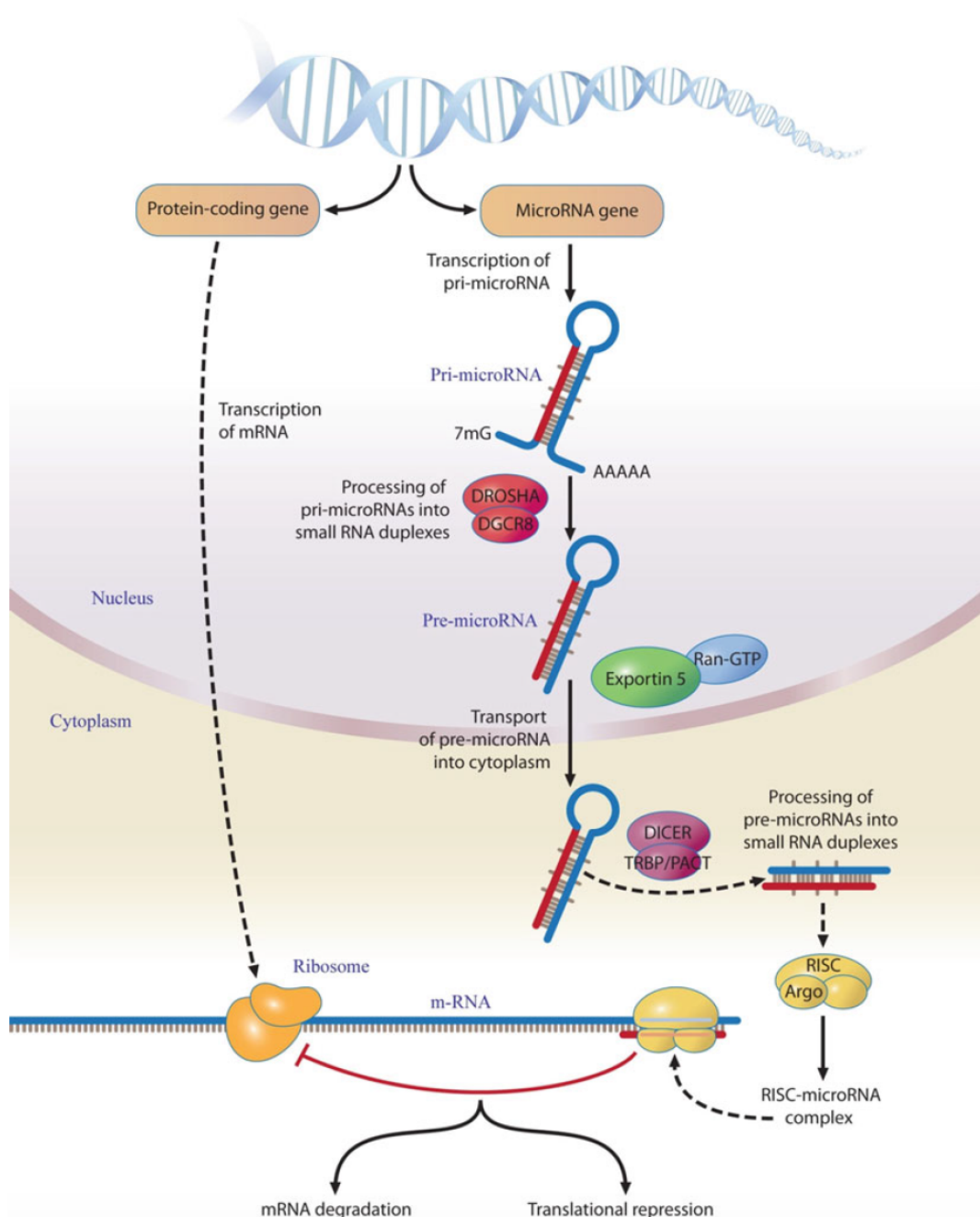


Figure 1.6. Canonical miRNA biogenesis pathway and mechanisms of mRNA silencing. From miRNA Maturation, C. Arenz, Humana Press (2014).

The duplex comprises a 5p strand, arising from the 5' arm of the pre-miRNA hairpin, and a 3p strand. Although both molecules can be potentially loaded into Argonaute (AGO) proteins, the preference between 5p and 3p miRNA is given to the strand possessing the less stable paired 5' end or an A or U as 5'-terminal nucleotide (Figure 1.6). In addition to the canonical pathway described above, alternative biogenesis routes independent of Drosha/DGCR8 or Dicer have been found for mirtrons and 7-methylguanine capped pre-miRNA as well as shRNA pre-miRNA, respectively (reviewed in Gebert and MacRae, 2019). Regardless of the biogenesis pathway used, the function of the AGO loaded miRNA is to guide an effector riboprotein complex called 'RISC' (RNA-induced silencing complex) to the target transcripts, via full or partial sequence complementarity. For this reason, the RISC loaded miRNA is also called 'guide miRNA' in contrast to the discarded one defined 'passenger miRNA' (reviewed in Gebert and MacRae, 2019).

In animals, miRNA targets are dictated by the seed sequence, a small region extending from nucleotide 2 to 8 at the 5' end of the guide miRNA. In most cases, miRNAs interact with the 3' untranslated region (3'UTR) of multiple target transcripts to induce mRNA degradation and translational repression. However, miRNA binding sites have also been detected in other mRNA regions including the 5' UTR and coding sequence, as well as within promoter regions. Interestingly, while the targeting of mRNA transcript regions under normal conditions has silencing effects, the interaction of miRNAs with gene promoters can induce transcription (reviewed in O'Brien et al., 2018).

2.2 miRNAs in adult V-SVZ NSCs and their progeny

An increasing number of miRNAs have been found to regulate adult NSCs and their progeny *in vivo* and in culture. Indeed, miRNAs have been implicated in multiple steps of OB neurogenesis, from stem cell self-renewal and proliferation to fate specification and functional integration of new neurons. For instance, miR-137 and miR-184, which are expressed in the adult V-SVZ, sustained NSC proliferation and inhibited neuronal differentiation by repressing the NSC fate-regulator Numbl-like (Numbl) and the polycomb methyltransferase Ezh2, respectively (Szulwach et al., 2010; Liu et al., 2010). Similarly, the miR-106b-25 cluster promoted the proliferation of primary cultured NSCs isolated from the adult forebrain. However, it also enhanced neurogenesis in differentiation conditions (Brett et al., 2011). miR-124, the most abundant miRNA in the adult brain, was found to promote the temporal progression of neurogenesis in the adult V-SVZ by repressing the expression of the transcription factor Sox9 in neuroblasts (Cheng et al., 2009). In a similar manner, the miRNAs

let-7b and miR-9, inhibited NSC proliferation and triggered neuronal differentiation by suppressing *Tlx* and the oncogenic chromatin regulator *Hmga2* (Zhao et al., 2010; Zhao et al., 2009). Moreover, since TLX protein can repress miR-9 expression, the negative feedback regulatory loop between mir-9 and TLX further controlled the balance between proliferation and differentiation during neurogenesis. In later stages of neurogenesis, miR-125b and miR-132 regulated the maturation and synaptic integration of newly-generated neurons in OB in an opposite manner: miR-125b by slowing the kinetics of this process likely allowing appropriate synapse formation and miR-132 by enhancing the synaptic integration and survival of new neurons. However, the targets mediating these phenotypes are still unknown (Akerblom et al., 2014; Pathania et al., 2012) (Figure 1.7).

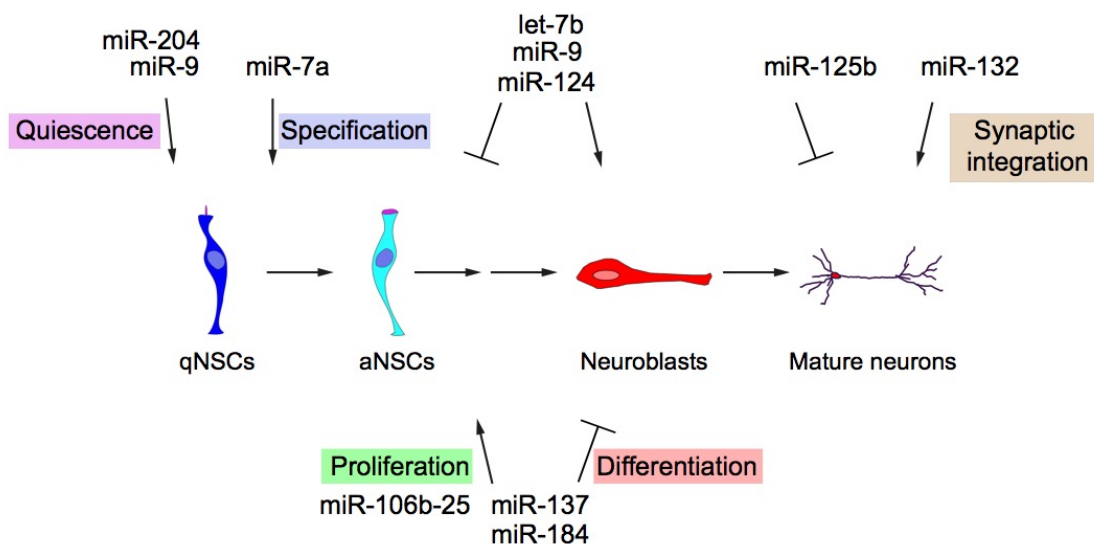


Figure 1.7. Summary of miRNA functional analyses during OB neurogenesis.

miRNAs have been found to contribute to the regionalization and fate specification of V-SVZ NSCs. For example, the expression of Pax6, which determines the generation of dopaminergic OB interneurons from NSCs, is regionally restricted to the dorsal V-SVZ by miR-7a. Indeed, whereas Pax6 mRNA is widely expressed in this germinal niche, the expression of miR-7a in V-SVZ progenitors follows a ventro-dorsal decreasing gradient and thus limits the appearance of PAX6 protein to the only dorsal domain (De Chevigny et al., 2012). miRNAs can also be secreted in extracellular fluids to modulate the activity of distant target cells. One example is the choroid plexus-derived miR-204 which was recently shown to regulate the number and undifferentiated state of V-SVZ qNSCs by repressing the translation of neurogenic mRNAs (Lepko et al., 2019).

Finally, miRNAs were also reported to maintain the quiescent state of adult stem cells. This is the case of miR-9, described in the zebrafish brain, and miR-195, miR-489, miR-497 and miR-708, found in the mouse skeletal muscle. Interestingly, whereas miR-195, miR-489 and miR-497 maintained the quiescent state through the suppression of cell cycle regulators, both miR-9 and miR-708 controlled the balance between stem cell quiescence and activation by modulation components of the Notch signaling (Katz et al., 2016; Sato et al., 2014; Cheung et al., 2012; Baghdadi et al., 2018).

3. THE miR-17~92 CLUSTER: MORE THAN A MERE ONCOGENE

miR-17~92 is one of the best-characterized miRNA clusters. It encodes six distinct miRNAs (-17, -18a, -19a and b, -20a, and -92a), as well as their passenger strands, that can be grouped into four families based on seed sequence homology. In mammals, miR-17~92 has two paralogs, miR-106a~363 and miR-106b~25, that likely originated through a series of duplication and deletion events during early vertebrate evolution (Concepcion et al., 2012). Whereas miR-17~92 and miR-106b~25 display similar expression patterns and are particularly abundant in embryonic stem cells and during embryogenesis, miR-106a~363 is generally expressed at lower levels (Concepcion et al., 2012) (Figure 1.8). Functionally, miR-17~92 was originally identified as an oncogene due to its frequent amplification in hematopoietic malignancies where different members of the cluster contributed to its overall oncogenic activity by promoting proliferation and survival of cancer cells. Its tumorigenic role was further demonstrated in a variety of solid tumors including lung cancer, neuroblastoma and medulloblastoma (Concepcion et al., 2012). In contrast to its paralogs, whose single and compound deletions do not result in any obvious abnormalities, miR-17~92 plays important roles during normal development and homeostasis, and its ablation is embryonically lethal (Ventura et al., 2008). Indeed, miR-17~92 is essential for normal lung and heart development, B cell survival as well as for axial patterning control in vertebrates (Ventura et al., 2008; Han et al., 2015).

In the developing forebrain, miR-17~92 maintains asymmetric neural stem division by restricting the expression pattern of *Tis21* (Fei et al., 2014) and modulates RGC expansion and transition to intermediate progenitors through repression of *Pten* and *Tbr2* as well as the cell-cycle regulator *p21* (Bian et al., 2013; Chen et al., 2014). In addition, miR-17~92 regulates the neurogenic-to-gliogenic transition by promoting neurogenesis and inhibiting the acquisition of gliogenic competence through the silencing of *p38* (Naka-Kaneda et al., 2014). Similarly, miR-17~92 induces neurogenesis at the expense of astrocytogenesis by targeting *Bmpr2* (Mao et al.,

2014). Moreover, miR-17~92 cluster is also needed for normal spinal cord motor neuron patterning (Chen et al., 2011) as well as for survival of limb-innervating motor neurons (Tung et al., 2015). miR-17~92 also promotes proliferation of embryonic primary cultured OPCs by targeting Akt signaling (Budde et al., 2010), but its expression is downregulated during differentiation *in vitro* (de Faria O Jr et al., 2012).

In the adult brain, miR-17~92 controls hippocampal neurogenesis and, thus, affects mood and anxiety-related behavior (Jin et al., 2016) as well as spatial memory (Pan et al., 2019). Furthermore, miR-17~92 expression in adult V-SVZ neural progenitors elevates following experimental stroke to sustain their proliferation and survival (Liu et al., 2013). However, to date, the role of the miR-17~92 cluster in the adult V-SVZ under normal conditions has not yet been elucidated. Recently, in the context of brain metastasis, astrocytes were found to secrete exosomes containing the most oncogenic member of the miR-17~92 cluster, miR-19a. Uptake of miR-19a-containing exosomes by cancer cells led to the recruitment of IBA⁺ myeloid cells to further support cancer cell proliferation and survival (Zhang et al., 2015). Thus, miR-17~92 can potentially act in both cell-autonomous and non-autonomous manners.

In conclusion, the miR-17~92 cluster has been implicated in different cellular processes where it has pleiotropic functions in a cell type and context-dependent manner.

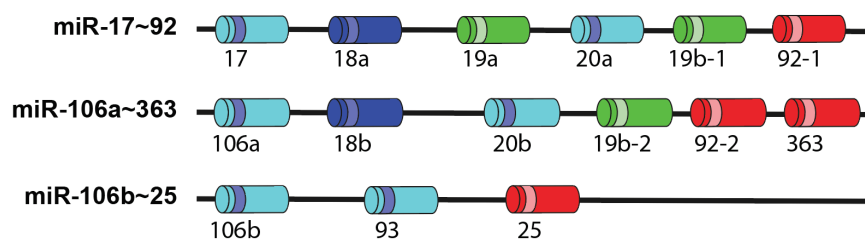


Figure 1.8. Schematics of the miR-17~92 cluster and paralogs, miR-106a~363 and miR-106b~25. miRNAs sharing the same seed sequence are illustrated in the same color.

AIMS

In the adult mammalian brain, the ventricular-subventricular zone (V-SVZ) generates neurons and glia throughout life. In this germinal niche, neural stem cells (NSCs) coexist in quiescent and activated states. However, the molecular mechanisms underlying this transition remain elusive. miRNAs are emerging as important regulators of global cell state and NSC functions, and have been implicated in stem cell self-renewal and differentiation. However, their role in adult NSC activation is unknown.

By miRNA profiling of FACS-purified cells of the early V-SVZ lineage, the Doetsch group found the miR-17~92 cluster to be significantly upregulated in activated NSCs (aNSCs) and transit-amplifying cells (TACs) in comparison to quiescent NSCs (qNSCs). Previous work in the laboratory has shown that conditional ablation of miR-17~92 cluster in FACS-purified aNSCs *in vitro* reduced their neurosphere formation and their ability to be passaged suggesting a potential role of the cluster in stem cell proliferation and self-renewal. In addition, in a 1-month-chase analysis after tamoxifen (Tmx) administration to a conditional knock-out (cKO) mouse model in which GFAP⁺ astrocytes can be recombined (GFAP-CreERT2; miR-17~92fl/fl; R26R Tomato mice), loss of miR-17~92 was found to increase the proportion of GFAP⁺ astrocytes and decrease that of MCM2⁺ proliferating cells, as well as reduce the percentage of DCX⁺ neuroblasts (NBs) in the V-SVZ.

Although these results support the evidence that miR-17~92 is important for adult V-SVZ neurogenesis, its role in the V-SVZ niche has not yet been fully characterized. Moreover, it remains unclear whether the miR-17~92 cluster regulates the cell fate of V-SVZ NSCs towards an oligodendroglial lineage. Therefore, the major aims of my PhD thesis will be:

- a) To elucidate the role of the cluster in adult neural stem cell activation, proliferation and fate specification;
- b) To identify miR-17~92 targets that could mediate its function.

Chapter 2: miR-17~92 Regulation of Adult Neural Stem Cells

Introduction

In the V-SVZ, adult NSCs exist in both quiescent and activated states. Currently, little is understood about the molecular pathways that regulate the adult neural stem cell switch from a quiescent to an activated state.

miRNAs (miRs) are small non-coding RNAs able to rapidly sculpt cell transcriptomes and modulate global cell state by targeting hundreds of mRNAs simultaneously at the post-transcriptional level. microRNAs have been implicated in stem cell differentiation and self-renewal, as well as stem cell quiescence (Brett et al., 2011; Zhao et al., 2009; Cheung et al., 2013). To date, the role of miRNAs in regulating the transition from quiescence to activation in neural stem cells has not been explored.

Previous work in the Doetsch laboratory identified, through miRNA expression profiling of FACS-purified V-SVZ cells, the miR-17~92 cluster as highly upregulated in activated stem cells in comparison to their quiescent counterparts. Preliminary data suggested that miR-17~92 is important for adult V-SVZ neurogenesis. However, its role in the V-SVZ niche has not yet been fully characterized.

In this chapter, I validate the expression profiling of miR-17~92 by quantitative PCR (qPCR) and investigate the functional role of this cluster in the V-SVZ upon conditional deletion of miR-17~92 *in vitro* and *in vivo*, to test whether this miRNA cluster is necessary for activation, proliferation and fate specification of adult neural stem cells. I also perform pathway analysis of computationally predicted miRNA targets expressed in FACS-purified populations to identify potentially relevant targets of miR-17~92 in the early NSC lineage of the adult V-SVZ. Altogether, these analyses reveal that miR-17~92 plays pleiotropic functions in the adult V-SVZ.

Results

qPCR validation of miR-17~92 expression profile in the adult SVZ NSC lineage

Quiescent (qNSCs) and activated (aNSCs) neural stem cells as well as transit amplifying cells (TACs) can be directly FACS-purified from the adult V-SVZ niche by combining fluorescently complexed EGF-ligand and antibodies against CD24 and CD133 in *hGFAP::GFP* mice, in which astrocytes express GFP under the GFAP promoter (Codega et al., 2014) (Fig. 2.1 A). To validate the finding from the expression profiling that miR-17~92 is enriched in aNSCs versus qNSCs, and to determine whether individual members of the miR-17~92 cluster were all expressed at the same level, I performed qPCR analysis of FACS-purified qNSCs,

aNSCs and TACs using probes for all mature forms of the different members of the cluster. This analysis revealed that all members of miR-17~92 were expressed at low levels in qNSCs and were significantly upregulated in aNSCs and TACs over qNSCs (Fig. 2.1 B and C).

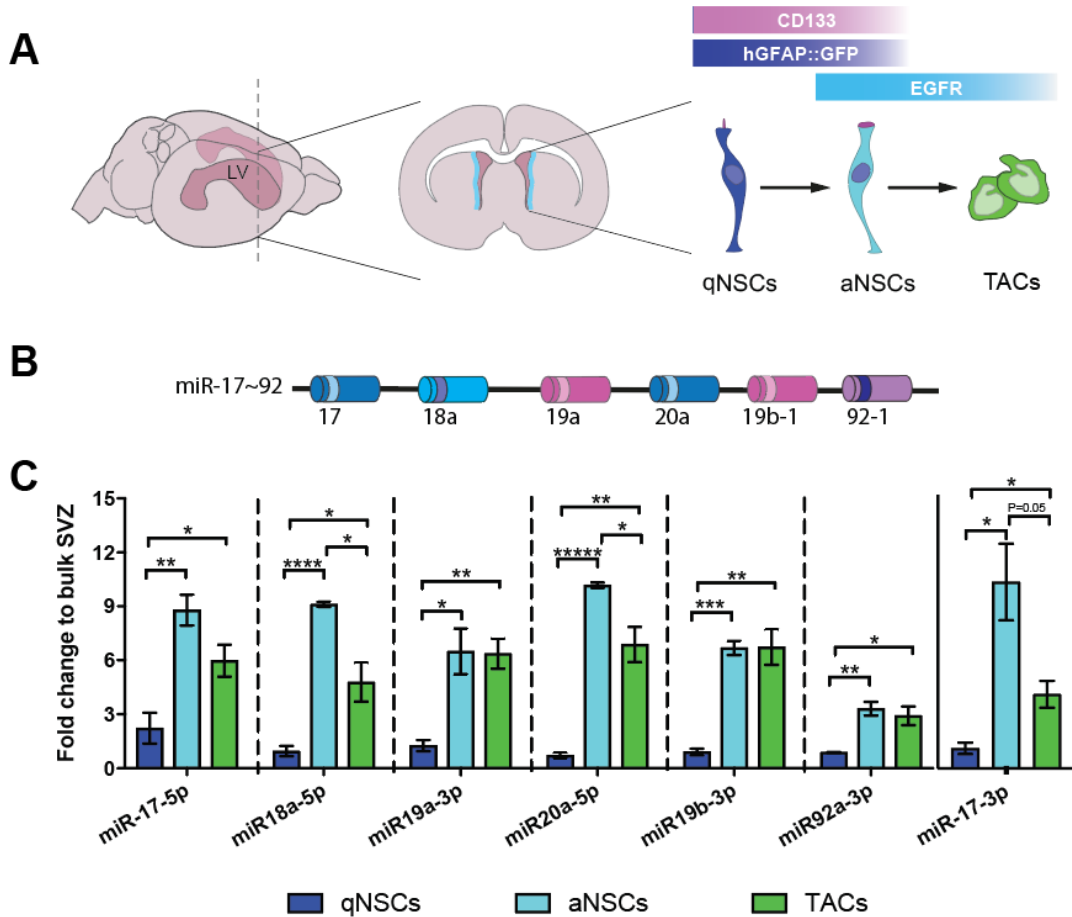


Figure 2.1 qPCR validation of miR-17~92 expression profiling in the early V-SVZ lineage

(A) left: Schema of the whole mouse brain showing the LVs (dark color); middle: schema of coronal section displaying the V-SVZ (light blue); right: schema of V-SVZ early lineage and markers for FACS-purification. (B) Schematic representation of the miR-17~92 cluster. (C) Fold change expression to bulk SVZ of miR-17~92 members in qNSCs, aNSCs and TACs (n = 3; *p < 0.05, **p < 0.01, ***p < 0.001, ****p < 0.0001, *****p < 0.00001, unpaired two-tailed Student's t test; mean ± SEM).

Depending on the strand of the pre-miRNA harpin from which they arise, mature miRNAs are distinguished as guide and star (also known as passenger) forms. Analysis of the relative abundance of miR-17~92 guide and star forms to the housekeeping miRNA miR-16-5p highlighted that the guide forms of miR-19b, miR-20a and miR-92a were the most abundantly expressed miRNAs of the cluster in the profiled populations (Fig. 2.2 A). While both guide and star form of miR-17 were expressed at similar levels, the expression of all other star forms of

the cluster were very low as compared to the guide forms (Fig. 2.2 B) and thus unlikely to play a pivotal role in the control of the gene regulatory network of adult V-SVZ stem cells.

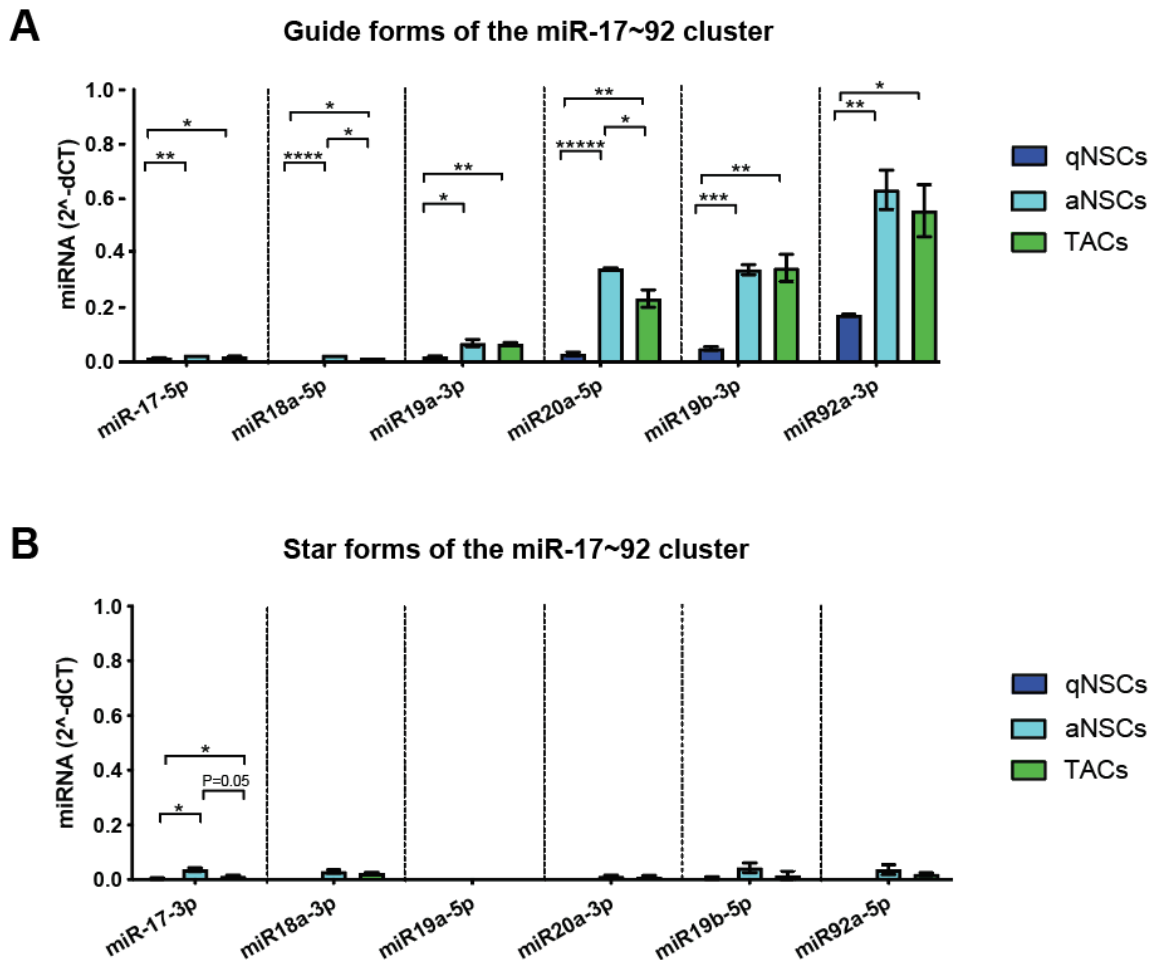


Figure 2.2 Relative abundance of miR-17~92 guide and star members in the early V-SVZ lineage

Relative abundance of miR-17~92 guide (A) and star (B) members in qNSCs, aNSCs and TACs (n = 3; *p < 0.05, **p < 0.01, ***p < 0.001, ****p < 0.0001, *****p < 0.00001, unpaired two-tailed Student's t test; mean ± SEM).

miR-17~92 deletion reduces adult NSC proliferation and colony formation *in vitro*

To investigate the effect of miR-17~92 deletion on NSC proliferation and self-renewal, we performed *in vitro* assays using FACS-purified NSCs from adult CAGG-CreERT2^{+/+}; miR-17~92^{fl/fl} or miR-17~92^{+/+}; R26R Tomato eGFP mice in which, upon administration of hydroxytamoxifen (4OHT), a ubiquitously expressed CreERT2 recombinase induces deletion of the miR-17~92 cluster, as well as rearrangement of the reporter locus to switch from expression of the tdTomato to the eGFP reporter (Fig. 2.3A). In neurosphere assays, in which NSCs are cultured in non-adherent conditions, the ability of NSCs to form spheres is used as a readout of their proliferation and self-renewal capabilities. Previous work in the lab has shown that conditional deletion of miR-17~92 cluster in FACS-purified aNSCs *in vitro* reduced their

neurosphere formation and their ability to be passaged suggesting a potential role of the cluster in stem cell proliferation and self-renewal.

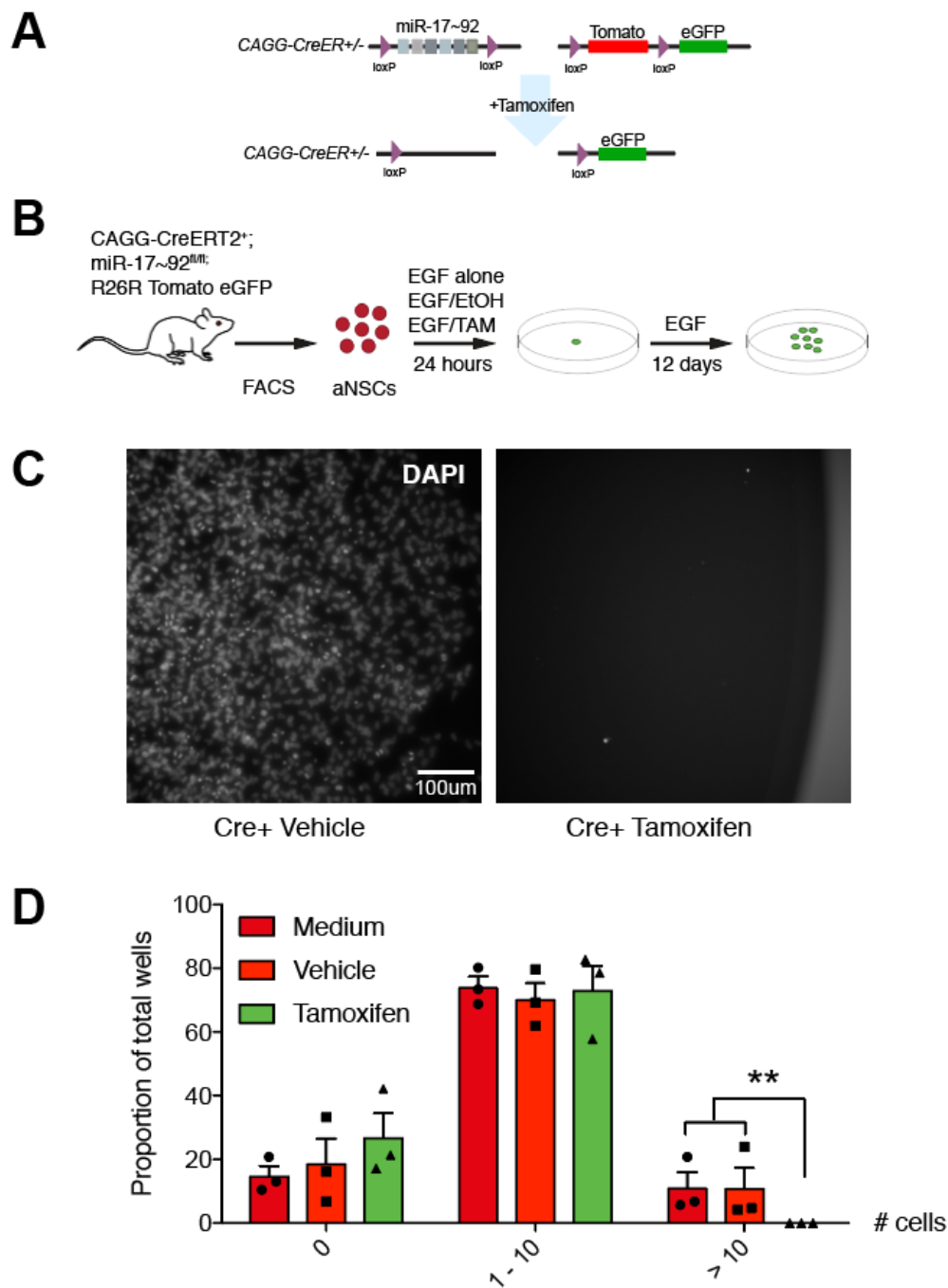


Figure 2.3 Conditional deletion of miR-17~92 *in vitro* reduces neural stem cell proliferation

(A) Schematic of miR-17~92 recombination strategy *in vitro*. (B) Schematic of experimental paradigm. (C) Representative fluorescent images of Cre+ aNSCs 13 days after plating. Cells treated with Vehicle (Ethanol) are on the left, cells treated with Tamoxifen on the right. Scale bar, 100 μ m. (D) Quantification of total cells per well at the end of cell culture. Each data point represents an independent experiment ($n = 3$; $**p < 0.01$, two-sided Wilcoxon rank sum test followed by Fisher's exact test; mean \pm SEM).

To be able to assess the effect of miR-17~92 deletion on stem cell proliferation at the single cell level, we utilized an adherent assay. FACS-purified aNSCs were plated as single cells per well, exposed to tamoxifen, vehicle (ethanol) or medium for 24 hours and subsequently grown for 12 days under adherent conditions with EGF (Fig. 2.3 B). At the end of the culture, cells were fixed and stained with DAPI to visualize cell nuclei. I then quantified the number of cells per well in each condition. Interestingly, while control cells underwent a massive expansion giving rise to very large clones, miR-17~92-deleted cells exhibited very modest proliferation and failed to generate large colonies (Fig. 2.3 C and D). Moreover, no significant difference was found in the number of wells containing less than ten cells or no cells (Fig. 2.3 C and D). Together, these results show an important function of the cluster in the proliferation and colony formation of adult NSCs, and suggest that miR-17~92 is not important for their survival at short time points.

Deletion of miR-17~92 in NSCs *in vivo* decreases stem cell proliferation and expands oligodendrogenic transit amplifying cells at short time points

To investigate the role of miR-17~92 in V-SVZ stem cells *in vivo* I selectively deleted the miR-17~92 cluster in GFAP⁺ NSCs. To do this, I used adult miR-17~92 floxed (GFAP-CreERT2^{+/+}; miR-17~92^{fl/fl}; R26R lslTomato^{+/+}) or control (GFAP-CreERT2^{+/+}; miR-17~92^{+/+}; R26R lslTomato^{+/+}) mice in which administration of tamoxifen (Tmx) induces miR-17~92 deletion and initiates tdTomato reporter expression in GFAP⁺ cells (Fig. 2.5 A). To study the effect of the deletion of cluster at short time points, I performed immunohistochemistry (IHC) analysis for cells at different stages of the lineage in coronal brain sections of miR-17~92 control and deleted mice after three pulses of tamoxifen followed by a one-day chase (1 dpi) (Fig. 2.4, Fig. 2.5 B).

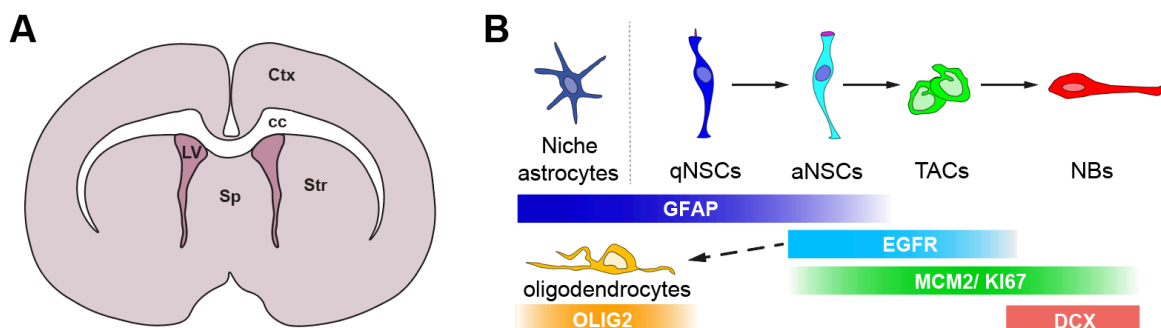


Figure 2.4 Summary of markers of the adult V-SVZ neural stem cell lineage

(A) Schema of mouse brain coronal section showing brain regions relevant to this work. (B) Schematic of neurogenic and oligodendrogenic NSC lineages showing cell markers. Ctx: cortex, cc: *corpus callosum*, LV: lateral ventricle, Sp: *septum*, Str: *striatum*.

I then quantified Tomato⁺ (Tom⁺) cells along the entire dorsoventral extent of the V-SVZ, in the lateral and septal walls, of four different rostro-caudal levels.

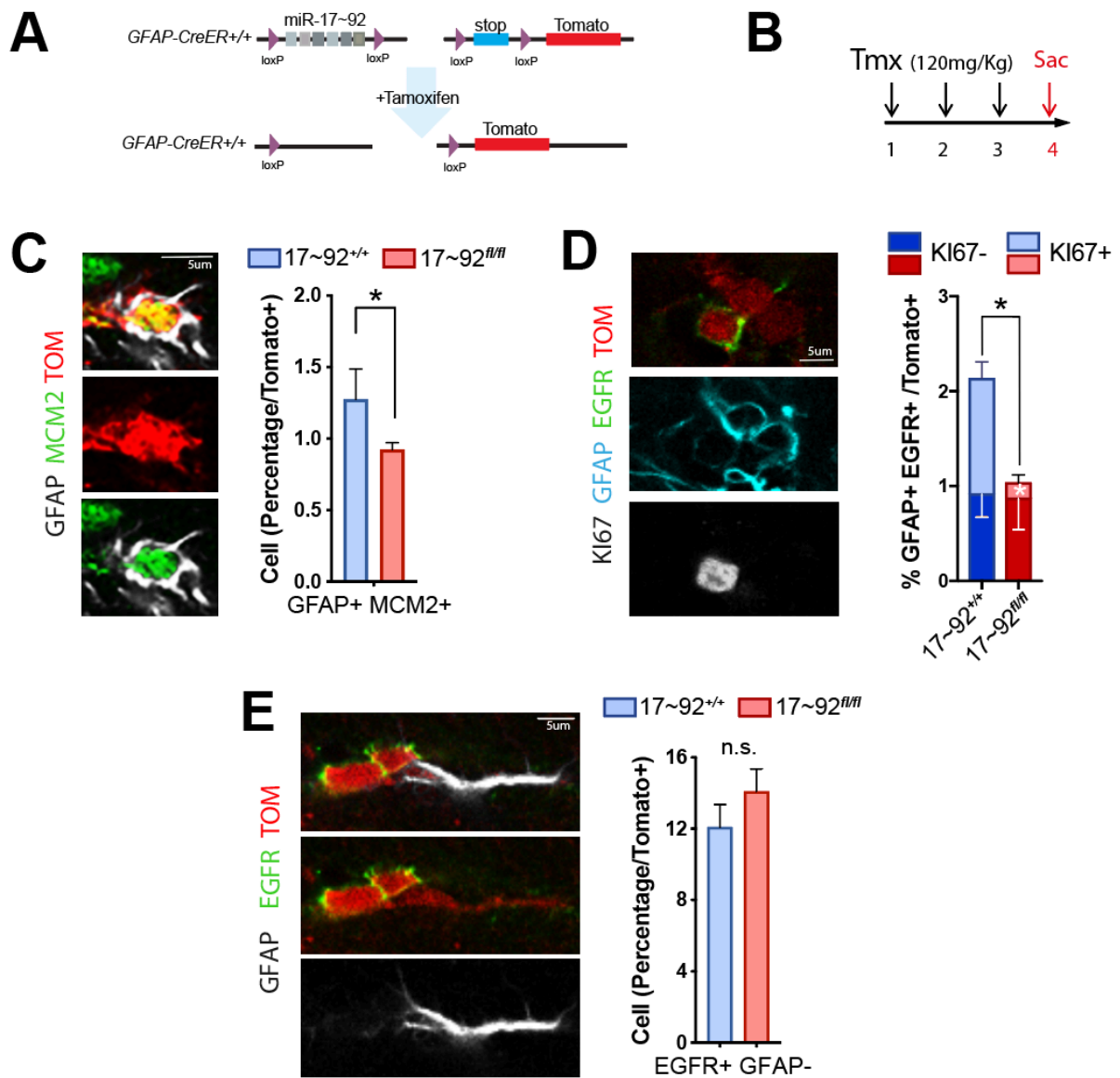


Figure 2.5 Deletion of miR-17~92 in NSCs *in vivo* reduces stem cell proliferation at short time points

(A) Schematic of miR-17~92 recombination strategy *in vivo*. (B) Schematic of experimental paradigm. (C-F) Representative confocal images and related quantification. miR-17~92 deletion reduces the percentage of Tom⁺ GFAP⁺ MCM2⁺ dividing NSCs (C) and Tom⁺ GFAP⁺ EGFR⁺ KI67⁺ cycling aNSCs (D). Loss of miR-17~92 does not change the proportion of total TACs (E). (C-E) Scale bar, 5 μ m. (n = 3; *p < 0.05, two-tailed unpaired Student's t test; mean \pm SEM).

In the V-SVZ, qNSCs express the astrocytic marker GFAP and upregulate EGFR upon activation. aNSCs, in turn, give rise to TACs which retain EGFR expression but lose that of

GFAP. To discriminate qNSCs, aNSCs and TACs, I therefore immunostained with antibodies against the early lineage markers GFAP and EGFR, whereas to assess changes in stem cell proliferation I immunostained with antibodies against the intrinsic proliferation markers MCM2 and KI67.

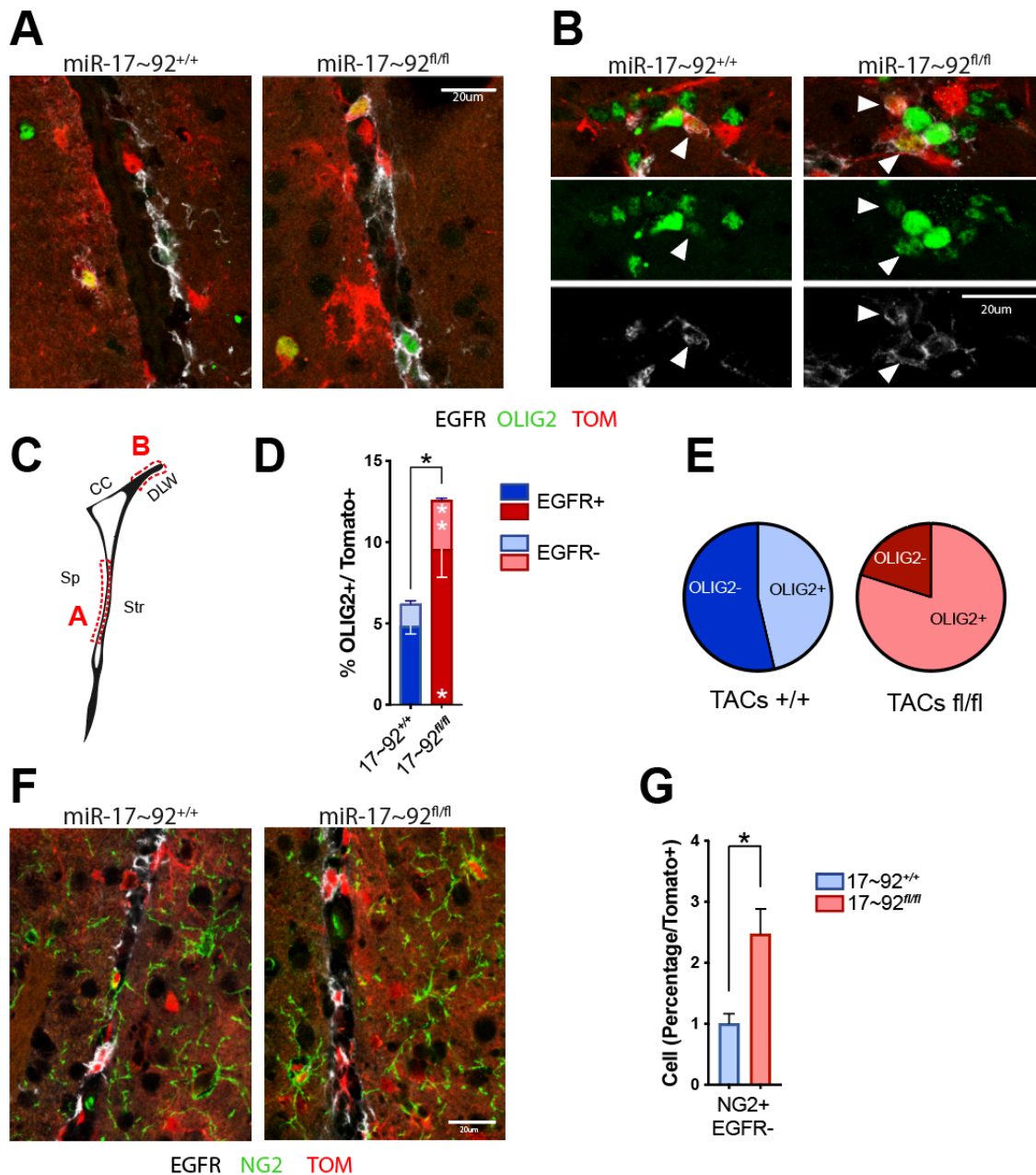


Figure 2.6 Loss of miR-17~92 in NSCs *in vivo* increases OLIG2⁺ TACs and NG2⁺ OPCs at short time points (A, B, F) Representative confocal images showing OLIG2⁺ TACs and NG2⁺ OPCs in the intermediate (A, F) and dorsal (B) regions of the V-SVZ. (A-D) miR-17~92 deletion increases the percentage of Tom⁺ OLIG2⁺ EGFR⁺ and Tom⁺ OLIG2⁺ EGFR⁻ cells. (C) Schema of the V-SVZ showing the location of the regions (dotted boxes) of images in A and B. (E) Deletion of miR-17~92 increases the proportion of oligodendrogenic TACs. (F-G) miR-17~92 loss increases the percentage of Tom⁺ NG2⁺ EGFR⁻ cells. Scale bar, 20 μ m. (n = 3; *p < 0.05, **p < 0.01, two-tailed unpaired Student's t test; mean \pm SEM). CC: *corpus callosum*, DLW: dorsolateral wedge, Sp: *septum* and Str: *striatum*.

At 1 dpi, deletion of the cluster reduced the proportion of dividing NSCs (GFAP⁺ MCM2⁺) and activated NSCs (GFAP⁺ EGFR⁺) over total Tomato⁺ (Tom) cells (Fig. 2.5 C and D). The decrease in aNSCs was due to a selective loss of cycling aNSCs suggesting that the miR-17~92 cluster plays a critical function in stem cell proliferation *in vivo*.

No change was observed in the proportion of total Tom⁺ TACs (GFAP⁻ EGFR⁺) (Fig. 2.5 E) or neuroblasts (NBs, DCX⁺, data not shown) at short time points after miR-17~92 deletion.

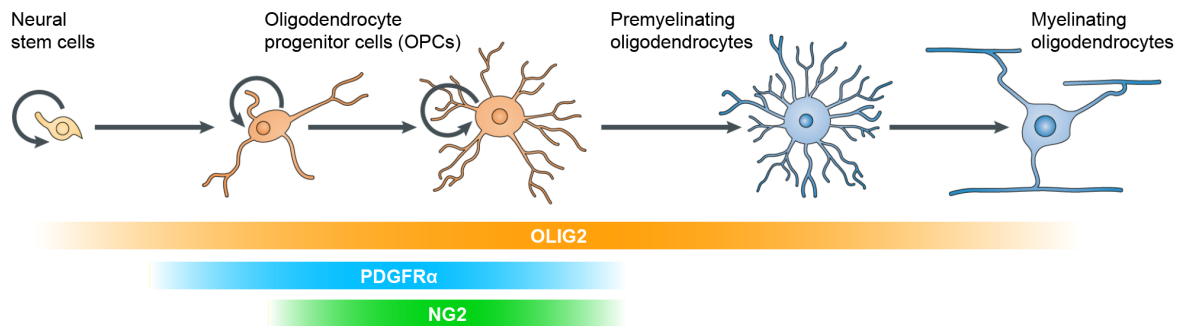


Figure 2.7 Summary of cellular markers of the oligodendrocyte lineage. Image modified from Nishiyama et al., Nature Reviews Neuroscience (2009).

Beside NBs, V-SVZ NSCs also generate a small number of oligodendrocytes (Chaker et al., 2016). To assess a potential function of the miR-17~92 cluster in cell fate specification, I immunostained miR-17~92 control and deleted mice for the oligodendrocyte lineage marker OLIG2 (Fig. 2.7). Strikingly, miR-17~92 loss increased the percentage of Tom⁺ OLIG2⁺ cells, the majority of which co-expressed EGFR, over total Tom⁺ cells (Fig. 2.6 A-D).

OLIG2⁺ cells were distributed throughout the V-SVZ niche but were especially enriched in the intermediate and dorsal regions which are emerging as the most oligodendrogenic aspects of the adult V-SVZ (Ortega et al., 2013; Delgado et al., bioRxiv 2019) (Fig. 2.6 C). Almost all Tom⁺ OLIG2⁺ EGFR⁺ were negative for GFAP. As such deletion of the cluster significantly shifted the pool of recombined TACs towards more oligodendrogenic progenitors and fewer neurogenic progenitors (Fig. 2.6 E). Interestingly, miR-17~92 loss also increased the percentage of V-SVZ Tom⁺ NG2⁺ cells, all of which were EGFR⁻ (Fig. 2.6 F-G), which likely correspond to the Tom⁺ OLIG2⁺ EGFR⁻ cells that were also increased following miR-17~92 deletion (Fig. 2.6 D). Altogether, these data show an important function of the miR-17~92 cluster in cell proliferation of adult NSCs and suggest a potential role in cell specification.

miR-17~92 deletion *in vivo* reduces NSC activation and neurogenesis at long time points

To study the effect of miR-17~92 deletion following a longer time period, miR-17~92 control and floxed mice were injected with Tmx once a day for three consecutive days and

chased for thirty days (30 dpi). To identify possible label-retaining (LR) cells in the V-SVZ, 5-bromo-2'-deoxyuridine (BrdU) was co-administered on the last two days of Tmx injections (Fig. 2.8 A).

Within the Tom⁺ population, deletion of the cluster increased the proportion of Tom⁺ qNSCs (GFAP⁺ EGFR⁻) and reduced the percentage of Tom⁺ aNSCs (GFAP⁺ EGFR⁺) suggesting a defect in stem cell activation at long time points following miR-17~92 deletion (Fig. 2.8 B and C). Loss of the cluster also decreased the proportion of dividing aNSCs (based on KI67) indicating a reduced stem cell proliferation when miR-17~92 is deleted (Fig. 2.8 B and C). In support of this, IHC analysis of Tom⁺ BrdU-LRCs distribution in the V-SVZ revealed the appearance of LR-aNSCs (Tom⁺ BrdU⁺ GFAP⁺ EGFR⁺) only in mice that had lost miR-17~92 expression (Fig. 2.8 D). Thus, deletion of the miR-17~92 cluster in NSCs not only decreases their proliferation but may also impair their activation.

Unexpectedly, no change was found in the proportion of total Tom⁺ TACs at long time points after miR-17~92 deletion (data not shown). However, I still observed a significant increase in the percentage of Tom⁺ OLIG2⁺ cells, many of which co-expressed EGFR (data not shown), in the V-SVZ of mice that had lost miR-17~92 expression (Fig. 2.9 A and B) suggesting that oligodendrogenic TACs are still generated at the expense of neurogenic TACs at long time points. Indeed, miR-17~92 deletion reduced the proportion of DCX⁺ neuroblasts in the V-SVZ (Fig. 2.8 E and F).

Although V-SVZ-derived neuroblasts largely give rise to OB GABAergic neurons (Mullen et al., 1992), a small subset of *Tbr2*-expressing progenitor cells located in the dorsal aspect of the V-SVZ has been shown to generate glutamatergic neurons (Brill et al., 2009). Since *Tbr2* is a validated miR-17~92 functional target during neocortex development (Bian et al., 2013), I asked whether deletion of the cluster might affect the proportion and distribution of TBR2⁺ progenitors. Interestingly, miR-17~92 loss resulted in a higher proportion of TBR2-expressing cells within the Tom⁺ population (Fig. 2.8 E-G). As in their wild-type counterparts, these TBR2⁺ cells were only found in the dorsal V-SVZ suggesting that, independently of miR-17~92 mediated silencing, *Tbr2* expression is restricted to a subpopulation of dorsal V-SVZ cells unlike *Pax6*, whose dorsally confined protein expression is spatially limited by its targeting miRNA, miR-7a, and becomes extended to the entire V-SVZ upon miR-7a deletion (De Chevigny et al., 2012). It will be interesting to check the number of V-SVZ-derived glutamatergic and GABAergic neurons in the OB to confirm whether deletion of miR-17~92 causes a shift in glutamatergic versus GABAergic neuronal production.

Altogether, these results provide evidence for a role of miR-17~92 in stem cell activation and proliferation as well as neurogenesis.

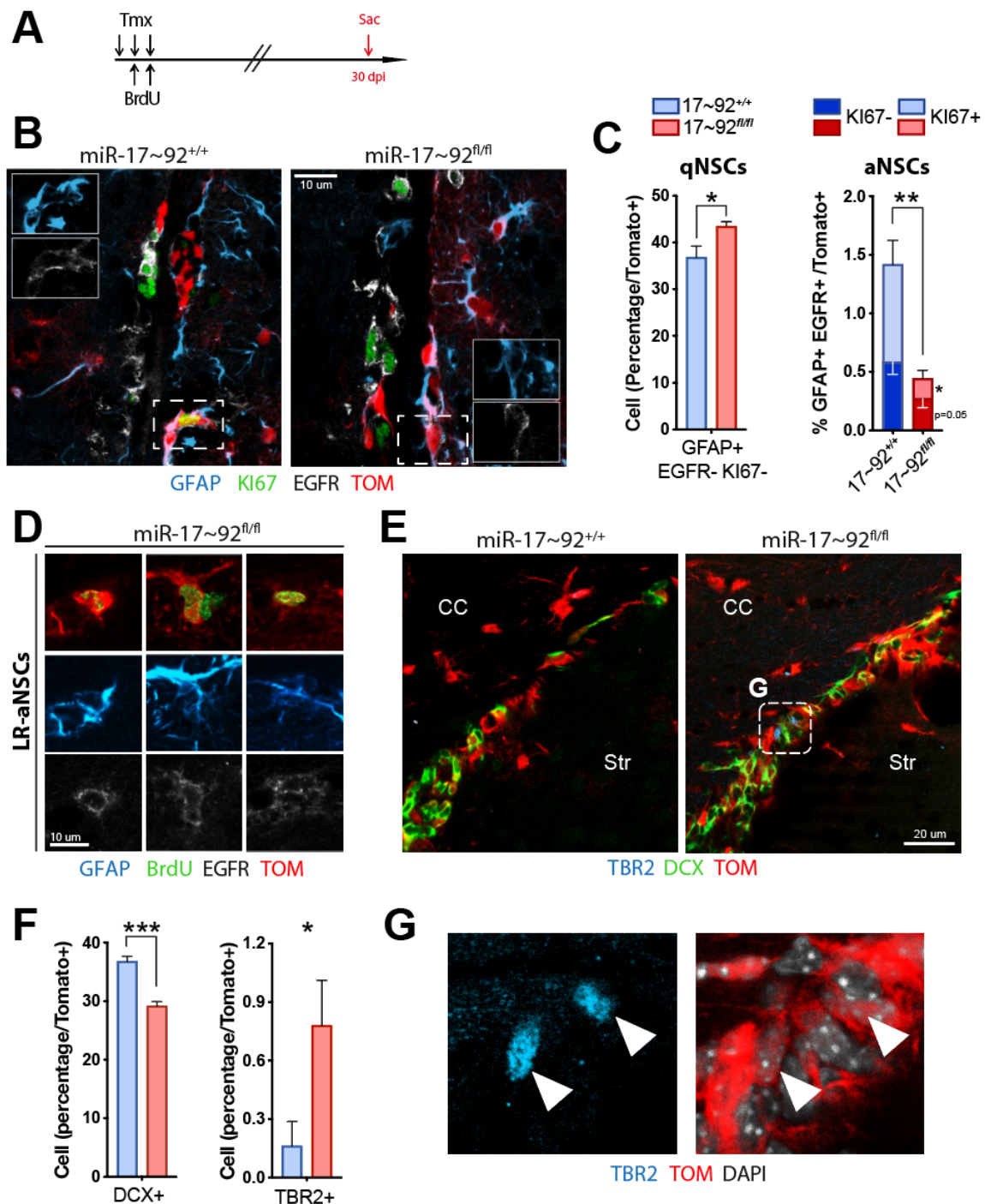


Figure 2.8 miR-17~92 deletion in NSCs *in vivo* reduces NSC activation and neurogenesis at long time points (A) Schematic of experimental paradigm. (B-C) miR-17~92 deletion increases the percentage over total Tom⁺ of qNSCs (GFAP⁺ EGFR⁻ KI67⁻) and reduces that of total aNSCs (GFAP⁺ EGFR⁺) and non-dividing (KI67⁻) aNSCs. (D) Label retaining-aNSCs only appear following miR-17~92 deletion. (E-G) Loss of miR-17~92 decreases the proportion of DCX⁺ neuroblasts (E-F) and increases the percentage of TBR2⁺ cells (F-G). (G) Blow-up of detail in image E. Scale bar, 10 μ m (B and D) and 20 μ m (E). (n = 3; *p < 0.05, **p < 0.01, ***p < 0.001, two-tailed unpaired Student's t test; mean \pm SEM). CC: *corpus callosum* and Str: *striatum*.

miR-17~92 ablation *in vivo* promotes oligodendrogenesis at long time points

Under normal conditions, V-SVZ NSCs generate a small number of oligodendrocytes which are destined for the *corpus callosum* (Menn et al., 2006). Since deletion of the miR-17~92 cluster at short time points increased the proportion of oligodendrogenic TACs (Fig. 2.6 E), I investigated the generation of oligodendrocytes at long time points following miR-17~92 loss.

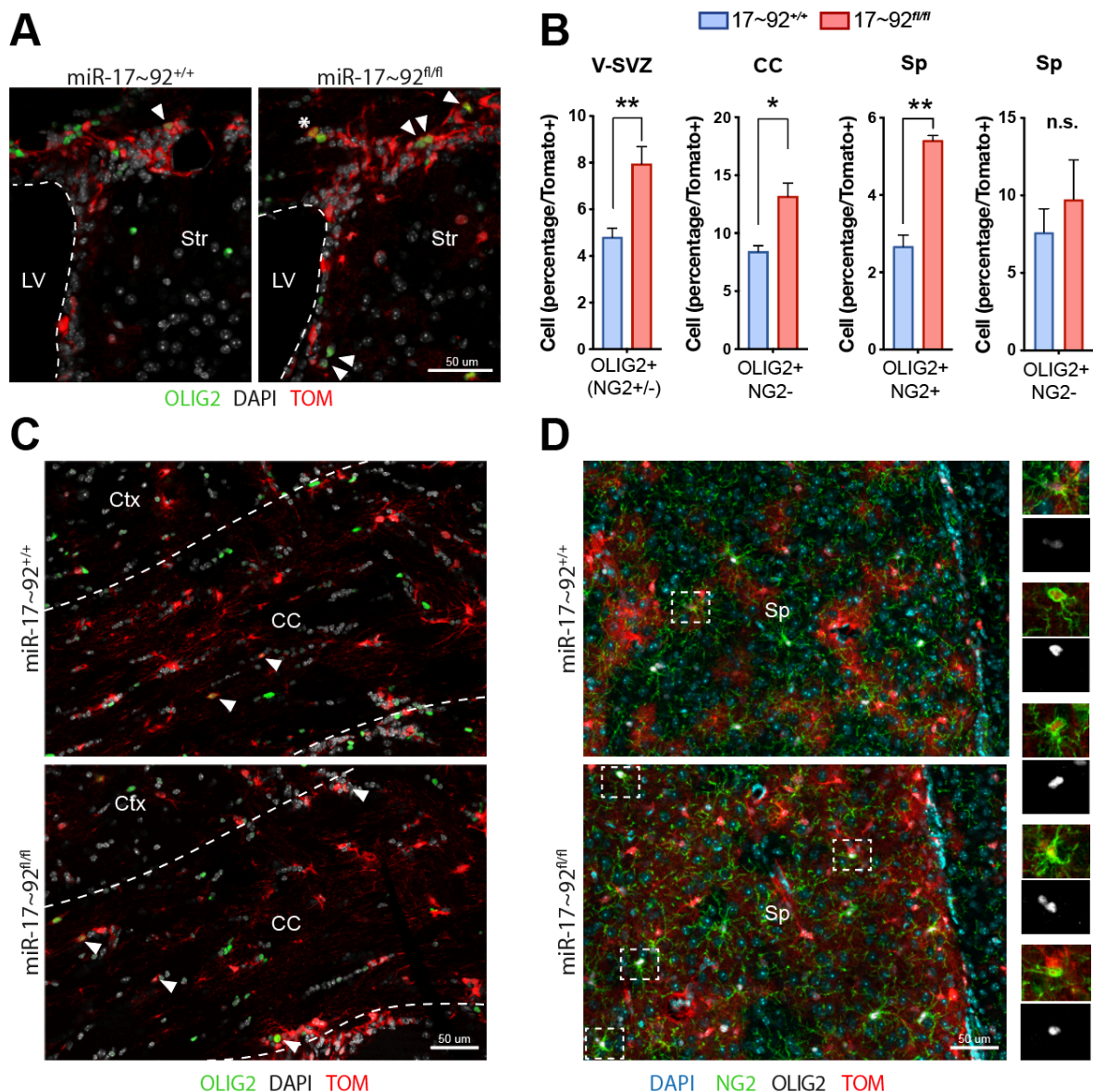


Figure 2.9 Deletion of miR-17~92 in NSCs *in vivo* promotes oligodendrogenesis at long time points

(A, C, D) Representative confocal tile scan images showing Tom⁺ OLIG2⁺ cells in the V-SVZ (A), *corpus callosum* (C) and *septum* (D). (A-D) miR-17~92 deletion increases the percentage of Tom⁺ OLIG2⁺ (NG2^{+/-}) cells in the V-SVZ (A), Tom⁺ OLIG2⁺ NG2⁻ cells in the CC (C), but not in the Sp, and Tom⁺ OLIG2⁺ NG2⁺ cells in the Sp (D). (B) Quantification of cells illustrated in images A, C and D. Scale bar, 50 μ m. (n = 3; *p < 0.05, **p < 0.01, two-tailed unpaired Student's t test; mean \pm SEM). LV: lateral ventricle, Str: *striatum*, CC: *corpus callosum*, Ctx: cortex and Sp: *septum*.

Importantly, thirty days after Tmx administration, miR-17~92 loss increased the proportion of Tom⁺ OLIG2⁺ NG2⁻ differentiated oligodendrocytes, but not Tom⁺ OLIG2⁺ NG2⁺ OPCs (data not shown), in the *corpus callosum* (CC) (Fig. 2.9 B and C). No change in differentiated Tom⁺ oligodendrocytes was found in the *septum* (Fig. 2.9 B). However, intriguingly, deletion of miR-17~92 significantly increased the percentage of Tom⁺ OLIG2⁺ NG2⁺ OPCs in this brain region (Fig. 2.9 B and D) revealing that V-SVZ NSCs deleted for miR-17~92 contribute OPCs to this brain area. Altogether, these results highlight an important function of the miR-17~92 cluster in regulating oligodendrogenesis.

Computational identification of biological pathways regulated by the miR-17~92 cluster

miRNAs are a class of small non-coding RNA molecules able to sculpt cell transcriptomes by targeting hundreds of mRNAs simultaneously, either repressing their translation or promoting their degradation (O'Brien et al., 2018).

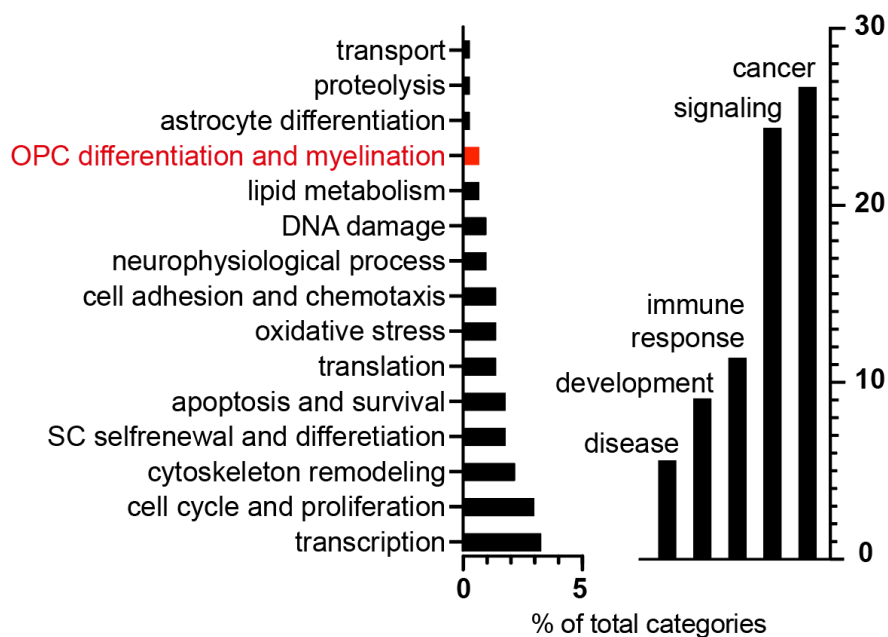


Figure 2.10 Pathway analysis of computationally predicted miR-17~92 targets expressed in V-SVZ NSCs

Selected top-enriched pathway maps from Metacore analysis exhibiting a False Discovery Rate $< 3 \times 10^{-5}$. Data show pathway abundance as percentage of total categories containing miR-17~92 targets.

To identify miR-17~92 targets that might be relevant for adult V-SVZ NSC functions, I performed bioinformatic analyses. First, I compiled a shortlist of miR-17~92 targets expressed in qNSCs, aNSCs and TACs from FACS-purified populations and multiple online available prediction algorithms (TargetsScan, PicTar, microcosm, miRDB). I then carried out pathway analysis of the predicted targets using Metacore. In line with published works investigating the

function of the miR-17~92 cluster in several cellular and physiopathological contexts, the bulk of miR-17~92 targets were found in the gene categories related to ‘cancer’, ‘immune response’, ‘development’ and ‘apoptosis and survival’ (Olive et al., 2013; Conception et al., 2012; Ventura et al., 2008; Han et al., 2015; Xu et al., 2015). In addition to these, miR-17~92 targets were also in pathways related to the categories of ‘cell adhesion’ and ‘lipid metabolism’, two gene categories enriched in quiescent stem cells across different compartments (Codega et al., 2014). Strikingly, pathway analysis also identified ‘OPC differentiation and myelination’ among gene categories enriched for miR-17~92 targets (Fig. 2.10).

| miR-17~92 targets in 'OPC differentiation and myelination' | | | | | |
|---|-------|--------|--------|---------|--------|
| Akt1 | Fzd1 | Hn1 | Nkx2-2 | Qk | Sp1 |
| Akt3 | Fzd3 | Id2 | Notch1 | Raf1 | Tcf4 |
| Ascl1 | Fzd4 | Id4 | Nrg1 | Rbpj | Tcf712 |
| Bad | Fzd5 | Jag1 | Olig2 | Rps6ka1 | Ugt8a |
| Chuk | Fzd7 | Mtf1 | Pdgfra | Rps6kb1 | Ywhab |
| Eif4ebp1 | Gsk3b | Myt1 | Pik3ca | Sox10 | Yy1 |
| Fyn | Hes1 | Nfkbia | Pik3r1 | Sox21 | |

Table 2.1 miR-17~92 targets enriched in the gene category of ‘OPC differentiation and myelination’

The identification of a gene category related to oligodendrogenesis is exciting as it complements my functional data showing an increase in oligodendrogenesis following miR-17~92 deletion at both short and long time points. Interestingly, among the miR-17~92 predicted targets in this category there were two key regulators of oligodendrogenesis, *Olig2* and *Pdgfra* (Table 2.1). *Olig2* is expressed in both parenchymal and V-SVZ OPCs and has been validated as a functional target of miR-17-3p during spinal cord progenitor patterning in embryogenesis (Cheng et al., 2011). *Pdgfra* is also highly expressed in OPCs and is, together with its ligand platelet-derived growth factor-A (PDGF-A), of critical importance for oligodendrocyte formation in the developing and adult mouse central nervous system (Barres et al., 1992; Nishiyama et al., 2009; Noble et al., 1988; Pringle et al., 1992; Đăng et al., 2019). However, so far no studies have addressed the relationship between *Pdgfra* and the miR-17~92 cluster. I therefore focused on this miR-17~92 predicted target for further functional studies.

***Pdgfra* is a functional miR-17~92 target in the V-SVZ**

Prediction algorithms of miRNA targets identified binding sites for all four seed families of the miR-17~92 cluster in the 3’UTR of the *Pdgfra* gene (Fig. 2.11). To validate

whether *Pdgfra* is a target of miR-17~92, I performed luciferase assays using constructs containing the 3'UTR of different genes together with a miRNA vector encoding the whole miR-17-92 cluster.

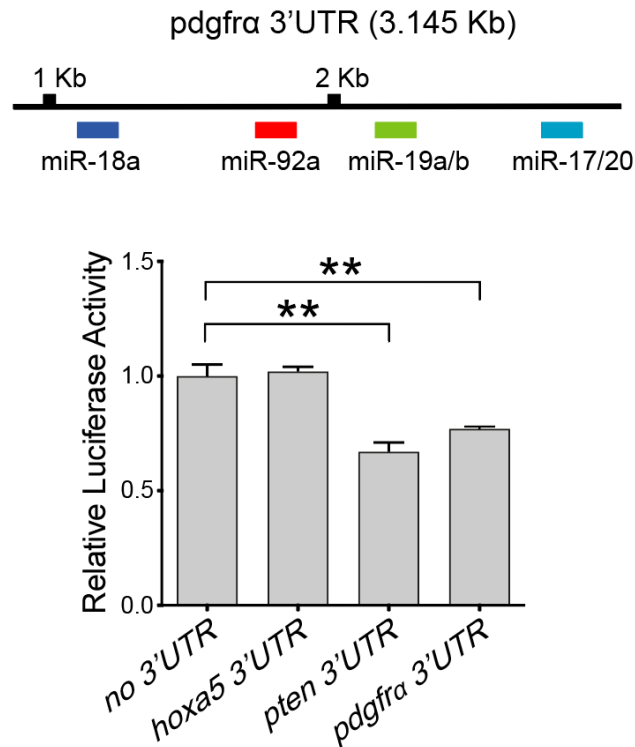


Figure 2.11 The miR-17~92 cluster regulates *Pdgfra* expression via its 3'UTR

(Top) Schematic representation of the 3'UTR of the *Pdgfra* gene showing the binding sites for different members of the miR-17~92 cluster in distinct colors. (Bottom) Luciferase reporter assay validating *Pdgfra* as biochemical miR-17~92 target. *Hoxa5*: non-targeted negative control, *Pten*: validated positive control (Tun et al., 2015) (n=3, **p<0.01, two-tailed unpaired Student's t test, mean \pm SEM).

Compared to the blank luciferase reporter lacking any 3'UTR, I observed a robust reduction in luciferase activity for luciferase reporters containing the 3'UTR of *Pdgfra* and the validated miR-17~92 target *Pten* (Tun et al., 2015) but not for the negative control *Hoxa5* (Tun et al., 2015), indicating that *Pdgfra* is a target of the miR-17~92 cluster.

To define if *Pdgfra* is an *in vivo* target of the cluster, I performed IHC analysis of PDGFR α protein expression and distribution in early NSC lineage of miR-17~92 control and deleted mice at 1dpi by immunostaining for PDGFR α as well as for the lineage markers GFAP and EGFR (Fig 2.12). Under normal conditions PDGFR α is only expressed by extremely rare NSCs in the V-SVZ but not in TACs (Chojnacki et al., 2011). Therefore, if *Pdgfra* is a functional target of miR-17~92, deletion of the cluster is expected to expand PDGFR α expression along

the lineage leading to the appearance of EGFR co-positive cells. Indeed, IHC analysis revealed the presence of very rare Tom⁺ qNSCs expressing PDGFR α protein in both miR-17~92 control and deleted mice. However, no Tom⁺ aNSCs and TACs were found immunopositive for PDGFR α in control mice. In contrast, deletion of miR-17~92 led to appearance of Tom⁺ PDGFR α ⁺ aNSCs but especially Tom⁺ PDGFR α ⁺ TACs in the V-SVZ. Thus, this result shows that *Pdgfra* is an *in vivo* functional target of the miR-17~92 cluster.

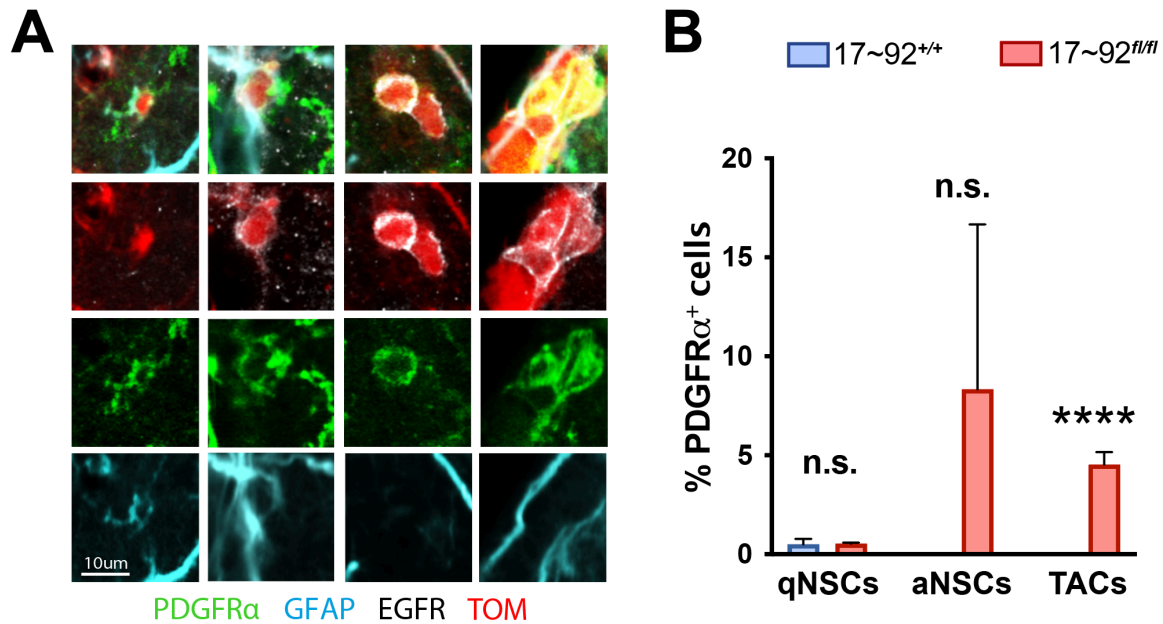


Figure 2.12 *Pdgfra* is a functional target of the miR-17~92 cluster *in vivo*

(A) Representative confocal images of Tom⁺ PDGFR α ⁺ cells found in the V-SVZ of miR-17~92 deleted mice. (B) Quantification of Tom⁺ PDGFR α ⁺ qNSCs, aNSCs and TACs at 1 dpi (n=3, n.s.: not significant, ****p<0.00001, two-tailed unpaired Student's t test, mean \pm SEM).

Conclusions

In this chapter, I have shown that all detectable members of the miR-17~92 cluster are expressed at low levels in qNSCs and are significantly upregulated in aNSCs and TACs in comparison to qNSCs. I have also shown that miR-17~92 guide and star forms are not equally expressed, with the guide forms of miR-19b, miR-20a and miR-92a being the most abundantly expressed miRNAs of the cluster in the profiled populations and the star forms of all the members of the cluster except miR-17 being extremely low and thus unlikely to play a key role in the control of the gene regulatory network of adult V-SVZ stem cells.

By quantifying an *in vitro* assay based on the plating of single FACS-purified aNSCs in adherent cultures, I have shown that conditional deletion of miR-17~92 reduced the

proliferation of adult neural stem cells but had no effect of their survival of short time points. Indeed, although a similar proportion of wells containing control and deleted NSCs was found, only miR-17~92 deleted NSCs exhibited a scarce proliferation and failed to give rise to large colonies.

After conditionally deleting miR-17~92 in adult NSCs *in vivo*, I have observed a smaller percentage of dividing NSCs (GFAP⁺ MCM2⁺) and cycling aNSCs (GFAP⁺ EGFR⁺ KI67⁺) at short time points confirming that the miR-17~92 cluster is essential for their proliferation. Interestingly, following a longer chase period from miR-17~92 deletion, the reduced percentage of aNSCs was coupled to an increase in the proportion of qNSCs indicating a role of the miR-17~92 cluster in stem cell activation. As a consequence of the activation and proliferation defects due to miR-17~92 deletion, I was able to detect LR-aNSCs only in miR-17~92 deleted mice. At long time points, I have also shown that miR-17~92 loss significantly reduced neurogenesis. Interestingly, although overall neurogenesis was decreased in the V-SVZ, deletion of the cluster increased the proportion of TBR2-expressing cells located in the dorsal V-SVZ, which likely correspond to glutamatergic neuronal progenitors.

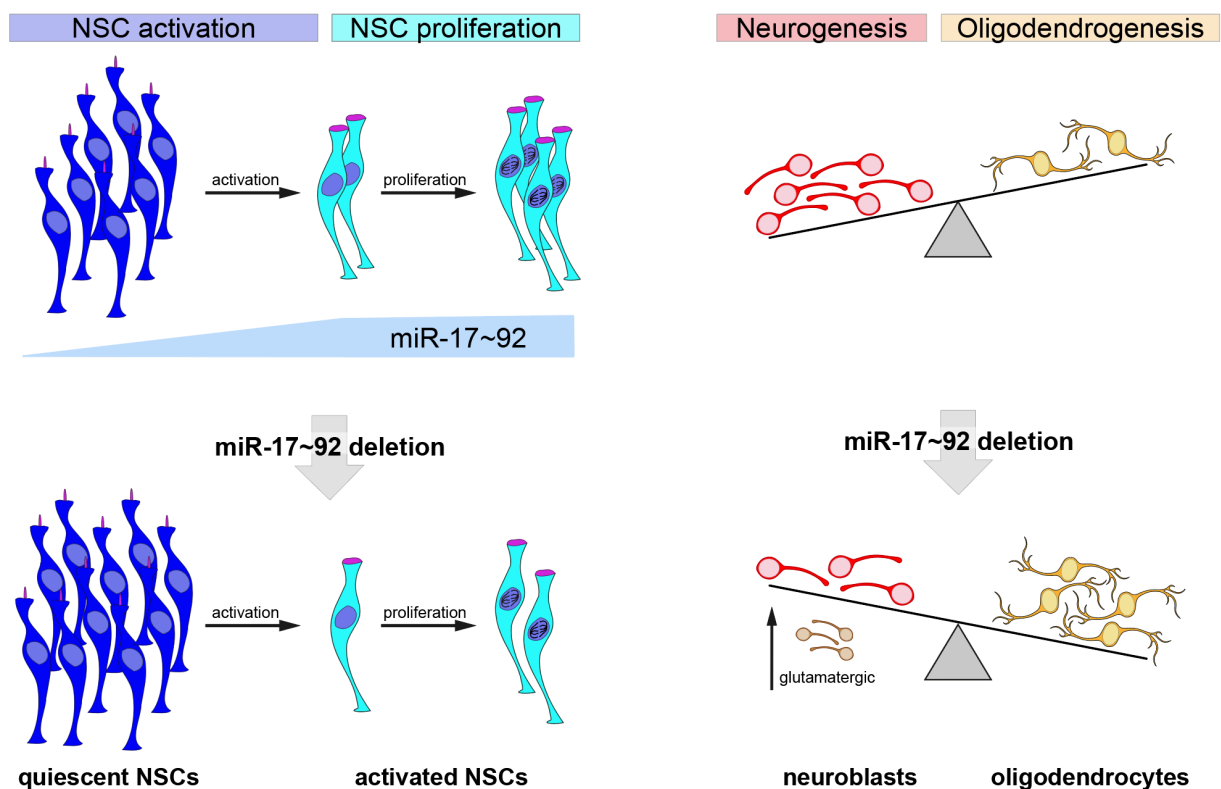


Figure 2.9 Summary of the pleiotropic functions of the miR-17~92 cluster in the V-SVZ

The miR-17~92 cluster is expressed at low levels in qNSCs and is upregulated upon activation. Deletion of miR-17~92 in NSCs *in vivo* reduces NSC activation and proliferation, and promotes oligodendrogenesis at the expense of neurogenesis, despite possibly increasing glutamatergic neuronal production.

Excitingly, my work also shows a role of the miR-17~92 cluster in regulating oligodendrogenesis (Fig. 2.9). Following miR-17~92 deletion, I have found an increase in oligodendrogenesis in the V-SVZ, *corpus callosum* and *septum*, with more mature oligodendrocytes in the *corpus callosum* but not in the *septum*, and more OPCs in the *septum* but not in the *corpus callosum*. Importantly, this increased oligodendrogenesis was due to an expansion of oligodendrogenic TACs.

Finally, by performing pathway analysis of computationally predicted miR-17~92 targets expressed in FACS-purified NSC populations I have identified a gene category related to oligodendrogenesis. Among the targets enriched in this category, I have validated the Platelet-Derived Growth Factor Receptor α (PDGFR α), a regulator of oligodendrocyte generation, as miR-17~92 functional target by luciferase reporter assay and *in vivo* analysis of PDGFR α protein expression in miR-17~92 control and deleted mice.

Materials and Methods

FACS-purification strategy

The V-SVZs from 3-4 month old mice were dissected from heterozygous hGFAP::GFP mice (Jackson Labs) or wildtype CD-1 mice (Charles River), digested with papain (Worthington, 1,200 units per 5 mice, 10 min at 37°C) in PIPES solution [120 mM NaCl, 5 mM KCl, 50 mM PIPES (Sigma), 0.6% glucose, 1X Antibiotic/Antimycotic (Gibco), and phenol red (Sigma) in water, pH adjusted to 7.6] and mechanically dissociated to single cells after adding ovomucoid (Worthington, 0.7 mg per 5 mice) and DNase (Worthington, 1,000 units per 5 mice). Cells were centrifuged for 10 min at 4°C without brake in 22% Percoll (Sigma) to remove myelin. Cell stainings were done in 3 steps: First, cells were incubated for 20 min with PE-conjugated rat anti-mCD24 (1:500; BD Pharmingen) and biotinylated rat anti-mCD133 (1:300, clone 13A4, eBioscience). Cells were washed by centrifugation at 1300rpm for 5min. Next, cells were incubated for 10 min with Streptavidin PE-Cy7 (1:500; eBioscience), and washed by centrifugation. Finally, cells were incubated with A647-complexed EGF (1:300; Molecular Probes) for 15 min, and washed by centrifugation. All stainings and washes were carried out on ice in 1% BSA, 0.1% Glucose HBSS solution. To assess cell viability, 4',6-diamidino-2-phenylindole (DAPI; 1:1000; Sigma) was added to the cell suspension. All cell populations were isolated in a single sort using a Becton Dickinson FACS Aria II using 13 psi pressure and 100- μ m nozzle aperture and were collected in Neurosphere medium (NSM) [DMEM/F12 (Life Technologies) supplemented with 0.6% Glucose (Sigma), 1X HEPES (Life Technologies), 1X Insulin-Selenium-Transferrin (Life Technologies), N-2 (Life Technologies), and B-27

supplement (Life Technologies)]. Gates were set manually using single-color control samples and FMO controls. Data were analyzed with FlowJo 9.3 data analysis software and displayed using bi-exponential scaling.

qPCR analysis of miRNA expression

RNA from FACS-purified populations was extracted from a miR-rich fraction using the miRNeasy kit as described in Codega et al., 2014. miR-rich cDNA was then generated using the Exiqon miRCURY LNA Universal RT microRNA kit. qPCR for the guide and star forms of all six members of the miR-17~92 cluster was performed using Exiqon miRCURY LNA probes for the mature forms of the miRs, in accordance with the LNA probes. Data were normalized to miR-16-5p expression and analyzed by the $2^{-\Delta\Delta CT}$ method (Livak & Schmittgen, 2001).

Mice breeding and usage for miR-17~92 *in vitro* deletion experiments

CAGG-CreERT2^{+/-}; miR-17~92^{fl/fl} mice were a generous gift from Jun-An Chen of the Wichterle lab. These were then bred to ROSA (ACTB-tdTomato,-EGFP^{+/+}) mice to generate CAGG-CreERT2^{+/-} or ^{-/-}; miR-17~92^{fl/fl}; ROSA (ACTB-tdTomato,-EGFP^{+/+}) mice. These mice express tdTomato before recombination, and eGFP afterwards, allowing tracking of recombination.

Sort Strategy for *in vitro* assays

CAGG-CreERT2^{+/-} or ^{-/-}; miR-17~92^{fl/fl}; ROSA (ACTB-tdTomato,-EGFP^{+/+}) mice were processed for FACS as in Codega et al. and stained with CD24-FITC (1:1000; BD Pharmingen), EGF-Alexa647 (1:300; Molecular Probes), and biotinylated rat anti-mCD133 (1:300, clone 13A4, eBioscience), which was followed by secondary staining with PE-Cy7-conjugated streptavidin (1:1000; eBioscience).

Single cell adherent assay

For single cell assays, one cell per well was manually plated into 96 well plates previously coated with Poly-D-Lysine (Sigma, 10 μ g/ml) and Fibronectin (Sigma, 2 μ g/ml). During the first 24 hours after plating, cells were treated with NSM + EGF, NSM + EGF + 250nM 4OHT, or NSM + EGF + vehicle (EtOH). At 24 hours, the entire media was replaced with NSM + EGF to prevent toxicity. Wells were fixed with 4% paraformaldehyde (PFA) in 0.1M phosphate buffer (PB) at 13 days post plating and stained with 4',6-Diamidino-2-Phenylindole

Dihydrochloride (DAPI, Sigma). Finally, the number of cells per well was quantified to assess changes in activation, proliferation and survival of adult neural stem cells. Two-sided Wilcoxon rank sum test was used to look at overall changes in the distribution of the outcomes (given number of cells per well), followed by Fisher's exact test, to later identify which of the outcomes was responsible for the difference.

Mice breeding and usage for miR-17~92 deletion *in vivo*

miR-17~92fl/fl mice were a generous gift from the Jeker lab (University of Basel). miR-17~92 fl/fl were crossed to GFAP-CreERT2^{+/+} mice and R26R lslTomato^{+/+} mice to generate GFAP-CreERT2^{+/+}; miR-17~92^{+/+} or fl/fl; R26R lslTomato^{+/+} mice.

Tamoxifen and BrdU injections

Cre-mediated recombination in CreER^{T2} transgenic mice was induced by administration of Tamoxifen (Sigma) dissolved at 30 mg/ml in 90% corn oil, 10% ethanol (Sigma). Mice were intraperitoneally injected at the dose of 120 mg/Kg once per day for three consecutive days and sacrificed at one and thirty days ending tamoxifen injections. To identify possible label-retaining (LR) cells in the V-SVZ, 5-bromo-2'-deoxyuridine (BrdU, 50 mg/kg, Sigma) was co-administered every 12 hours on the last two days of Tmx injections.

Tissue preparation for immunohistochemistry

Mice were anesthetized by intraperitoneal injection of pentobarbital (Escornarkon) and were sacrificed by intracardial perfusion of 4% paraformaldehyde (PFA) in 0.1M phosphate buffer (PB). Brains were extracted from the skull and post-fixed overnight. Coronal sections were cut at 25µm using a vibratome (Leica VT1000S).

Immunostaining

Tissue sections were incubated in blocking solution (PBS with 10% donkey normal serum and 0.03% Triton-X100 for antibodies against receptors or 0.3% Triton-X100 for all others) for 60 minutes and then incubated in primary antibodies in blocking solution for 36 hours at 4°C. After washing, sections were incubated with secondary antibodies for 1 hour at room temperature. After washing, sections were counterstained with 4',6-Diamidino-2-Phenylindole Dihydrochloride (DAPI, Sigma). Sections were mounted on slides with FluorSaveTM (Millipore Corporation).

Antibodies

The following primary antibodies were used: anti-BrdU (rat, 1:400, abcam); anti-doublecortin, DCX (goat, 1:100, Santa Cruz); anti-DsRed (rabbit, 1:500, Clontech); anti-EGFR (goat, 1:100, R&D); anti-EGFR (rabbit, 1:100, abcam); anti-GFAP (rat, 1:1000, Invitrogen); anti-Ki67 (rabbit, 1:100, abcam); anti-MCM2 (rabbit, 1:100, Cell signaling); anti-NG2 (rabbit, 1:100, Millipore); anti-OLIG2 (rabbit, 1:100, Millipore); anti-OLIG2 (goat, 1:150, R&D); goat anti-PDGFR α (1:100, R&D); anti-TBR2 (rabbit, 1:1000, abcam). The following secondary antibodies were used: Alexa Fluor-conjugated (405, 1:250, abcam; 488, 647, 568, 1:600, Molecular probes), Cy3-conjugated (1:1000, Jackson ImmunoResearch).

Brain section imaging and analysis

Tile scan imaging of the entire dorsoventral extent of the V-SVZ at least four different rostro-caudal levels (Bregmas: ~1mm, ~0.70mm, ~0.3mm and ~0mm) were taken on a Zeiss 880 confocal microscope with a 1.5 μ m distance between focal planes. Images were opened in FIJI and all Tom⁺ cells were quantified using the Cell Counter plug-in. For each rostro-caudal level, cell percentages of different cell populations over total Tom⁺ cells were calculated. These cell percentages were averaged and the average value from control and deleted mice were then compared to identify statistically significant differences in cell populations using unpaired two-tailed Student's t-test.

Bioinformatic analysis of miRNA-mRNA interactions in the early V-SVZ NSC lineage

A list of genes expressed in early stages of the lineage was compiled from gene expression datasets of FACS-purified V-SVZ NSC populations (PDGFR β ⁺ CD133⁺, PDGFR β ⁺ EGFR⁺ and EGFR⁺) (Delgado et al., 2019). Computationally predicted targets for the guide and star forms of individual members of the miR-17~92 cluster (miR-17, 18a, 19a, 20a, 19b, 92a and miR-17*) were generated from the online platforms Targetscan, PicTar, microcosm and miRDB. The gene expression list and miR target list were then compared to find overlap. Finally, the resulting list of miR-17~92 targets was analyzed using MetaCore (Thompson Reuters, New York, NY) performing enrichment analysis by pathway maps.

Luciferase reporter and miRNA expression constructs

A 1'791 nucleotide fragment of the *Pdgfra* 3'UTR, encompassing all four binding sites for members of the miR-17~92 cluster, was amplified from mouse genomic DNA by PCR using

the forward primer 5'-GTCTGTGACTTTTAAGGATGC-3' and reverse primer 5'-CCACACCACCATGTTGGGAAC-3' (Microsynth) and cloned into psiCHECK™-2 vector from Promega at the XhoI/NotI restriction sites (In-Fusion HD cloning kit, Clontech Laboratories). Psi-CHECK-2-pten 3'UTR and psi-CHECK2-hoxa5 3'UTR were generously provided by Jun-An Chen. All constructs were sequenced (Microsynth). To generate miR-17~92 expression construct, the entire miR-17~92 cluster sequence was amplified from the pKO-II-miR-17~92 vector (Addgene) by qPCR using the forward primer 5'-GCTGTAATTGATGTTTGTGAC -3' and the reverse primer 5'-ATCCCGTTTTACACCAACG -3', and cloned into the pSR-GFP expression vector (Cheng et al., 2009) at the HindIII/XhoI restriction sites (In-Fusion HD cloning kit, Clontech Laboratories).

Luciferase reporter assay

HEK293 cells were plated at a density of 9×10^5 cells in poly-L-lysine pre-coated 48-well plates, expanded for 18h, and transfected with 62.5 ng luciferase reporter and 187.5 ng miRNA vector (1:3 ratio) using 0.5 μ L of PLUS Reagent and 1 μ L of Lipofectamine 3000 (Life Technology). Cells were incubated with lipofectamine-DNA complexes for 24h prior to change medium containing lipofectamine with fresh medium. Transfected HEK293 were grown for additional 24 hours before performing luciferase assay. Finally, cells were lysed and processed for luciferase assays using the Dual-Luciferase Reporter Assay System (Promega). Luciferase activity was measured using the TECAN Spark Plate Reader. The ratio between renilla and firefly luciferase activities was calculated for all luciferase reporters. The data were then normalized to the respective miRNA empty vector conditions. All luciferase activity data are presented as means \pm SEM of values from three experiments, each performed in duplicates.

Chapter 3: Potential miR-17~92 targets for stem cell activation: *Slpr1* and *Pdgfrβ*

miRNAs are a class of small non-coding RNA molecules able to sculpt cell transcriptomes by targeting hundreds of mRNAs simultaneously, either repressing their translation or promoting their degradation (O'Brien et al., 2018). Since the interaction of miRNAs with their target genes is dynamic and dependent on several factors, including the abundance and affinity of miRNAs and their target mRNA transcripts, miRNAs can exert distinct functions depending on the cell type, or cellular transcriptional profile, in which they are expressed (O'Brien et al., 2018).

In Chapter 2, I have shown that the miR-17~92 cluster, whose expression is upregulated in aNSCs and TACs in comparison to qNSCs, regulates multiple aspects of NSC behavior including stem cell activation, proliferation, neurogenesis and oligodendrogenesis. In addition, I focused on miR-17~92 targets involved in oligodendrogenesis and I validated *Pdgfrα* as miR-17~92 functional target *in vivo*.

In this chapter, I perform bioinformatic analysis of predicted miR-17~92 targets upregulated in qNSCs versus aNSCs, and identify the Sphingosine-1-phosphate Receptor 1 (S1PR1) and the Platelet-Derived Growth Factor Receptor β (PDGFRβ) as potential targets of the miR-17~92 cluster for neural stem cell activation.

Results

Bioinformatic analysis of miRNA-mRNA interactions in the early V-SVZ NSC lineage

microRNAs repress the expression of target mRNA transcripts through a combination of translational repression and mRNA destabilization, with mRNA destabilization being the predominant mode of action of mammalian miRNAs, accounting for most (66% to 90%) of the miRNA-mediated silencing (Eichhorn et al., 2014). Since the mRNA destabilization mechanism results not only in the reduction of the final gene product, i.e. protein, but also in a measurable decrease in the amount of the targeted mRNA, I used gene expression datasets generated in the lab to focus on genes upregulated in qNSCs versus aNSCs in my search for potential miR-17~92 targets involved in stem cell activation.

Specifically, to identify potential candidate genes regulated by the miR-17~92 cluster, I performed the following bioinformatic analysis. I first used different on-line available algorithms (Targetscan, PicTar, microcosm, miRDB, TarBase) to compile a list of all predicted mRNA targets of individual members of the cluster. I then analyzed the expression of these mRNAs against a list of genes upregulated at least 1.5-fold in qNSCs over aNSCs. Among the targets identified by this analysis, genes related to cell adhesion, like *Ncam1*, *Vcam1* and

Tspan9, and lipid metabolism, such as *Crot* and *Elovl5*, as well as the G protein-coupled receptor *S1pr1* appeared particularly interesting as these gene categories have been shown to be enriched in quiescent stem cells across different compartments (Codega et al., 2014) (Fig. 3.1). Moreover, functional analysis showed that cell adhesion positively regulates stemness of embryonic and postnatal NSCs and that the cell adhesion molecule VCAM1 is a key regulator of NSC quiescence in the adult V-SVZ (Kokovay et al., 2012). In addition to the candidate targets above, *Dkk3* (Dickkopf WNT Signaling Pathway Inhibitor 3) and *Pdgfr β* also drew my attention since the former has been reported to play tumor suppressor roles (Gondkar et al., 2019) whereas the latter has been found to maintain the quiescent state of adult neural stem cells (Delgado et al., bioRxiv, 2019). As cell adhesion molecules and receptors are relatively easier to study than enzymes or soluble factors due to their localization at the cell surface, I focused on *Ncam1*, *Vcam1*, *Tspan9*, *S1pr1* and *Pdgfr β* for subsequent analysis.

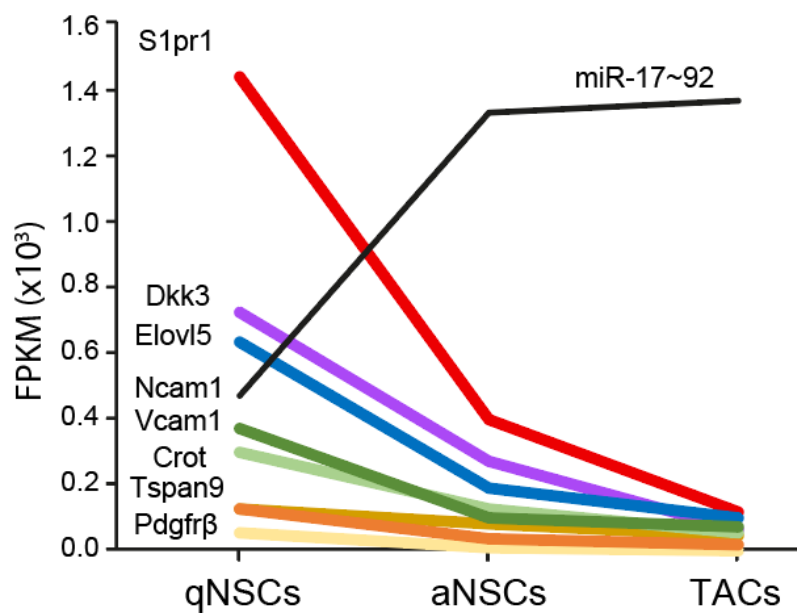


Figure 3.1 Bioinformatic analysis identifies miR-17~92 targets upregulated in qNSCs versus aNSCs

Expression pattern of selected miR-17~92 candidate targets (colored lines) along the early NSC lineage. Relative expression of target genes is estimated in FPKM. Black line represents the relative expression of the miR-17~92 cluster across qNSCs, aNSCs and TACs defined using Taqman low density array (TLDA) data.

The miR-17~92 cluster regulates the expression of *S1pr1*, *Pdgfr β* and *Ncam1*

To assess whether the miR-17~92 cluster can suppress the expression of the aforementioned candidate genes, I performed luciferase assays overexpressing luciferase reporters containing fragments of the 3'UTR or CDS of *Ncam1*, *Vcam1*, *Tspan9*, *S1pr1* or *Pdgfr β* together with a vector encoding the whole miR-17~92 cluster. Compared to the empty

luciferase reporter, I observed a robust reduction in luciferase activity for the luciferase reporter containing the 3'UTR of the validated miR-17~92 target *Pten* but not for the luciferase reporter containing the 3'UTR of *Hoxa5*, which is not a miR-17~92 target. Interestingly, I detected an equally marked decrease in luciferase activity for the *S1pr1* luciferase reporter and to a lesser extent for the luciferase reporters bearing the proximal CDS sequences of *Pdgfrβ* and *Ncam1*, but not for the other luciferase reporters. Thus, this result indicates that the miR-17~92 cluster represses the expression of *S1pr1*, *Pdgfrβ* and *Ncam1* (Fig. 3.2).

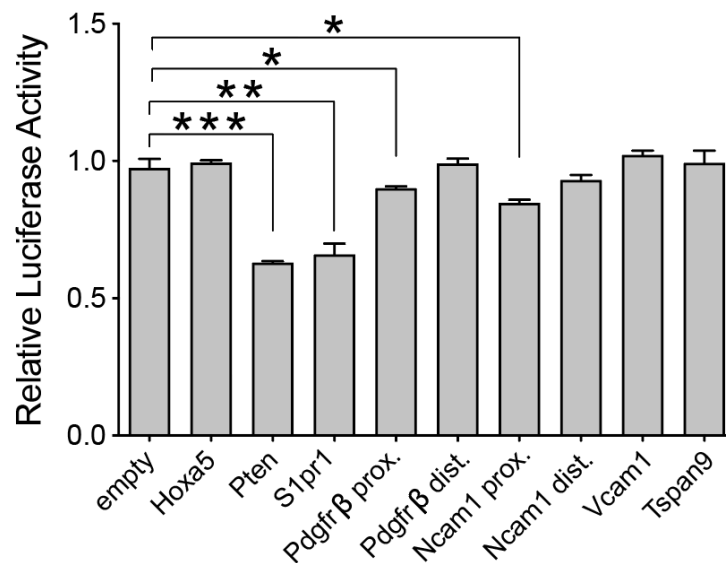


Figure 3.2 miR-17~92 downregulates the expression of *S1pr1*, *Pdgfrβ* and *Ncam1*

Luciferase reporter assay validating *S1pr1*, *Pdgfrβ* and *Ncam1* as biochemical miR-17~92 targets. Empty: blank luciferase reporter, *Hoxa5*: non-targeted negative control, *Pten*: validated positive control (Tun et al., 2015). Dist.: distal gene sequence, prox.: proximal gene sequence. (n=3, *p<0.05, **p<0.01, ***p<0.001, two-tailed unpaired Student's t test, mean ± SEM).

Of these three potential miR-17~92 targets for stem cell activation, I focused on *S1pr1* and *Pdgfrβ* for *in vivo* analysis since the former has already been reported to be an *in vivo* functional miR-17~92 target in the immune (Xu et al., 2015) and cardiovascular systems (Guzzolino et al., 2018) and the latter has been found by our group to maintain the quiescent state of adult neural stem cell *in vivo* (Delgado et al., bioRxiv, 2019). Moreover, these two receptors have also been shown to interact with each other within a protein complex (reviewed in Delcourt et al., 2007). Lastly, the S1PR1 ligand, Sphingosine-1-phosphate (S1P), was found by our group to reduce the activation of qNSCs (Codega et al., 2014). Thus, *S1pr1* and *Pdgfrβ* appear promising potential miR-17~92 targets for stem cell activation.

Characterization of S1PR1 expression and distribution in the V-SVZ

To characterize which cells express S1PR1 protein in the V-SVZ, I performed immunohistochemistry analysis in CD1 and gfapGFP mice for markers of the SVZ lineage as well as niche cell types. S1PR1 was highly expressed in the V-SVZ (Fig. 3.3) but also in parenchymal cells. Based on gfapGFP and S100 β staining, S1PR1 was predominantly found in astrocytes (Fig. 3.3 A and B). In addition, it was expressed in some CD13⁺ pericytes (Fig. 3.3 C) and IBA1⁺ microglia (Fig. 3.3 D) in both the V-SVZ and parenchyma.

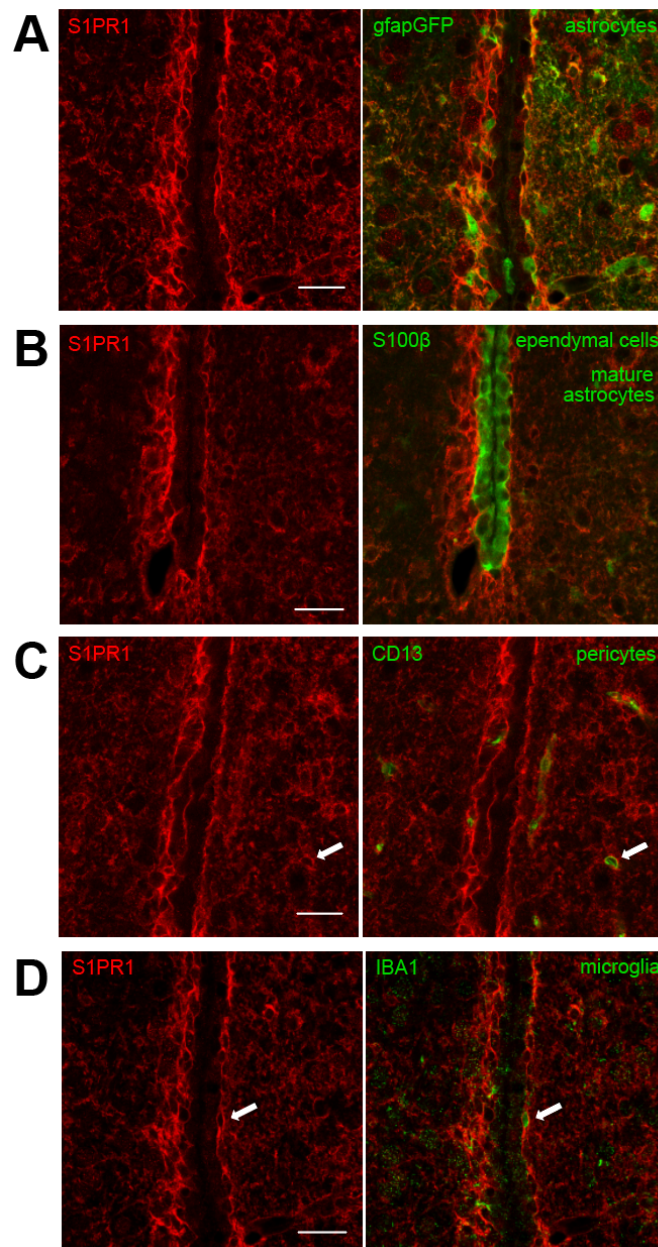


Figure 3.3 S1PR1 is highly expressed in V-SVZ

Representative confocal images (A-D) of S1PR1 expression and distribution in cell populations in the V-SVZ of gfapGFP and CD1 mice. (A) gfapGFP cells, (B) S100 β ependymal cells and mature astrocytes, (C) CD13 pericytes, (D) IBA1 microglia. Scale bar, 25 μ m.

In ependymal cells, labeled by S100 β , S1PR1 was expressed at low levels and in the nucleus rather than at the cell surface (Fig. 3.3 B).

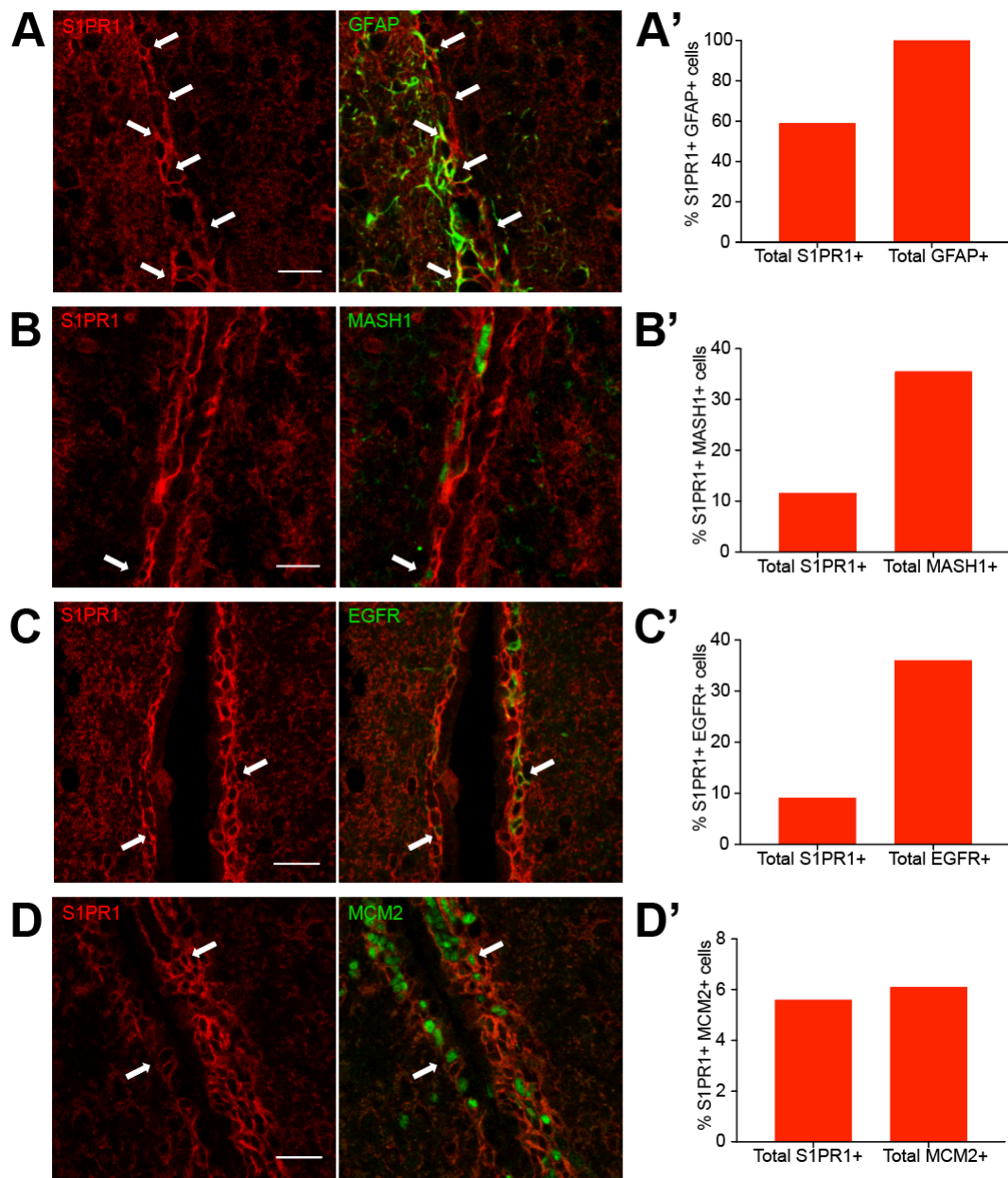


Figure 3.4 Quantification of S1PR1-expressing cells in different cell types in the V-SVZ

Representative confocal images (A-D) and quantification (A'-D') of S1PR1 co-positive cells in the V-SVZ of *gfapGFP* mice. (A) GFAP cells, (B) MASH1 aNSCs and TACs, (C) EGFR aNSCs and TACs, (D) MCM2 dividing cells. Scale bar, 25 μ m.

I then looked in more details at which cells in the lineage expressed S1PR1. All GFAP⁺ cells (100% of GFAP⁺ cells, ~50% of S1PR1⁺ cells) (Fig. 3.4 A and A') and almost all *gfapGFP* cells (~90% of *gfapGFP*, ~70% of S1PR1⁺ cells) were immunopositive for S1PR1 in the V-SVZ. As revealed by immunostaining for EGFR and MASH1, which are expressed by both

aNSCs and TACs, S1PR1 was found in ~35% of MASH1⁺ or EGFR⁺ cells (~10% of S1PR1⁺ cells) (Fig. 3.4 B, B', C and C'). The majority of S1PR1⁺ cells were not dividing. Indeed, S1PR1 was found in only 6% of MCM2⁺ proliferating cells corresponding to ~6% of S1PR1⁺ cells (Fig. 3.4 D and D'). Finally, S1PR1 was not expressed in DCX⁺ neuroblasts in the V-SVZ (Fig. 3.6 A).

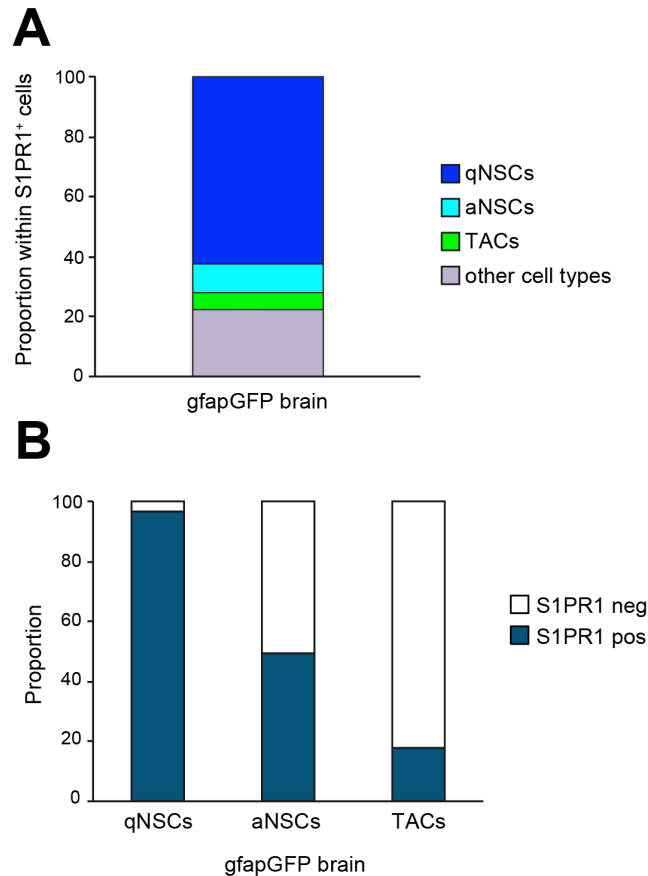


Figure 3.5 S1PR1 expression in neural stem cell lineage in the V-SVZ

(A-B) Stacked plots representing proportions of V-SVZ cell types within the S1PR1⁺ population (C) and the fractions of S1PR1 positive and negative cells within qNSCs, aNSCs and TACs (D). S1PR1 protein was not detected in neuroblasts. These analyses were carried out on gfapGFP brains.

As MASH1 and EGFR are expressed by both aNSCs and TACs, to better dissect S1PR1 expression in the early lineage I co-immunostained for S1PR1, GFAP and EGFR to discriminate qNSCs, aNSCs and TACs. IHC analysis revealed that most of the S1PR1⁺ cells (~60%) in the V-SVZ corresponded to qNSCs (Fig. 3.5 A) and that the proportion of S1PR1-expressing cells progressively decreased as cells transitioned down the lineage (Fig. 3.5 B), with neuroblasts being immunonegative for S1PR1 protein. Therefore, within the adult V-SVZ lineage, S1PR1 is mainly expressed in NSCs which are largely quiescent and is down-regulated as cells progress down the lineage.

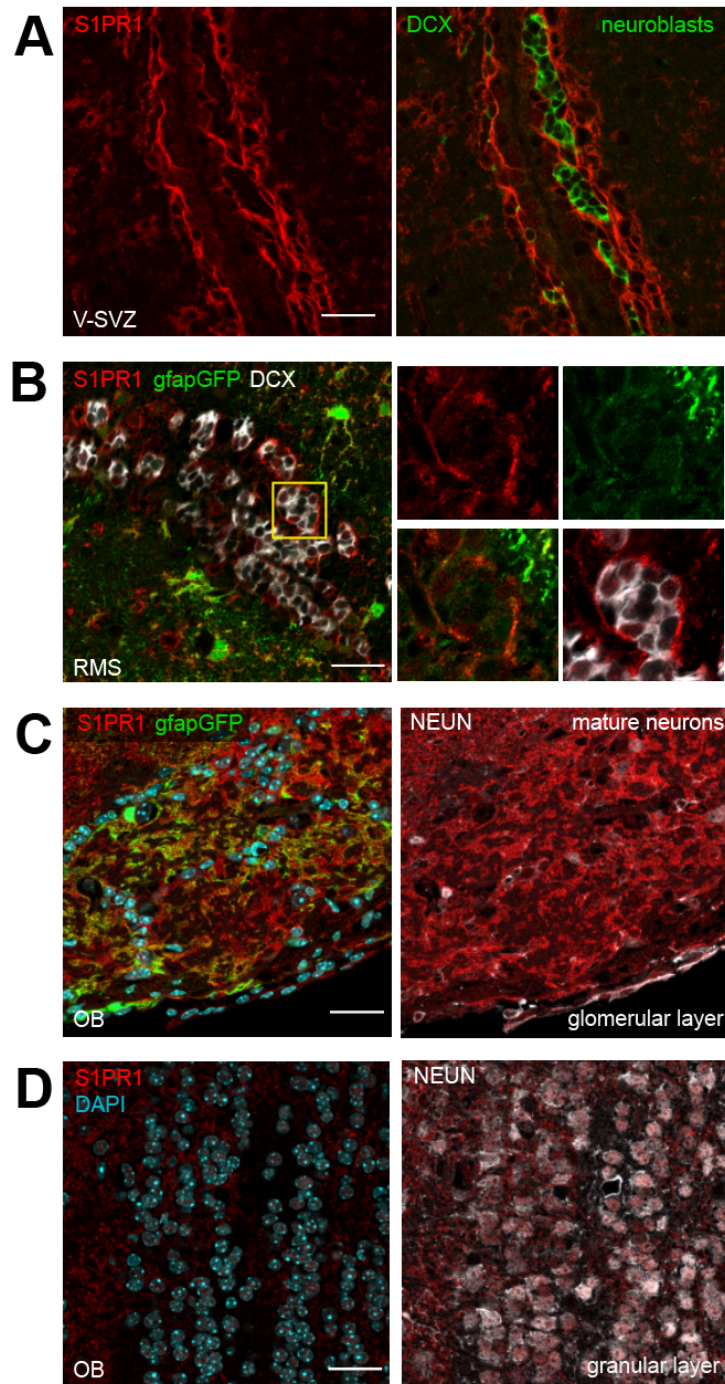


Figure 3.6 S1PR1 exhibits cell membrane and nuclear distribution across different cell types

Representative confocal images (A-G) of S1PR1 expression and distribution in cell populations in the V-SVZ (A, B, C, E), RMS (G) and OB (D, F) of *gfapGFP* mice. Scale bar, 25 μ m.

Interestingly, a second burst of S1PR1 expression was detected in the RMS (Fig. 3.6 B) and OB (Fig 3.6 C and D) where both migrating neuroblasts and mature neurons exhibited nuclear S1PR1 protein rather than expression of this receptor at their cell surface as in the cell types described above.

S1PR1 and PDGFR β are co-expressed in quiescent neural stem cells

Work in the Doetsch laboratory has shown that PDGFR β is expressed in the adult V-SVZ lineage *in vivo*. Indeed, by immunostaining with lineage markers, PDGFR β protein was found to be highly expressed in radial quiescent NSCs and in some activated NSCs, whose EGFR expression anti-correlated with that of PDGFR β , but not in transit amplifying cells or neuroblasts (Delgado et al., bioRxiv, 2019) (Fig 3.7 C). Moreover, PDGFR β protein had different localization along the dorsoventral axis of the V-SVZ. PDGFR β was distributed along the entire plasma membrane of NSCs in the dorsal V-SVZ (including the apical processes) but was only located in the apical processes of NSCs in the ventral V-SVZ (Fig. 3.7 A and B).

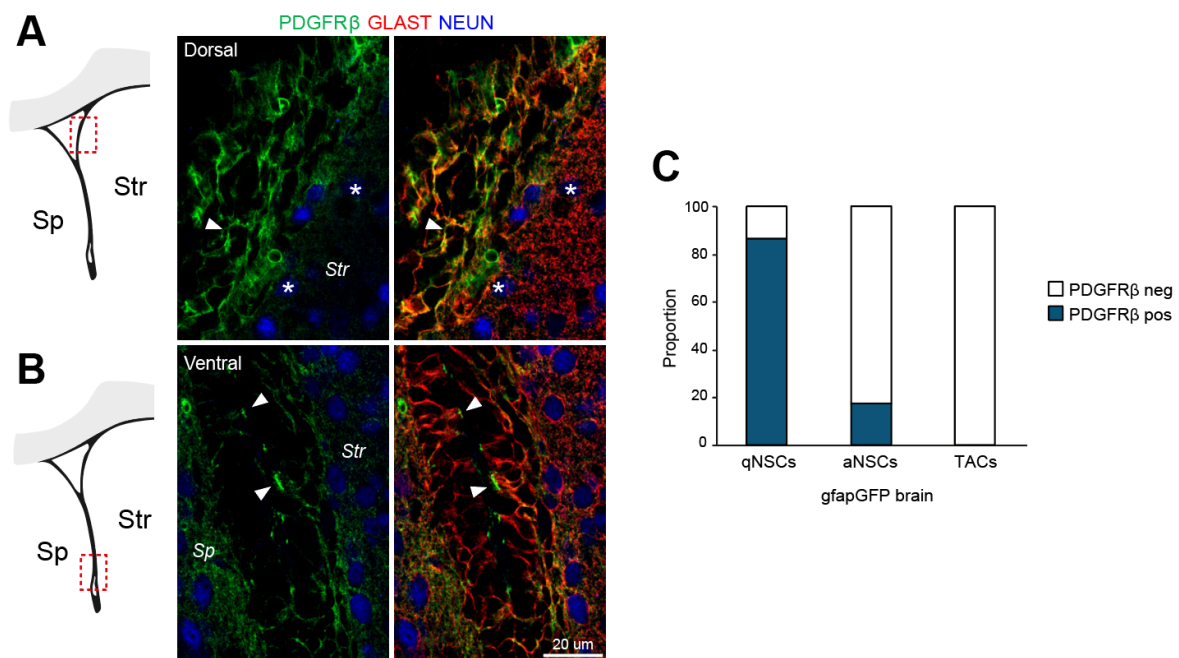


Figure 3.7 PDGFR β expression and protein distribution in the V-SVZ neural stem cell lineage

(A-B) Representative confocal images of PDGFR β distribution in the dorsal (A) and ventral (B) adult V-SVZ of CD1 mice. Images kindly provided by Ana Delgado. Scale bars: 20 μ m. (C) Stacked plots representing proportions of PDGFR β positive and negative cells within qNSCs, aNSCs and TACs in gfapGFP mice.

S1PR1 and PDGFR β can interact within a protein complex in airway smooth muscle cells (reviewed in Delcourt et al., 2007). I therefore performed co-immunostaining of S1PR1 and PDGFR β and found that they overlapped in the V-SVZ. However, while all PDGFR β ⁺ cells were co-labeled by S1PR1, some S1PR1⁺ cells, likely corresponding to TACs, were not immunopositive for PDGFR β . Thus, S1PR1 and PDGFR β are mostly co-expressed by quiescent NSCs and need to be downregulated for cells to progress down the lineage (Fig. 3.8).

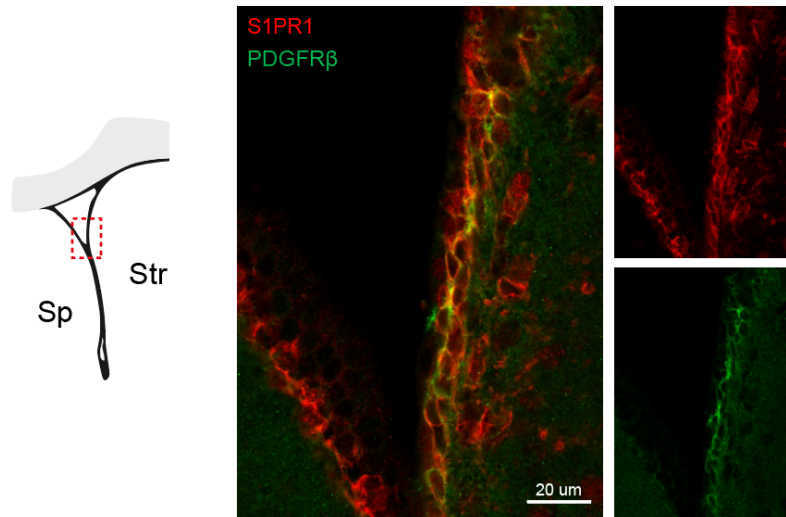


Figure 3.8 S1PR1 and PDGFRβ overlap in the adult V-SVZ

Representative confocal images showing co-expression of S1PR1 and PDGFRβ in the adult V-SVZ. Scale bars: 20 μm.

Finally, to define if *S1pr1* and *Pdgfrβ* are *in vivo* targets of the cluster, I performed immunohistochemistry analysis of S1PR1 and PDGFRβ protein expression and distribution in the early neural stem cell lineage in miR-17~92 control and deleted mice by co-immunostaining for EGFR.

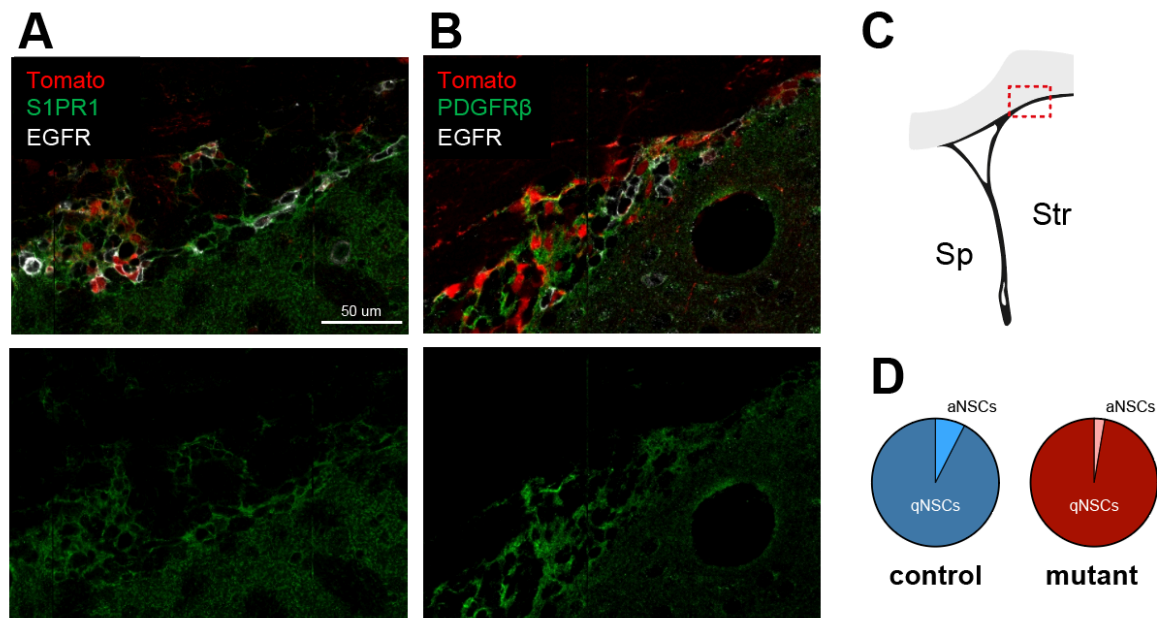


Figure 3.9 Analysis of S1PR1 and PDGFRβ distribution after deleting miR-17~92 *in vivo*

(A-B) Representative confocal images of S1PR1 and PDGFRβ protein distribution in the dorsal V-SVZ [red dotted box in V-SVZ schema in (C)] of miR-17~92 deleted mice. (D) miR-17~92 deletion reduces the proportion over total Tom of aNSCs. Scale bars: 20 μm.

If *Slpr1* and *Pdgfrβ* are functional targets of miR-17~92, deletion of the cluster is expected to expand the proportion of S1PR1⁺/EGFR⁺ cells and PDGFRβ⁺/EGFR⁺ cells. However, the complex staining pattern of these two receptors, especially of PDGFRβ, and the very limited number of aNSCs occurring after deleting miR-17~92 made the quantification of S1PR1⁺ and PDGFRβ⁺ cells extremely difficult, thereby precluding their validation as miR-17~92 functional target *in vivo* (Fig. 3.9).

Conclusions

In this chapter, I have performed bioinformatic analysis of predicted miR-17~92 targets upregulated in qNSCs versus aNSCs, and I have identified a set of target genes potentially regulated by miR-17~92 for neural stem cell activation. By luciferase reporter assay, I have shown that the expression of some of these genes, including *Slpr1*, *Pdgfrβ* and *Ncam1*, is regulated by the miR-17~92 cluster. I have focused on *Slpr1* and *Pdgfrβ* for *in vivo* analysis since the former has already been reported an *in vivo* functional miR-17~92 target in the immune (Xu et al., 2014) and cardiovascular systems (Guzzolino et al., 2018) and the latter has been found by our group to maintain the quiescent state of adult neural stem cell *in vivo* (Delgado et al., bioRxiv, 2019). As S1PR1 and PDGFRβ proteins are highly expressed by qNSCs and the proportion of S1PR1- and PDGFRβ- expressing cells progressively decreases as cells transitioned down the lineage these receptors are attractive miR-17~92 targets in the regulation of stem cell activation. However, their validation as miR-17~92 functional target *in vivo* remains open.

Materials and Methods

Bioinformatic analysis of miRNA-mRNA interactions in the early V-SVZ NSC lineage

A list of genes enriched at least 1.5- fold in qNSCs versus aNSCs was compiled from gene expression datasets of V-SVZ populations (Delgado et al, bioRxiv 2019). In parallel, computationally predicted targets for guide and star forms of individual members of the miR-17~92 cluster (miR-17, 18a, 19a, 20a, 19b, 92a and miR-17*) were downloaded from online available platforms including Targetscan, PicTar, microcosm, miRDB and TarBase. The gene expression list and miR target list were then compared to find overlap. Finally, the resulting list of miR-17~92 targets expressed in the V-SVZ populations was manually screened to identify potential targets for stem cell activation.

Luciferase reporter and miRNA expression constructs

Fragments of the CDS of *Ncam1*, *Vcam1*, *Tspan9* and *Pdgfrβ*, encompassing binding sites for members of the miR-17~92 cluster, were amplified by PCR from the cDNA derived from NIH3T3 cells. *Slpr1* 3'UTR was amplified by qPCR from the GeneCopoeia luciferase vector MmiT026983-MT01. PCR products were then cloned into psiCHECK™-2 vector from Promega at the XhoI/NotI restriction sites (In-Fusion HD cloning kit, Clontech Laboratories). Psi-CHECK-2-pten 3'UTR and psi-CHECK2-hoxa5 3'UTR were generously provided by Jun-An Chen. All constructs were sequenced (Microsynth).

To generate miR-17~92 expression construct, the entire miR-17~92 cluster sequence was amplified by qPCR from the pKO-II-miR-17~92 vector (Addgene) and cloned into the pSR-GFP expression vector (Cheng et al., 2009) at the HindIII/XhoI restriction sites (In-Fusion HD cloning kit, Clontech Laboratories).

Sequences of primers are as follows: *Ncam1* proximal CDS: F: 5'-CAGTTTACAATGCTGCGAAC-3', R: 5'-CATTACACGATGCTCTGTCTG-3'; *Ncam1* distal CDS: F: 5'-TGAAACCTGAGACGAGGTAC-3', R: 5'-CTGTACTTGACCAGATAGTG-3'; *Vcam1*: F: 5'-ACAGCCTCTTTATGTCAACG-3', R: 5'-GGAGAGACTTGGATAATCAG-3'; *Tspan9*: F: 5'-GTACGACGCCTGAGGCTGCG-3', R: 5'-GGCATCTTTGGCAAGTCTGC-3'; *Pdgfrβ* proximal CDS: F: 5'-GTCCGTGTTATGGCTCCTGG-3', R: 5'-CCTGGAGGCTGTAGACGTAG-3'; *Pdgfrβ* distal CDS: F: 5'-GGCAAGCTGGTCAAGATCTG-3', R: 5'-GCTTGTGGCAGTGTAGCTGC-3'; *Slpr1*: F: 5'-AAGCTGTTGATACTGAGGGAAGC-3', R: 5'-CAGTTTATTAATGTTTAAAAGTTG-3'; miR-17~92: F: 5'-GCTGTAATTGATGTTTGTGAC-3', R: 5'-ATCCCGTTTTACACACCAACG-3'.

Luciferase reporter assay

HEK293 cells were plated at a density of 9×10^5 cells in poly-L-lysine pre-coated 48-well plates, expanded for 18h, and transfected with 62.5 ng luciferase reporter and 187.5 ng miRNA vector (1:3 ratio) using 0.5 μ L of PLUS Reagent and 1 μ L of Lipofectamine 3000 (Life Technology). Cells were incubated with lipofectamine-DNA complexes for 24h prior to change medium containing lipofectamine with fresh medium. Transfected HEK293 were grown for additional 24 hours before performing luciferase assay. Finally, cells were lysed and processed for luciferase assays using the Dual-Luciferase Reporter Assay System (Promega). Luciferase activity was measured using the TECAN Spark Plate Reader. The ratio between renilla and firefly luciferase activities was calculated for all luciferase reporters. The data were then

normalized to the respective miRNA empty vector conditions. All luciferase activity data are presented as means \pm SEM of values from three experiments, each performed in duplicates.

Analysis of S1PR1 and PDGFR β expression *in vivo*

Adult CD1, gfap::GFP and GFAP-CreERT2^{+/+}; miR-17~92^{+/+} or ^{fl/fl}; R26R lslTomato^{+/+} mice, aged 3-4 months, were used in this study. Cre-mediated recombination in CreERT² transgenic mice was induced by administration of Tamoxifen (Sigma) dissolved at 30 mg/ml in 90% corn oil, 10% ethanol (Sigma). Specifically, mice were intraperitoneally injected at the dose of 120 mg/Kg once per day for three consecutive days and sacrificed 24h after tamoxifen injections. All mice were intracardially perfused with 4% paraformaldehyde (PFA) in 0.1M phosphate buffer (PB). Brains were extracted from the skull and post-fixed overnight. Coronal sections were cut at 25 μ m using a vibratome (Leica VT1000S). These sections were then stained with the following primary antibodies: anti-CD13 (rat, 1:100, abcam); anti-DCX (goat, 1:100, Santa Cruz); anti-EGFR (goat, 1:100, R&D); anti-GFAP (rat, 1:1000, Invitrogen); anti-GFAP (chicken, 1:600, Millipore); anti-GFP (goat, 1:500, Rockland); anti-GFP (rat, 1:500, Nacalai Tesque, Inc); anti-GLAST (guinea pig, 1:1000, Chemicon); anti-IBA1 (goat, 1:200, abcam); anti-MASH1 (mouse, 1:50, R&D); anti-MCM2 (rabbit, 1:100, Cell signaling); anti-NeuN (mouse, 1:100, Millipore); anti-PDGFR β (goat, 1:100, R&D); anti-S100 β (mouse, 1:100, sigma) and anti-S1PR1 (rabbit, 1:50, Santa Cruz). Alexa Fluor-conjugated (488, 647, 1:600, Molecular probes) and Cy3-conjugated (1:1000, Jackson ImmunoResearch) were used as secondary antibodies. Sections were imaged on Zeiss 700 confocal microscope and quantified in FIJI using the Cell Counter plug-in.

Chapter 4: Discussion and future directions

Over the course of this dissertation, I have shown that the proto-oncogenic miR-17~92 cluster is highly upregulated in activated NSCs and TACs in comparison to quiescent NSCs, and that it plays important roles beyond the control of cell proliferation. Indeed, my work shows that miR-17~92 is involved in NSC activation, proliferation and neurogenesis. Moreover, it also regulates oligodendrogenesis and possibly glutamatergic neuronal production through the repression of *Pdgfra* and *Tbr2* respectively, with *Pdgfra* being identified and validated as miR-17~92 functional target for the first time in this dissertation.

miR-17~92 expression in the V-SVZ NSC lineage

The miR-17~92 cluster encodes six distinct miRNAs (miR-17, -18a, -19a and b, -20a, -92a) that can be grouped into four families based on seed sequence homology (Concepcion et al., 2012). Here, I performed qPCR measurement of miR-17~92 members in FACS-purified populations of qNSCs, aNSCs and TACs. Interestingly, through analysis of the relative abundance of miR-17~92 guide and star members to the housekeeping miRNA miR-16-5p, I found that not all cluster members are equally expressed and that the guide forms of miR-19b, miR-20a and miR-92a are the most represented miRNAs of the cluster in the profiled populations. The observation that the expression levels of mature miRNAs do not necessarily correlate with those of their pri-miRNAs is not surprising and it has already been reported in other studies (Obernosterer et al., 2006; Wulczyn et al., 2007; Thomson et al., 2006). Indeed, since miRNA biogenesis occurs in a multiple step process, distinct members of the miR-17~92 cluster can be individually and uniquely regulated beyond transcription (Concepcion et al., 2012). Intriguingly, although the individual members of the cluster are expressed at different levels within a given cell type, they exhibit a comparable ratio across the profiled populations suggesting that the individual members of the miR-17~92 cluster are processed with similar efficiencies or that they display similar stabilities in the early neural stem lineage.

Through an allelic series of genetically engineered mice harboring selective targeted deletions of individual members of the miR-17~92 cluster, recent work has shown the coexistence of functional cooperation and specialization among cluster members. Perinatal lethality, cardiac defects and lung hypoplasia only occurred when the whole miR-17~92 cluster was deleted, demonstrating a functional cooperation of all cluster members. In contrast, axial patterning defects, as well as the oncogenic activity of the cluster in Myc-driven tumors, were examples of functional specialization of miR-17 and miR-19, respectively (Han et al, 2015). In the future, it will be important to dissect whether specific members of the miR-17~92 cluster

are responsible for the different aspects of the phenotype I observed following miR-17~92 deletion in adult V-SVZ NSCs. It will also be important to test the expression of miR-17~92 in V-SVZ-derived neuroblasts and OPCs.

miR-17~92 underlies neural stem cell activation and proliferation

Several miRNAs have been implicated in the maintenance of stem cell quiescence but so far no study has shown that miRNAs can underlie stem cell activation (Katz et al., 2016; Sato et al., 2014; Cheung et al., 2012; Baghdadi et al., 2018). By performing immunohistochemistry analysis at long time points (one month) after miR-17~92 conditional deletion, I have shown that endogenous miRNAs can be involved in stem cell activation *in vivo*. miR-17~92 deletion increased the proportion of qNSCs and reduced the percentage of aNSCs showing that ablation of the cluster in NSCs impaired their activation causing a shift, within the NSC pool, towards more quiescent NSCs and fewer aNSCs. The higher proportion of qNSCs in deleted mice also suggest that in addition to defects in stem cell activation, loss of the cluster could promote the return of NSCs to the quiescent state, a transition already observed in both V-SVZ and SGZ niches *in vivo* (Basak et al., 2018; Urban et al., 2016). This idea is further supported by the appearance of LR- aNSCs only in miR-17~92 deleted mice at long time points suggesting that aNSCs that initially entered cell cycle reverted back to a quiescent or ‘resting’ state without down-regulating EGFR expression. To date, no studies have so far addressed whether LR-NSCs retain expression of EGFR. Another hypothesis is that LR-aNSCs lacking miR-17~92 expression failed to divide. By conditionally deleting miR-17~92 in NSCs *in vitro* and *in vivo*, I have shown that the miR-17~92 cluster also plays a critical role in supporting the proliferation of adult neural stem cells. Compared to their wild type counterparts, miR-17~92 deleted NSCs *in vitro* exhibited a scarce proliferation and failed to give rise to large colonies while *in vivo*, miR-17~92 deletion at short time points resulted in a reduced percentage of dividing NSCs and cycling aNSCs. The pro-proliferation function of the cluster is in line with previous reports showing that miR-17~92 promotes cell proliferation and survival in the hematopoietic system as well as in cancers (Mavrakis et al., 2010; Mu et al., 2009; Olive et al., 2009; Ventura et al., 2008). Although miR-17~92 also acted in a pro-survival manner in these contexts, I did not observe any defects in survival in miR-17~92 deleted NSCs *in vitro*. Thus, it is possible that miR-17~92 is not important for the survival of neural stem cells or that it plays a pro-survival function at longer time points or at later stages in the V-SVZ lineage, such as in newly generated neurons, as was shown during the development of limb innervating motor neurons (Tung et al., 2015).

One of the best characterized direct transcriptional activators of the miR-17~92 cluster is Myc (O'Donnell et al., 2005; de Pontual et al., 2011; Liu et al., 2013). Interestingly, Myc has been shown to control a gene regulatory network, including miR-22, that underlies the transition from quiescence to proliferation of primary human fibroblasts *in vitro* (Polioudakis et al., 2013). It would therefore be exciting to determine whether miR-22 is co-expressed, together with miR-17~92, by activating qNSCs and if it might functionally cooperate with miR-17~92 to promote NSC activation and proliferation in the adult V-SVZ.

Since quiescent NSCs exhibit a similar transcriptome to cortical astrocytes, it would be also exciting to determine whether miR-17~92 overexpression, either using a viral approach or by means of conditionally inducible mice, might induce astrocytes in non-neurogenic brain regions to become actively dividing and generate neuronal or glial progeny.

Recently, in the context of brain metastasis, astrocytes were found to secrete exosomes enriched for miR-19a that, upon uptake by cancer cells, led to the recruitment of IBA⁺ myeloid cells to further support cancer cell proliferation and survival (Zhang et al., 2015). Although this work highlights a possible cell non-autonomous function for the miR-17~92 cluster, quantification of total V-SVZ qNSCs, aNSCs, TACs and NBs (both Tomato positive or negative) at 1dpi did not reveal changes in Tomato negative cells suggesting that miR-17~92 acts in a cell-autonomous manner under normal conditions in adult NSCs.

miR-17~92 regulates neurogenesis and oligodendrogenesis *in vivo*

In the developing forebrain, miR-17~92 regulates the neurogenic-to-gliogenic transition by promoting neurogenesis and inhibiting astrocytogenesis through the silencing of *p38* (Naka-Kaneda et al., 2014) and *Bmpr2* (Mao et al., 2014). Indeed, an increase in GFAP⁺ astrocytes concomitant with a reduction in TuJ1⁺ neurons was found in both studies after miR-17~92 deletion *in vitro*. In the adult brain, I observed that V-SVZ neurogenesis was decreased one month following miR-17~92 deletion *in vivo*. A comparable drop in neurogenesis after deletion of miR-17~92 was also described in the adult hippocampus (Jin et al., 2016; Pan et al., 2019). However, these studies on hippocampal neurogenesis did not address how deletion of the cluster affected individual stages of the lineage. According to the data presented here the reduction in neurogenesis following miR-17~92 loss, at least in the V-SVZ, is likely due to a reduction in stem cell activation and divisions, as well as to a possible change in fate specification of NSCs. However, it is still unclear whether the decrease in adult neurogenesis observed following miR-17~92 deletion may in part also be due to neuroblast proliferation and survival.

miR-17~92 is expressed by OPCs during embryonic development (Budde et al., 2010). However, no studies have so far investigated whether miR-17~92 deletion in NSCs might affect oligodendrogenesis. Here, I have shown, for the first time, that deletion of the cluster in V-SVZ NSCs *in vivo* increased oligodendrogenesis in the V-SVZ, *corpus callosum* and *septum*. In line with previous work showing that SVZ-derived OLs are generated through TACs (Menn et al., 2006), the increased oligodendrogenesis I found in miR-17~92 deleted mice was caused by an expansion of oligodendrogenic TACs. However, due to the concomitant reduction in aNSC proportion following miR-17~92 deletion, it remains unclear whether the increased oligodendrogenesis triggered by miR-17~92 loss is initiated in a subset of aNSCs or in TACs themselves. Interestingly, oligodendrogenic TACs were distributed throughout the V-SVZ niche but especially enriched in the intermediate and dorsal regions, which are emerging as the most oligodendrogenic aspects of the adult V-SVZ (Ortega et al., 2013; Delgado et al., bioRxiv 2019). Since only approximately one third of the recombined TACs were affected by miR-17~92 deletion, it might be that the cluster is not broadly expressed throughout the V-SVZ but rather displays a restricted expression in specific domains of the niche. This idea is further supported by the fact that most of the phenotype observed after miR-17~92 loss is more pronounced in the dorsal V-SVZ. *In situ* hybridization experiments will therefore be key to define the spatial expression of the miR-17~92 cluster members and determine whether individual mature miRNAs of the cluster might be differentially distributed along the V-SVZ. Moreover, it would be interesting to assess whether loss of cluster in NSCs can increase oligodendrogenesis *in vitro* in differentiation assays. Recently, Delgado et al. identified a novel population of intraventricular OPCs bathed by the cerebrospinal fluid (CSF) and in contact with supraependymal axons from distant brain regions (Delgado et al., bioRxiv, 2019). In the future, it will be important to assess whether miR-17~92 deletion *in vivo* also affects this cell population. Finally, it would be also interesting to assess changes in astrocytogenesis *in vivo* following miR-17~92 deletion. This could be done, for instance, by immunostaining for Glutamine Synthetase (GS) and Olig2 to quantify GS⁺ OLIG2⁻ astrocytes in the septal wall of the V-SVZ and in the *septum*, which have recently been described to be the regions where astrocytes likely arise from and migrate to (Delgado et al., bioRxiv, 2019).

miR-17~92 targets for neural stem cell activation and fate specification

Slpr1 and *Pdgfrβ* are potential targets of miR-17~92 for stem cell activation

NSC quiescence is an actively maintained state (Codega et al., 2014). While a direct role for PDGFRβ in neural stem cell quiescence has recently been shown (Delgado et al.,

bioRxiv, 2019), treatment of FACS-purified NSCs with the S1PR1 physiological ligand, S1P, suggested a similar function for this latter receptor. Indeed, S1P was found to inhibit the activation of qNSCs indicating that S1PR1 might actively maintain the quiescent state of NSCs (Codega et al., 2014). During my thesis work, I have identified *Slpr1* and *Pdgfr β* as potential genes regulated by miR-17~92 for stem cell activation. I have shown that both genes are downregulated by miR-17~92 in luciferase assays and that, *in vivo*, both receptors were co-expressed by V-SVZ NSCs that were largely quiescent. Importantly, within the neurogenic lineage, I have shown that the proportion of S1PR1- and PDGFR β - expressing cells decreases as NSCs transition down the lineage. However, while PDGFR β expression was only retained by few aNSCs, S1PR1 expression was also found in some TACs. Together, these results suggest that both receptors are co-expressed in qNSCs and need to be downregulated for NSC to become activated and generate progeny. Unfortunately, the complex staining patterns of S1PR1 and especially of PDGFR β , as well as the very limited number of aNSCs after miR-17~92 deletion precluded their validation as miR-17~92 functional targets *in vivo*. In the future, one could test if they are functional targets by performing immunostaining analysis of S1PR1 and PDGFR β expression in FACS-sorted NSCs *in vitro* following transfection of miR-17~92 AgomiRs or AntagomiRs or conditional genetic deletion. Furthermore, to more globally identify miR-17~92 targets *in vivo*, RNASeq and Mass Spec analyses using FACS-sorted cells from control and miR-17~92 deleted mice would provide a powerful approach to identify individual targets or pathways involved in a specific cellular transition at a large scale.

The miR-17~92 target Tbr2 promotes glutamatergic neuronal production

Expression of the transcription factor *Tbr2* in radial glial cells (RGCs) during neocortex development is a critical step underlying the transition from RGCs into intermediate progenitors (IPs), one of the two types of progenitor cells, together with RGCs, for glutamatergic, pyramidal-projection neurons (Englund et al., 2005). The same *Tbr2*-mediated specification of glutamatergic neuronal progenitors also occurs, in the adult V-SVZ, in a small subset of dorsally located NSCs retaining the expression of this transcription factor (TF) (Brill et al., 2009). However, adult-born glutamatergic neurons are destined for the olfactory bulb, and differentiate into cortical neurons only in the context of cerebral cortex lesion (Brill et al., 2009). *Tbr2* has been validated as a miR-17~92 functional target in the developing neocortex where deletion of the cluster, through derepression of this TF, resulted in a premature transition of radial glial cells (RGCs) into intermediate progenitors (IPs). My results show that miR-17~92 also regulates *Tbr2* expression in the adult V-SVZ. miR-17~92 deletion in adult NSCs *in vivo*

increased the proportion of TBR2-expressing cells but did not expand their distribution in the V-SVZ suggesting that *Tbr2* expression might only be initiated in dorsal V-SVZ cells unlike Pax6, whose dorsally restricted protein expression becomes extended to the whole dorsoventral extent of the V-SVZ upon deletion of its targeting miRNA miR-7a (De Chevigny et al., 2012). A next important step is to determine whether the increased proportion of TBR2-expressing cells in the V-SVZ results in an increase in glutamatergic neuronal production in the OB. This could be tested by quantifying changes in GABAergic and glutamatergic neurons in the OB of miR-17~92 control and deleted mice by immunostaining for GAD65 (or 67) and VGLUT2 respectively.

The oligodendrogenesis regulator Pdgfra is a functional target of miR-17~92

Here, I have shown that one of the major phenotypes triggered by conditional deletion of miR-17~92 in NSCs *in vivo* is an increased oligodendrogenesis in the V-SVZ, *corpus callosum* and *septum*, due to an expansion of oligodendrogenic TACs. These functional data were complemented by the identification, through bioinformatic analysis, of an oligodendrocyte-related pathway among the gene categories enriched for miR-17~92 targets, and the validation of *Pdgfra* as miR-17~92 functional target by luciferase reporter assay and *in vivo* analysis. *Pdgfra* is, indeed, a key regulator of oligodendrocyte generation. In the brain, *Pdgfra* is highly expressed by parenchymal and V-SVZ OPCs and, together with its ligand PDGF-A, promotes oligodendrocyte formation by supporting OPC proliferation and survival, and preventing their premature differentiation (Menn et al., 2006; Barres et al., 1992; Nishiyama et al., 2009; Noble et al., 1988; Pringle et al., 1992). PDGF-A deletion resulted in ablation of PDGFR α ⁺ cells and subsequent loss of oligodendrocytes and myelin, indicating that PDGFR α -expressing cells are the main source of oligodendrocytes throughout the brain (Fruttiger et al., 1999). In the future, to more robustly establish a functional link between miR-17~92 and *Pdgfra*, one could perform immunostaining analysis of PDGFR α expression after conditionally deleting miR-17~92 in NSCs *in vitro*. Using a lentiviral approach, it will be also interesting to manipulate the expression of miR-17~92 or *Pdgfra* in cultured cells, and perform rescue experiments.

Final conclusions

One important question still open in the field is whether individual NSCs with tri- or bi-lineage potential exist in the adult V-SVZ *in vivo*. Fate mapping has shown that V-SVZ NSCs can give rise to neurons, oligodendrocytes and astrocytes (reviewed in Chaker et al., 2016).

However, it is still unclear whether all NSCs *in vivo* are tri-potent or whether they are restricted to neuronal or glial lineages. *In vitro*, both multipotent and unipotent NSCs were detected after culturing single FACS-purified cells or time-lapse imaging of individual cells suggesting that NSCs with different potencies might coexist within the same niche (Codega et al., 2014; Ortega et al., 2013). One hypothesis could be that NSCs are progressively restricted in their lineage potential during development to become unipotent NSCs in the adult V-SVZ. Another hypothesis is that adult NSCs are intrinsically tri- or bi-potent and their multipotency is constitutively repressed by niche signals. Since the data presented here show a shift in the balance between neurogenesis and oligodendrogenesis following miR-17~92 deletion, it is tempting to speculate that the miR-17~92 cluster might be a critical regulator of NSC potency. Moreover, miR-17~92 might spatially segregate neurogenic and oligodendrogenic lineages according to a potential regional expression of the cluster itself. Indeed, as already mentioned above, most of the phenotype observed after deleting miR-17~92 was found to be more pronounced in specific domains of niche, including the intermediate and dorsal regions of the V-SVZ, suggesting that the expression of the miR-17~92 cluster might be spatially restricted.

In addition to the heterogeneity of NSCs, TACs have also been shown to be heterogeneous with respect to their cell cycle dynamics and transcriptional signatures (Ponti et al., 2013; Azim et al., 2015). Interestingly, my work further provides important evidence of the cellular diversity within the TAC population. Indeed, my work suggests that at least three subpopulations of TACs might exist in the adult V-SVZ. These include oligodendrogenic and neurogenic TACs, with neurogenic progenitors further subdivided into GABAergic and glutamatergic progenitors. In the future, it will be interesting to dissect whether the heterogeneity of TACs is intrinsically inherited by the NSCs they arise from or if it stems from additional regulators coming into play once TACs are generated.

Finally, the data in this dissertation uncover an additional layer of cell intrinsic regulation of adult NSC behavior highlighting novel functions of the miR-17~92 cluster in adult NSC activation and oligodendrogenesis. Importantly, my work provides the first evidence that miRNAs are involved in the transition from adult neural stem cell quiescence to activation. As such, exploring the gene regulatory network regulated by the miR-17~92 cluster could therefore provide insights into pathways that might prove pivotal to harness or fine-tuning adult neural stem cells for brain repair after injury, stroke, or onset of neurodegenerative disorder, either controlling neuronal production or oligodendrogenesis. Moreover, since overexpression of the miR-17~92 cluster is often associated with the onset of brain tumors, including neuroblastoma

and medulloblastoma (Concepcion et al., 2012), my work might also suggest which cells in the adult brain might give rise to tumor-initiating cells during neoplastic transformation.

Acknowledgements

Heartful thank to:

Valerie Crotet, my dear Zia Val, for starting just as a colleague and ending up being family, as well as for her professional and technical help with cloning and ISH exps;

Ana Delgado for sharing her broad experience on the field but especially for always being ready to help, professionally and personally;

Violeta Silva-Vargas for the stimulating professional and personal discussions, for making me see the silver lining of the darkest situations;

Zayna Chaker for her constructive feedback and frank opinions, for being a model of professionalism;

Thomas von Känel for his ability to fix almost everything in Illustrator and for helping me represent what I meant;

Other members of the Doetsch, Scheiffele and Tan labs for being generous with their time, ideas, reagents and friendship;

People from the IMFC facility, especially Kai Schleicher, and FACS facility, Janine Bögli and Stella Stefanova, for their important support with imaging and cell sorting;

Annina DeLeo for starting this exciting project;

My thesis committee, Drs. Peter Schiffele and Joerg Betschinger, for their invaluable insights;

and Dr. Fiona Doetsch for taking me into her lab and giving me the chance to work on this project in the first place, as well as for teaching me to be critical with the data and always be open to alternative interpretations.

References

- Aguirre A., Rizvi T.A., Ratner N., Gallo V. (2005). Overexpression of the epidermal growth factor receptor confers migratory properties to nonmigratory postnatal neural progenitors. *J Neurosci.* 25 (48):11092-106.
- Akerblom M., Petri R., Sachdeva R., Klussendorf T., Mattsson B., Gentner B. et al. (2014). microRNA-125 distinguishes developmentally generated and adult-born olfactory bulb interneurons. *Development* 141, 1580-1588.
- Altman J. (1962a). Are New Neurons Formed in the Brains of Adult Mammals? *Science*, 135 (3509), 1127–1128. <http://doi.org/10.1126/science.135.3509.1127>
- Altman J. (1962b). Autoradiographic study of degenerative and regenerative proliferation of neuroglia cells with tritiated thymidine. *Experimental Neurology*, 6 (2), 142–151. [http://doi.org/10.1016/0014-4886\(62\)90084-5](http://doi.org/10.1016/0014-4886(62)90084-5)
- Altman J. (1963). Autoradiographic investigation of cell proliferation in the brains of rats and cats. *The Anatomical Record*, 145, 573–591.
- Altman J. (1969). Autoradiographic and histological studies of postnatal neurogenesis. IV. Cell proliferation and migration in the anterior forebrain, with special reference to persisting neurogenesis in the olfactory bulb. *The Journal of Comparative Neurology*, 137 (4), 433–457. <http://doi.org/10.1002/cne.901370404>
- Altman J., & Chorover S. L. (1963). Autoradiographic investigation of the distribution and utilization of intraventricularly injected adenine-3h, uracil-3h and thymidine-3h in the brains of cats. *The Journal of Physiology*, 169 (4), 770–779. [http://doi.org/10.1111/\(ISSN\)14697793](http://doi.org/10.1111/(ISSN)14697793)
- Altman J., & Das G. D. (1965). Autoradiographic and histological evidence of postnatal hippocampal neurogenesis in rats. *The Journal of Comparative Neurology*.
- Altman J., & Das G. D. (1966). Autoradiographic and histological studies of postnatal neurogenesis. I. A longitudinal investigation of the kinetics, migration and transformation of cells incorporating tritiated thymidine in neonate rats, with special reference to postnatal neurogenesis in some brain regions. *The Journal of Comparative Neurology*, 126 (3), 337-389. <http://doi.org/10.1002/cne.901260302>
- Augusto-Oliveira M., Arrifano G.P.F, Malva J.O., Crespo-Lopez M.E. (2019). Adult Hippocampal Neurogenesis in Different Taxonomic Groups: Possible Functional Similarities and Striking Controversies. *Cells*. 8 (2). pii: E125. doi: 10.3390/cells8020125.
- Arenz C. et al. (2014). miRNA Maturation. Springer Protocols. Humana Press.
- Azim K., Angonin D., Marcy G., Pieropan F., Rivera A., Donega V., Cantù C., Williams G., Berninger B., Butt A.M., Raineteau O. (2017). Pharmacogenomic identification of small molecules for lineage specific manipulation of subventricular zone germinal activity. *PLoS Biol.* 15 (3):e2000698. doi: 10.1371/journal.pbio.2000698.
- Azim K., Berninger B., Raineteau O. (2016). Mosaic Subventricular Origins of Forebrain Oligodendrogenesis. *Front Neurosci.* 10:107. doi: 10.3389/fnins.2016.00107.

- Azim K., Fischer B., Hurtado-Chong A., Draganova K., Cantù C., Zemke M., Sommer L., Butt A., Raineteau O. (2014). Persistent Wnt/ β -catenin signaling determines dorsalization of the postnatal subventricular zone and neural stem cell specification into oligodendrocytes and glutamatergic neurons. *Stem Cells*. 32 (5):1301-12. doi: 10.1002/stem.1639.
- Azim K., Hurtado-Chong A., Fischer B., Kumar N., Zweifel S., Taylor V., Raineteau O. (2015). Transcriptional Hallmarks of Heterogeneous Neural Stem Cell Niches of the Subventricular Zone. *Stem Cells*. 33 (7):2232-42. doi: 10.1002/stem.2017.
- Baghdadi M.B., Firmino J., Soni K., Evano B., Di Girolamo D., Mourikis P., Castel D., Tajbakhsh S. (2018). Notch-Induced miR-708 Antagonizes Satellite Cell Migration and Maintains Quiescence. *Cell Stem Cell*. 23 (6):859-868.e5. doi: 10.1016/j.stem.2018.09.017.
- Barman B., Bhattacharyya S.N. (2015). mRNA targeting to endoplasmic reticulum precedes ago protein interaction and microRNA (miRNA)-mediated translation repression in mammalian cells. *J Biol Chem*. 290:24650–6. doi: 10.1074/jbc.C115.661868
- Barres B.A., Hart I.K., Coles H.S., Burne J.F., Voyvodic J.T., Richardson W.D. and Raff M.C. (1992). Cell death and control of cell survival in the oligodendrocyte lineage. *Cell* 70, 31-46.
- Barrey E., Saint-Auret G., Bonnamy B., Damas D., Boyer O., Gidrol X. (2011). PremicroRNA and mature microRNA in human mitochondria. *PLoS ONE* 6:e20220. doi: 10.1371/journal.pone.0020220
- Basak O., Krieger T.G., Muraro M.J., Wiebrands K., Stange D.E., Frias-Aldeguer J., Rivron N.C., van de Wetering M., van Es J.H., van Oudenaarden A., Simons B.D., Clevers H. (2018). Troy⁺ brain stem cells cycle through quiescence and regulate their number by sensing niche occupancy. *Proc Natl Acad Sci U S A*. 115 (4):E610-E619. doi: 10.1073/pnas.1715911114.
- Baser A., Skabkin M., Kleber S., Dang Y., Gülcüler Balta G.S., Kalamakis G., Göpferich M., Ibañez D.C., Schefzik R., Lopez A.S., Bobadilla E.L., Schultz C., Fischer B., Martin-Villalba A. (2019). Onset of differentiation is post-transcriptionally controlled in adult neural stem cells. *Nature*. 566 (7742):100-104. doi: 10.1038/s41586-019-0888-x.
- Bergmann O., Spalding K.L., Frisén J. (2015). Adult Neurogenesis in Humans. *Cold Spring Harb Perspect Biol*. 7 (7):a018994. doi: 10.1101/cshperspect.a018994.
- Bian S., Hong J., Li Q., Schebelle L., Pollock A., Knauss J.L., Garg V., Sun T. (2013). MicroRNA cluster miR-17-92 regulates neural stem cell expansion and transition to intermediate progenitors in the developing mouse neocortex. *Cell Rep*. 3 (5):1398-1406. doi: 10.1016/j.celrep.2013.03.037.
- Bose M., Barman B., Goswami A., Bhattacharyya S.N. (2017). Spatiotemporal uncoupling of MicroRNA-mediated translational repression and target RNA degradation controls microRNP recycling in mammalian cells. *Mol Cell Biol*. 37:e00464–16. doi: 10.1128/MCB.00464-16
- Bracken C.P., Scott H.S., Goodall G.J. (2016). A network-biology perspective of microRNA function and dysfunction in cancer. *Nat Rev Genet*. 17 (12):719-732. doi: 10.1038/nrg.2016.134.

- Brett J.O., Renault V.M., Rafalski V.A., Webb A.E., Brunet A. (2011). The microRNA cluster miR-106bB25 regulates adult neural stem/progenitor cell proliferation and neuronal differentiation. *Aging (Albany NY)* 3, 108-124.
- Brill M.S., Ninkovic J., Winpenny E., Hodge R.D., Ozen I., Yang R., Lepier A., Gascón S., Erdelyi F., Szabo G., Parras C., Guillemot F., Frotscher M., Berninger B., Hevner R.F., Raineteau O., Götz M. (2009). Adult generation of glutamatergic olfactory bulb interneurons. *Nat Neurosci.* 12 (12):1524-33. doi: 10.1038/nn.2416.
- Budde H., Schmitt S., Fitzner D., Opitz L., Salinas-Riester G., Simons M. (2010). Control of oligodendroglial cell number by the miR-17-92 cluster. *Development.* 137 (13):2127-32. doi: 10.1242/dev.050633.
- Calaora, V., Chazal, G., Nielsen, P. J., Rougon, G., & Moreau, H. (1996). mCD24 expression in the developing mouse brain and in zones of secondary neurogenesis in the adult. *Nsc*, 73 (2), 581–594.
- Carraro G., El-Hashash A., Guidolin D., Tiozzo C., Turcatel G., Young B.M., De Langhe S.P., Bellusci S., Shi W., Parnigotto P.P., Warburton D. (2009). miR-17 family of microRNAs controls FGF10-mediated embryonic lung epithelial branching morphogenesis through MAPK14 and STAT3 regulation of E-Cadherin distribution. *Dev Biol.* 333(2):238-50. doi: 10.1016/j.ydbio.2009.06.020.
- Cebrián-Silla A., Alfaro-Cervelló C., Herranz-Pérez V., Kaneko N., Park D.H., Sawamoto K., Alvarez-Buylla A., Lim D.A., García-Verdugo J.M. (2017). Unique Organization of the Nuclear Envelope in the Post-natal Quiescent Neural Stem Cells. *Stem Cell Reports.* 9 (1):203-216. doi: 10.1016/j.stemcr.2017.05.024.
- Chaker Z., Codega P., Doetsch F. (2016). A mosaic world: puzzles revealed by adult neural stem cell heterogeneity. *Wiley Interdiscip Rev Dev Biol.* 5 (6):640-658. doi: 10.1002/wdev.248.
- Chen J., Huang Z. P., Seok H. Y., Ding J., Kataoka M., Zhang Z., et al. (2013). mir-17-92 Cluster Is Required for and Sufficient to Induce Cardiomyocyte Proliferation in Postnatal and Adult Hearts. *Circulation Research*, 112 (12), 1557–1566.
- Chen J.A., Huang Y.P., Mazzoni E.O., Tan G.C., Zavadil J., Wichterle H. (2011). Mir-17-3p controls spinal neural progenitor patterning by regulating Olig2/Irx3 cross-repressive loop. *Neuron.* 69 (4):721-35. doi: 10.1016/j.neuron.2011.01.014.
- Chen Y., Bian S., Zhang J., Zhang H., Tang B., Sun T. (2014). The Silencing Effect of microRNA miR-17 on p21 Maintains the Neural Progenitor Pool in the Developing Cerebral Cortex. *Front Neurol.* 5:132. doi: 10.3389/fneur.2014.00132.
- Cheng L.C., Pastrana E., Tavazoie M., Doetsch F. (2009). miR-124 regulates adult neurogenesis in the subventricular zone stem cell niche. *Nat. Neurosci.* 12, 399-408.
- Cheung T.H., Quach N.L., Charville G.W., Liu L., Park L., Edalati A., Yoo B., Hoang P., Rando T.A. (2012). Maintenance of muscle stem-cell quiescence by microRNA-489. *Nature.* 482 (7386):524-8. doi: 10.1038/nature10834.

- Chojnacki A., Mak G., Weiss S. (2011). PDGFR α expression distinguishes GFAP-expressing neural stem cells from PDGF-responsive neural precursors in the adult periventricular area. *J Neurosci.* 31 (26):9503-12. doi: 10.1523/JNEUROSCI.1531-11.2011.
- Codega P., Silva-Vargas V., Paul A., Maldonado-Soto A. R., DeLeo A. M., Pastrana E., & Doetsch F. (2014). Prospective Identification and Purification of Quiescent Adult Neural Stem Cells from Their In Vivo Niche. *Neuron*, 82 (3), 545–559.
- Codega P., Silva-Vargas V., Paul A., Maldonado-Soto A.R., Deleo A.M., Pastrana E., Doetsch F. (2014). Prospective identification and purification of quiescent adult neural stem cells from their in vivo niche. *Neuron*. 82(3):545-59. doi: 10.1016/j.neuron.2014.02.039.
- Concepcion C.P., Bonetti C., Ventura A. (2012). The microRNA-17-92 family of microRNA clusters in development and disease. *Cancer J.* 18 (3) :262-7. doi: 10.1097/PPO.0b013e318258b60a.
- Costa M.R., Ortega F., Brill M.S., Beckervordersandforth R., Petrone C., Schroeder T., Götz M., Berninger B. (2011). Continuous live imaging of adult neural stem cell division and lineage progression in vitro. *Development*. 138 (6):1057-68. doi: 10.1242/dev.061663.
- Đặng T.C., Ishii Y., Nguyen V., Yamamoto S., Hamashima T., Okuno N., Nguyen Q.L., Sang Y., Ohkawa N., Saitoh Y., Shehata M., Takakura N., Fujimori T., Inokuchi K., Mori H., Andrae J., Betsholtz C., Sasahara M. (2019). Powerful Homeostatic Control of Oligodendroglial Lineage by PDGFR α in Adult Brain. *Cell Rep.* 27 (4):1073-1089.e5. doi: 10.1016/j.celrep.2019.03.084.
- Daynac M., Chicheportiche A., Pineda J.R., Gauthier L.R., Boussin F.D., Mouthon M.-A. (2013). Quiescent neural stem cells exit dormancy upon alteration of GABAAR signaling following radiation damage. *Stem Cell Res.* 11:516–528.
- Daynac M., Morizur L., Chicheportiche A., Mouthon M.A., Boussin F.D. (2016). Age-related neurogenesis decline in the subventricular zone is associated with specific cell cycle regulation changes in activated neural stem cells. *Sci Rep.* 6:21505. doi: 10.1038/srep21505.
- De Chevigny A., Core N., Follert P., Gaudin M., Barbry P., Beclin C. et al. (2012a). miR-7a regulation of Pax6 controls spatial origin of forebrain dopaminergic neurons. *Nat. Neurosci.* 15, 1120-1126.
- de Faria O Jr., Cui Q.L., Bin J.M., Bull S.J., Kennedy T.E., Bar-Or A., Antel J.P., Colman D.R., Dhaunchak A.S. (2012). Regulation of miRNA 219 and miRNA Clusters 338 and 17-92 in Oligodendrocytes. *Front Genet.* 3:46. doi: 10.3389/fgene.2012.00046.
- de Pontual L., Yao E., Callier P., Faivre L., Drouin V., Cariou S., Van Haeringen A., Geneviève D., Goldenberg A. et al. (2011). Germline deletion of the miR-17~92 cluster causes skeletal and growth defects in humans. *Nat Genet.* 43 (10):1026-30. doi: 10.1038/ng.915.
- Delcourt N., Bockaert J., Marin P. (2007). GPCR-jacking: from a new route in RTK signalling to a new concept in GPCR activation. *Trends Pharmacol Sci.* 28 (12):602-7.
- Delgado A., Maldonado-Soto A., Silva-Vargas V., Mizrak D., von Känel T., Paul A., Madar A., Cuervo H., Kitajewski J., Lin C.-S., Doetsch F. (2019). Release of stem cells from quiescence reveals multiple gliogenic domains in the adult brain. *bioRxiv*. doi: <https://doi.org/10.1101/738013>

- Detzer A., Engel C., Wunsche W., Sczakiel G. (2011). Cell stress is related to re-localization of Argonaute 2 and to decreased RNA interference in human cells. *Nucleic Acids Res.* 39:2727–41. doi: 10.1093/nar/gkq1216
- Doetsch, F., & Alvarez-Buylla, A. (1996). Network of tangential pathways for neuronal migration in adult mammalian brain. *Proceedings of the National Academy of Sciences of the United States of America*, 93 (25), 14895–14900.
- Doetsch, F., Caillé, I., Lim, D. A., García-Verdugo, J. M., & Alvarez-Buylla, A. (1999a). Subventricular zone astrocytes are neural stem cells in the adult mammalian brain. *Cell*, 97 (6), 703–716.
- Doetsch, F., García-Verdugo, J. M., & Alvarez-Buylla, A. (1997). Cellular composition and three-dimensional organization of the subventricular germinal zone in the adult mammalian brain. *The Journal of Neuroscience*, 17 (13), 5046–5061.
- Doetsch, F., García-Verdugo, J. M., & Alvarez-Buylla, A. (1999b). Regeneration of a germinal layer in the adult mammalian brain. *Proceedings of the National Academy of Sciences of the United States of America*, 96 (20), 11619–11624.
- Doetsch, F., Petreanu, L., Caille, I., Garcia-Verdugo, J. M., & Alvarez-Buylla, A. (2002). EGF converts transit-amplifying neurogenic precursors in the adult brain into multipotent stem cells. *Neuron*, 36 (6), 1021–1034.
- Dulken B.W., Leeman D.S., Boutet S.C., Hebestreit K., Brunet A. (2017). Single-Cell Transcriptomic Analysis Defines Heterogeneity and Transcriptional Dynamics in the Adult Neural Stem Cell Lineage. *Cell Rep.* Jan 17;18(3):777-790. doi: 10.1016/j.celrep.2016.12.060.
- Eichhorn S.W., Guo H., McGeary S.E., Rodriguez-Mias R.A., Shin C., Baek D., Hsu S.H., Ghoshal K., Villén J., Bartel D.P. (2014). mRNA destabilization is the dominant effect of mammalian microRNAs by the time substantial repression ensues. *Mol Cell*. 56 (1):104-15. doi: 10.1016/j.molcel.2014.08.028. Epub 2014 Sep 25.
- Englund C., Fink A., Lau C., Pham D., Daza R.A., Bulfone A., Kowalczyk T., Hevner R.F. (2005). Pax6, Tbr2, and Tbr1 are expressed sequentially by radial glia, intermediate progenitor cells, and postmitotic neurons in developing neocortex. *J Neurosci*. 25(1):247-51.
- Fei J.F., Haffner C., Huttner W.B. (2014). 3' UTR-dependent, miR-92-mediated restriction of Tis21 expression maintains asymmetric neural stem cell division to ensure proper neocortex size. *Cell Rep.* 7 (2):398-411. doi: 10.1016/j.celrep.2014.03.033.
- Fiorelli R., Azim K., Fischer B., Raineteau O. (2015). Adding a spatial dimension to postnatal ventricular-subventricular zone neurogenesis. *Development*. 142:2109–2120.
- Fontana L., Fiori M.E., Albini S., Cifaldi L., Giovinazzi S., Forloni M., Boldrini R., Donfrancesco A. et al. (2008). Antagomir-17-5p abolishes the growth of therapy-resistant neuroblastoma through p21 and BIM. *PLoS One*. 3 (5):e2236. doi: 10.1371/journal.pone.0002236.
- Fruttiger, M. et al. (1999). Defective oligodendrocyte development and severe hypomyelination in PDGF-A knockout mice. *Development* 126, 457–467.

- Fuentealba L.C., Rompani S.B., Parraguez J.I., Obernier K., Romero R., Cepko C.L., Alvarez-Buylla A. (2015). Embryonic Origin of Postnatal Neural Stem Cells. *Cell*. 161 (7):1644-55. doi: 10.1016/j.cell.2015.05.041.
- Furutachi S., Miya H., Watanabe T., Kawai H., Yamasaki N., Harada Y., Imayoshi I., Nelson M., Nakayama K.I., Hirabayashi Y., Gotoh Y. (2015). Slowly dividing neural progenitors are an embryonic origin of adult neural stem cells. *Nat Neurosci*. 18 (5):657-65. doi: 10.1038/nn.3989. Epub 2015 Mar 30.
- Gallo A., Tandon M., Alevizos I., Illei G.G. (2012). The majority of microRNAs detectable in serum and saliva is concentrated in exosomes. *PLoS ONE* 7:e30679. doi: 10.1371/journal.pone.0030679
- Garcia, A. D. R., Doan, N. B., Imura, T., Bush, T. G., & Sofroniew, M. V. (2004). GFAP-expressing progenitors are the principal source of constitutive neurogenesis in adult mouse forebrain. *Nature Neuroscience*, 7 (11), 1233–1241. <http://doi.org/10.1038/nm1340>
- Gebert L.F.R., MacRae I.J. (2019). Regulation of microRNA function in animals. *Nat Rev Mol Cell Biol*. 20 (1):21-37. doi: 10.1038/s41580-018-0045-7.
- Giachino C., Basak O., Lugert S., Knuckles P., Obernier K., Fiorelli R., Frank S., Raineteau O., Alvarez-Buylla A., Taylor V. (2014). Molecular diversity subdivides the adult forebrain neural stem cell population. *Stem Cells*, 32:70–84.
- Gibbins D.J., Ciaudo C., Erhardt M., Voinnet O. (2009). Multivesicular bodies associate with components of miRNA effector complexes and modulate miRNA activity. *Nat Cell Biol*. 11:1143–9. doi: 10.1038/ncb1929
- Gleeson, J. G., Lin, P. T., Flanagan, L. A., & Walsh, C. A. (1999). Doublecortin Is a Microtubule-Associated Protein and Is Expressed Widely by Migrating Neurons. *Neuron*, 23 (2), 257–271. [http://doi.org/10.1016/s0896-6273\(00\)80778-3](http://doi.org/10.1016/s0896-6273(00)80778-3)
- Gondkar K., Patel K., Patil Okaly G.V., Nair B., Pandey A., Gowda H., Kumar P. (2019). Dickkopf Homolog 3 (DKK3) Acts as a Potential Tumor Suppressor in Gallbladder Cancer. *Front Oncol*. 9:1121. doi: 10.3389/fonc.2019.01121.
- Gonzalez-Perez O., Quiñones-Hinojosa A. (2010). Dose-dependent effect of EGF on migration and differentiation of adult subventricular zone astrocytes. *Glia*. 58 (8):975-83. doi: 10.1002/glia.20979.
- Goodell M.A., Nguyen H., Shroyer N. (2015). Somatic stem cell heterogeneity: diversity in the blood, skin and intestinal stem cell compartments. *Nat Rev Mol Cell Biol*. 2015 May;16(5):299-309. doi: 10.1038/nrm3980.
- Grandel H., Brand M. (2013). Comparative aspects of adult neural stem cell activity in vertebrates. *Dev Genes Evol*. 223(1-2):131-47. doi: 10.1007/s00427-012-0425-5.
- Griffiths-Jones S. (2004). The microRNA registry. *Nucleic Acids Res*. 32, D109-111.
- Guzzolino E., Chiavacci E., Ahuja N., Mariani L., Evangelista M., Ippolito C., Rizzo M., Garrity D., Cremisi F., Pitto L. (2018). Post-transcriptional Modulation of Sphingosine-1-Phosphate Receptor 1 by miR-19a Affects Cardiovascular Development in Zebrafish. *Front Cell Dev Biol*. 6:58. doi: 10.3389/fcell.2018.00058.

- Han Y.C., Vidigal J.A., Mu P., Yao E., Singh I., González A.J., Concepcion C.P., Bonetti C., Ogradowski P., Carver B., Selleri L., Betel D., Leslie C., Ventura A. (2015). An allelic series of miR-17 ~ 92-mutant mice uncovers functional specialization and cooperation among members of a microRNA polycistron. *Nat Genet.* 47 (7):766-75. doi: 10.1038/ng.3321.
- Hayashita Y., Osada H., Tatematsu Y., Yamada H., Yanagisawa K., Tomida S., Yatabe Y., Kawahara K., Sekido Y., Takahashi T. (2005). A polycistronic microRNA cluster, miR-17-92, is overexpressed in human lung cancers and enhances cell proliferation. *Cancer Res.* 65(21):9628-32.
- Iftikhar H., Carney G.E. (2016). Evidence and potential in vivo functions for biofluid miRNAs: from expression profiling to functional testing: potential roles of extracellular miRNAs as indicators of physiological change and as agents of intercellular information exchange. *Bioessays* 38:367–78. doi: 10.1002/bies.201500130
- Jin J. et al. (2016). miR-17-92 Cluster Regulates Adult Hippocampal Neurogenesis, Anxiety, and Depression. *Cell Rep.* 16(6):1653-1663. doi: 10.1016/j.celrep.2016.06.101.
- Kaplan M.S., Hinds J.W. (1977). Neurogenesis in the adult rat: electron microscopic analysis of light radioautographs. *Science.* 197 (4308):1092-4. DOI: 10.1126/science.887941
- Katz S., Cussigh D., Urbán N., Blomfield I., Guillemot F., Bally-Cuif L., Coolen M. (2016). A Nuclear Role for miR-9 and Argonaute Proteins in Balancing Quiescent and Activated Neural Stem Cell States. *Cell Rep.* 17 (5):1383-1398. doi: 10.1016/j.celrep.2016.09.088.
- Khatri P., Obernier K., Simeonova I.K., Hellwig A., Hölzl-Wenig G., Mandl C., Scholl C., Wöfl S., Winkler J., Gaspar J.A., et al. (2014). Proliferation and cilia dynamics in neural stem cells prospectively isolated from the SEZ. *Sci Rep* 2014, 4:3803.
- Kokovay E., Wang Y., Kusek G., Wurster R., Lederman P., Lowry N., Shen Q., Temple S. (2012). VCAM1 is essential to maintain the structure of the SVZ niche and acts as an environmental sensor to regulate SVZ lineage progression. *Cell Stem Cell.* 2012 Aug 3;11(2):220-30. doi: 10.1016/j.stem.2012.06.016.
- Kozomara A., Griffiths-Jones S., (2014). miRBase: annotating high confidence microRNAs using deep sequencing data. *Nucleic Acids Res.* 42, D68-73.
- Lazarini F., Lledo P.M. (2011). Is adult neurogenesis essential for olfaction? *Trends Neurosci.* 34 (1):20-30. doi: 10.1016/j.tins.2010.09.006.
- Lee R.C., Feinbaum R.L., Ambros V. (1993). The *C. elegans* heterochronic gene *lin-4* encodes small RNAs with antisense complementarity to *lin-14*. *Cell.* 75 (5):843-54.
- Leeman D.S., Hebestreit K., Ruetz T., Webb A.E., McKay A., Pollina E.A., Dulken B.W., Zhao X., Yeo R.W., Ho T.T., Mahmoudi S., Devarajan K., Passequé E., Rando T.A., Frydman J., Brunet A. (2018). Lysosome activation clears aggregates and enhances quiescent neural stem cell activation during aging. *Science.* 359 (6381):1277-1283. doi: 10.1126/science.aag3048.
- Lepko T., Pusch M., Müller T., Schulte D., Ehses J., Kiebler M. et al. (2019). Choroid plexus-derived miR-204 regulates the number of quiescent neural stem cells in the adult brain. *EMBO J.* 38 (17):e100481. doi: 10.15252/embj.2018100481.

- Li Y., Vecchiarelli-Federico L.M., Li Y.J., Egan S.E., Spaner D., Hough M.R., Ben-David Y. (2012). The miR-17-92 cluster expands multipotent hematopoietic progenitors whereas imbalanced expression of its individual oncogenic miRNAs promotes leukemia in mice. *Blood*. 119(19):4486-98. doi: 10.1182/blood-2011-09-378687.
- Lim D.A. and Alvarez-Buylla A. (2014). S., Gregory R.I. (2015). Adult neural stem cells stake their ground. *Trends Neurosci*. Oct;37(10):563-71. doi: 10.1016/j.tins.2014.08.006.
- Lin S., Gregory R.I. (2015). MicroRNA biogenesis pathways in cancer. *Nat Rev Cancer*. 15 (6):321-33. doi: 10.1038/nrc3932.
- Liu C., Teng Z.Q., Santistevan N.J., Szulwach K.E., Guo W., Jin P., et al. (2010). Epigenetic regulation of miR-184 by MBD1 governs neural stem cell proliferation and differentiation. *Cell Stem Cell* 6, 433-444.
- Liu X.S., Chopp M., Wang X.L., Zhang L., Hozeska-Solgot A., Tang T., Kassis H., Zhang R.L., Chen C., Xu J., Zhang Z.G. (2013). MicroRNA-17-92 cluster mediates the proliferation and survival of neural progenitor cells after stroke. *J Biol Chem*. 288 (18):12478-88. doi: 10.1074/jbc.M112.449025.
- Livak K.J., Schmittgen T.D. (2001). Analysis of relative gene expression data using real-time quantitative PCR and the 2(-Delta Delta C(T)) Method. *Methods*. 25 (4):402-8.
- Lledo P.M., Valley M. (2016). Adult Olfactory Bulb Neurogenesis. *Cold Spring Harb Perspect Biol*. 8 (8). pii: a018945. doi: 10.1101/cshperspect.a018945.
- Llorens-Bobadilla E., Zhao S., Baser A., Saiz-Castro G., Zwadlo K., & Martin-Villalba A. (2015). Single-cell transcriptomics reveals a population of dormant neural stem cells that become activated upon brain injury. *Cell Stem Cell* 2015, 17:329–340.
- Lois C., García-Verdugo J.M., Alvarez-Buylla A. (1996). Chain migration of neuronal precursors. *Science*. 271 (5251):978-81.
- Lu Y., Thomson J.M., Wong H.Y., Hammond S.M., Hogan B.L. (2007). Transgenic over-expression of the microRNA miR-17-92 cluster promotes proliferation and inhibits differentiation of lung epithelial progenitor cells. *Dev Biol*. 310(2):442-53.
- Malvaut S. and Saghatelian A. (2016). The Role of Adult-Born Neurons in the Constantly Changing Olfactory Bulb Network. *Neural Plast*. 2016: 1614329. doi: 10.1155/2016/1614329
- Mao S., Li H., Sun Q., Zen K., Zhang C.Y., Li L. (2014). miR-17 regulates the proliferation and differentiation of the neural precursor cells during mouse corticogenesis. *FEBS J*. 281 (4):1144-58. doi: 10.1111/febs.12680.
- Matsubara H., Takeuchi T., Nishikawa E., Yanagisawa K., Hayashita Y., Ebi H. et al. (2007). Apoptosis induction by antisense oligonucleotides against miR-17-5p and miR-20a in lung cancers overexpressing miR-17-92. *Oncogene*. 26(41):6099-105.
- Mavrakis K.J., Wolfe A.L., Oricchio E., Palomero T., de Keersmaecker K., McJunkin K., Zuber J., James T., Khan A.A., Leslie C.S., et al. (2010). Genome-wide RNA-mediated interference screen identifies miR-19 targets in Notch-induced T-cell acute lymphoblastic leukaemia. *Nat. Cell Biol*. 12, 372–379.

- Meenhuis A., van Veelen P.A., de Looper H., van Boxtel N., van den Berge I.J., Sun S.M., Taskesen E., Stern P., de Ru A.H., van Adrichem A.J., Demmers J., Jongen-Lavrencic M., Löwenberg B., Touw I.P., Sharp P.A., Erkeland S.J. (2011). MiR-17/20/93/106 promote hematopoietic cell expansion by targeting sequestosome 1-regulated pathways in mice. *Blood*. 118(4):916-25. doi: 10.1182/blood-2011-02-336487.
- Menn, B., Garcia-Verdugo, J. M., Yaschine, C., Gonzalez Perez, O., Rowitch, D., & Alvarez-Buylla, A. (2006). Origin of oligodendrocytes in the subventricular zone of the adult brain. *Journal of Neuroscience*, 26(30), 7907–7918. <http://doi.org/10.1523/JNEUROSCI.1299-06.2006>
- Merkle F.T., Fuentealba L.C., Sanders T.A., Magno L., Kessar N., Alvarez-Buylla A. (2014). Adult neural stem cells in distinct microdomains generate previously unknown interneuron types. *Nat Neurosci*. 17 (2):207-14. doi: 10.1038/nn.3610.
- Merkle F.T., Mirzadeh Z., Alvarez-Buylla A. (2007). Mosaic organization of neural stem cells in the adult brain. *Science*. 317 (5836):381-4.
- Miao L., Yao H., Li C., Pu M., Yao X., Yang H., et al. (2016). A dual inhibition: microRNA-552 suppresses both transcription and translation of cytochrome P450 2E1. *Biochim Biophys Acta* 1859:650–62. doi: 10.1016/j.bbagr.2016.02.016
- Mich J.K., Signer R.A.J., Nakada D., Pineda A., Burgess R.J., Vue T.Y., Johnson J.E., Morrison S.J. (2014). Prospective identification of functionally distinct stem cells and neurosphere-initiating cells in adult mouse forebrain. *eLife*, 2014:1–27.
- Mirzadeh Z., Merkle F.T., Soriano-Navarro M., Garcia-Verdugo J.M., Alvarez-Buylla A. (2008). Neural stem cells confer unique pinwheel architecture to the ventricular surface in neurogenic regions of the adult brain. *Cell Stem Cell*. Sep 11;3(3):265-78. doi: 10.1016/j.stem.2008.07.004.
- Mizrak D., Levitin H.M., Delgado A.C., Crotet V., Yuan J., Chaker Z., Silva-Vargas V., Sims P.A., Doetsch F. (2019). Single-Cell Analysis of Regional Differences in Adult V-SVZ Neural Stem Cell Lineages. *Cell Rep*. 26 (2):394-406.e5. doi: 10.1016/j.celrep.2018.12.044.
- Mu P., Han Y.C., Betel D., Yao E., Squatrito M., Ogradowski P., de Stanchina E., D'Andrea A., Sander C., and Ventura, A. (2009). Genetic dissection of the miR-17~92 cluster of microRNAs in Myc-induced B-cell lymphomas. *Genes Dev*. 23, 2806–2811.
- Mullen, R. J., Buck, C. R., & Smith, A. M. (1992). NeuN, a neuronal specific nuclear protein in vertebrates. *Development*, 116(1), 201–211.
- Nacher, J., Crespo, C., & McEwen, B. S. (2001). Doublecortin expression in the adult rat telencephalon. *European Journal of Neuroscience*, 14 (4), 629–644.
- Nait-Oumesmar B., Decker L., Lachapelle F., Avellana-Adalid V., Bachelin C., & Baron-Van Evercooren A. (1999). Progenitor cells of the adult mouse subventricular zone proliferate, migrate and differentiate into oligodendrocytes after demyelination. *The European Journal of Neuroscience*, 11(12), 4357–4366.
- Naka-Kaneda H., Nakamura S., Igarashi M., Aoi H., Kanki H., Tsuyama J., Tsutsumi S., Aburatani H., Shimazaki T., Okano H. (2014). The miR-17/106-p38 axis is a key regulator

- of the neurogenic-to-gliogenic transition in developing neural stem/progenitor cells. *Proc Natl Acad Sci U S A.* 111(4):1604-9. doi: 10.1073/pnas.1315567111.
- Nishi K., Takahashi T., Suzawa M., Miyakawa T., Nagasawa T., Ming Y., et al. (2015). Control of the localization and function of a miRNA silencing component TNRC6A by Argonaute protein. *Nucleic Acids Res* 43:9856–73. doi: 10.1093/nar/gkv1026
- Nishiyama A., Komitova M., Suzuki R. and Zhu, X. (2009). Polydendrocytes (NG2 cells): multifunctional cells with lineage plasticity. *Nat. Rev. Neurosci.* 10, 9–22.
- Noble M., Murray K., Stroobant P., Waterfield M.D. and Riddle P. (1988). Platelet-derived growth factor promotes division and motility and inhibits premature differentiation of the oligodendrocyte/type-2 astrocyte progenitor cell. *Nature* 333, 560–562.
- O'Brien J., Hayder H., Zayed Y., Peng C. (2018). Overview of MicroRNA Biogenesis, Mechanisms of Actions, and Circulation. *Front Endocrinol (Lausanne).* 9:402. doi: 10.3389/fendo.2018.00402.
- O'Donnell K.A., Wentzel E.A., Zeller K.I., Dang C.V., Mendell J.T. (2005). c-Myc-regulated microRNAs modulate E2F1 expression. *Nature.* 435:839Y843.
- Obernier K., Alvarez-Buylla A. (2019). Neural stem cells: origin, heterogeneity and regulation in the adult mammalian brain. *Development.* 146 (4). pii: dev156059. doi: 10.1242/dev.156059.
- Obernier K., Cebrian-Silla A., Thomson M., Parraguez J.I., Anderson R., Guinto C., Rodas Rodriguez J., Garcia-Verdugo J.M., Alvarez-Buylla A (2018). Adult Neurogenesis Is Sustained by Symmetric Self-Renewal and Differentiation. *Cell Stem Cell.* 22 (2):221-234.e8. doi: 10.1016/j.stem.2018.01.003.
- Obernosterer G1, Leuschner PJ, Alenius M, Martinez J. (2006). Post-transcriptional regulation of microRNA expression. *RNA.* 12 (7):1161-7.
- Olive V., Bennett M.J., Walker J.C., Ma C., Jiang I., Cordon-Cardo C., Li Q.J., Lowe S.W., Hannon G.J., and He L. (2009). miR-19 is a key oncogenic component of mir-17-92. *Genes Dev.* 23, 2839–2849.
- Olive V., Li Q., He L. (2013). mir-17-92: a polycistronic oncomir with pleiotropic functions. *Immunol Rev.* 253 (1):158-66. doi: 10.1111/imr.12054.
- Ortega F., Gascón S., Masserdotti G., Deshpande A., Simon C., Fischer J., Dimou L., Lie D.C., Schroeder T., Berninger B. (2013). Oligodendroglial and neurogenic adult subependymal zone neural stem cells constitute distinct lineages and exhibit differential responsiveness to Wnt signalling. *Nat Cell Biol.* Jun;15(6):602-13. doi: 10.1038/ncb2736.
- Ota A., Tagawa H., Karnan S., Tsuzuki S., Karpas A., Kira S., Yoshida Y., Seto M. (2004). Identification and characterization of a novel gene, C13orf25, as a target for 13q31-q32 amplification in malignant lymphoma. *Cancer Res.* 64(9):3087-95.
- Pan W.L., Chopp M., Fan B., Zhang R., Wang X., Hu J., Zhang X.M., Zhang Z.G., Liu X.S. (2019). Ablation of the microRNA-17-92 cluster in neural stem cells diminishes adult hippocampal neurogenesis and cognitive function. *FASEB J.* 33 (4):5257-5267. doi: 10.1096/fj.201801019R.

- Pastrana E., Cheng L.C., Doetsch F. (2009). Simultaneous prospective purification of adult subventricular zone neural stem cells and their progeny. *Proc Natl Acad Sci U S A.* 106 (15):6387-92. doi: 10.1073/pnas.0810407106.
- Pathania M., Torres-Reveron J., Yan L., Kimura T., Lin T.V., Gordon V. et al. (2012). miR-132 enhances dendritic morphogenesis, spine density, synaptic integration, and survival of newborn olfactory bulb neurons. *PLoS ONE* 7, e38174.
- Paton J.A., Nottebohm F.N. (1984). Neurons generated in the adult brain are recruited into functional circuits. *Science.* 225 (4666):1046-8. doi: 10.1126/science.6474166.
- Paul A., Chaker Z., Doetsch F. (2017). Hypothalamic regulation of regionally distinct adult neural stem cells and neurogenesis. *Science.* 356 (6345):1383-1386. doi: 10.1126/science.aal3839.
- Petrocca F., Visone R., Onelli M.R., Shah M.H., Nicoloso M.S., de Martino I., Iliopoulos D., Pilozi E. et al. (2008). E2F1-regulated microRNAs impair TGFbeta-dependent cell-cycle arrest and apoptosis in gastric cancer. *Cancer Cell.* 13 (3):272-86. doi: 10.1016/j.ccr.2008.02.013.
- Picard-Riera N., Decker L., Delarasse C., Goude K., Nait-Oumesmar B., Liblau R., Pham-Dinh D., Baron-Van Evercooren A. (2002). Experimental autoimmune encephalomyelitis mobilizes neural progenitors from the subventricular zone to undergo oligodendrogenesis in adult mice. *Proc Natl Acad Sci U S A.* 99 (20):13211-6.
- Polioudakis D., Bhinge A.A., Killion P.J., Lee B.K., Abell N.S., Iyer V.R. (2013). A Myc-microRNA network promotes exit from quiescence by suppressing the interferon response and cell-cycle arrest genes. *Nucleic Acids Res.* 41 (4):2239-54. doi: 10.1093/nar/gks1452.
- Ponti G., Obernier K., Guinto C., Jose L., Bonfanti L., Alvarez-Buylla A. (2013). Cell cycle and lineage progression of neural progenitors in the ventricular-subventricular zones of adult mice. *Proc Natl Acad Sci U S A.* 110 (11):E1045-54. doi: 10.1073/pnas.1219563110.
- Pringle N.P., Mudhar H.S., Collarini E.J. and Richardson W.D. (1992). PDGF receptors in the rat CNS: during late neurogenesis, PDGF alpha-receptor expression appears to be restricted to glial cells of the oligodendrocyte line- age. *Development* 115, 535–551.
- Reynolds B.A., Weiss S. (1992). Generation of neurons and astrocytes from isolated cells of the adult mammalian central nervous system. *Science.* 255 (5052):1707-10.
- Samanta J., Grund E.M., Silva H.M., Lafaille J.J., Fishell G., Salzer J.L. (2015). Inhibition of Gli1 mobilizes endogenous neural stem cells for remyelination. *Nature.* 526(7573):448-52. doi: 10.1038/nature14957.
- Sanai N., Nguyen T., Ihrie R. A., Tsai H.-H., Wong M., Gupta N., et al. (2011). Corridors of migrating neurons in the human brain and their decline during infancy. *Nature*, 478 (7369), 382–386. <http://doi.org/10.1038/nature10487>
- Sanai N., Tramontin A. D., Quiñones Hinojosa A., Barbaro N. M., Gupta N., Kunwar S., et al. (2004). Unique astrocyte ribbon in adult human brain contains neural stem cells but lacks chain migration. *Nature*, 427 (6976), 740–744. <http://doi.org/10.1038/nature02301>

- Sato T., Yamamoto T., Sehara-Fujisawa A. (2014). miR-195/497 induce postnatal quiescence of skeletal muscle stem cells. *Nat Commun.* 5:4597. doi: 10.1038/ncomms5597.
- Schulte J.H., Horn S., Otto T., Samans B., Heukamp L.C., Eilers U.C., Krause M., Astrahantseff K., Klein-Hitpass L. et al. (2008). MYCN regulates oncogenic MicroRNAs in neuroblastoma. *Int J Cancer.* 122(3):699-704.
- Seri, B., García-Verdugo, J. M., McEwen, B. S., & Alvarez-Buylla, A. (2001). Astrocytes give rise to new neurons in the adult mammalian hippocampus. *The Journal of Neuroscience*, 21 (18), 7153–7160.
- Shen Q., Wang Y., Kokovay E., Lin G., Chuang S.M., Goderie S.K., Roysam B., Temple S. (2008). Adult SVZ stem cells lie in a vascular niche: a quantitative analysis of niche cell-cell interactions. *Cell Stem Cell.* 3 (3):289-300. doi: 10.1016/j.stem.2008.07.026.
- Sohn J., Orosco L., Guo F., Chung S.H., Bannerman P., Mills Ko E., Zarbalis K., Deng W., Pleasure D. (2015). The subventricular zone continues to generate corpus callosum and rostral migratory stream astroglia in normal adult mice. *J Neurosci.* 35 (9):3756-63. doi: 10.1523/JNEUROSCI.3454-14.2015.
- Szulwach K.E., Li X., Smrt R.D., Li Y., Luo Y., Lin L. et al. (2010). Cross talk between microRNA and epigenetic regulation in adult neurogenesis. *J. Cell Biol.* 189, 127-141.
- Tavazoie M., Van der Veken L., Silva-Vargas V., Louissaint M., Colonna L., Zaidi B., Garcia-Verdugo J.M., Doetsch F. (2008). A specialized vascular niche for adult neural stem cells. *Cell Stem Cell.* 3 (3):279-88. doi: 10.1016/j.stem.2008.07.025.
- Thomson J.M., Newman M., Parker J.S., Morin-Kensicki E.M., Wright T., Hammond S.M. (2006). Extensive post-transcriptional regulation of microRNAs and its implications for cancer. *Genes Dev.* 20 (16):2202-7.
- Tong C.K., Fuentealba L.C., Shah J.K., Lindquist R.A., Ihrle R.A., Guinto C.D., Rodas-Rodriguez J.L., Alvarez-Buylla A. (2015). A Dorsal SHH-Dependent Domain in the V-SVZ Produces Large Numbers of Oligodendroglial Lineage Cells in the Postnatal Brain. *Stem Cell Reports.* 5 (4):461-70. doi: 10.1016/j.stemcr.2015.08.013.
- Trompeter H.I., Abbad H., Iwaniuk K.M., Hafner M., Renwick N., Tuschl T., Schira J., Müller H.W., Wernet P. (2011). MicroRNAs MiR-17, MiR-20a, and MiR-106b act in concert to modulate E2F activity on cell cycle arrest during neuronal lineage differentiation of USSC. *PLoS One.* 6 (1):e16138. doi: 10.1371/journal.pone.0016138.
- Tüfekci K.U., Oner M.G., Meuwissen R.L., Genç S. (2014). The role of microRNAs in human diseases. *Methods Mol Biol.* 1107:33-50. doi: 10.1007/978-1-62703-748-8_3.
- Tung Y.T., Lu Y.L., Peng K.C., Yen Y.P., Chang M., Li J., Jung H., Thams S., Huang Y.P., Hung J.H., Chen J.A. (2015). Mir-17~92 Governs Motor Neuron Subtype Survival by Mediating Nuclear PTEN. *Cell Rep.* 11(8):1305-18.
- Urbán N., van den Berg D.L.C., Forget A., Andersen J., Demmers J.A.A., Hunt C., Ayrault O., Guillemot F. (2011). Return to quiescence of mouse neural stem cells by degradation of a proactivation protein. *Science.* Jul 15;353(6296):292-5. doi: 10.1126/science.aaf4802.

- Turchinovich A., Weiz L., Langheinz A., Burwinkel B. (2011). Characterization of extracellular circulating microRNA. *Nucleic Acids Res.* 39:7223–33. doi: 10.1093/nar/gkr254
- Uziel T., Karginov F.V., Xie S., Parker J.S., Wang Y.D., Gajjar A., He L., Ellison D., Gilbertson R.J., Hannon G., Roussel M.F. (2009). The miR-17~92 cluster collaborates with the Sonic Hedgehog pathway in medulloblastoma. *Proc Natl Acad Sci U S A.* 106 (8):2812-7. doi: 10.1073/pnas.0809579106.
- Van Den Berge S. A., Middeldorp J., Zhang C. E., Curtis M. A., Leonard B. W., Mastroeni D., et al. (2010). Longterm quiescent cells in the aged human subventricular neurogenic system specifically express GFAP- δ . *Aging Cell*, 9 (3), 313–326.
- Ventura A., Young A.G., Winslow M.M., Lintault L., Meissner A., Erkeland S.J., Newman J., Bronson R.T., Crowley D., Stone J.R., Jaenisch R., Sharp P.A., Jacks T. (2008). Targeted deletion reveals essential and overlapping functions of the miR-17 through 92 family of miRNA clusters. *Cell.* 132 (5):875-86. doi: 10.1016/j.cell.2008.02.019.
- Venturini L., Battmer K., Castoldi M., Schultheis B., Hochhaus A., Muckenthaler M.U., Ganser A., Eder M., Scherr M. (2007). Expression of the miR-17-92 polycistron in chronic myeloid leukemia (CML) CD34+ cells. *Blood.* 109 (10):4399-405.
- Volinia S., Calin G.A., Liu C.G., Ambs S., Cimmino A., Petrocca F., Visone R., Iorio M., Roldo C. et al. (2006). A microRNA expression signature of human solid tumors defines cancer gene targets. *Proc Natl Acad Sci U S A.* 2006 Feb 14;103(7):2257-61.
- Wichterle H., Garcia-Verdugo J.M., Alvarez-Buylla A. (1997). Direct evidence for homotypic, glia-independent neuronal migration. *Neuron.* 18 (5):779-91.
- Wightman B., Ha I., Ruvkun G. (1993). Posttranscriptional regulation of the heterochronic gene *lin-14* by *lin-4* mediates temporal pattern formation in *C. elegans*. *Cell.* 75 (5):855-62.
- Wulczyn F.G., Smirnova L., Rybak A., Brandt C., Kwidzinski E., Ninnemann O., Strehle M., Seiler A., Schumacher S., Nitsch R. (2007). Post-transcriptional regulation of the *let-7* microRNA during neural cell specification. *FASEB J.* 21 (2):415-26.
- Xiao M., Li J., Li W., Wang Y., Wu F., Xi Y., et al. (2017). MicroRNAs activate gene transcription epigenetically as an enhancer trigger. *RNA Biol.* 14:1326–34. doi: 10.1080/15476286.2015.1112487
- Xu S., Ou X., Huo J., Lim K., Huang Y., Chee S., Lam K.P. (2015). Mir-17-92 regulates bone marrow homing of plasma cells and production of immunoglobulin G2c. *Nat Commun.* 6:6764. doi: 10.1038/ncomms7764.
- Yang X., Du W.W., Li H., Liu F., Khorshidi A., Rutnam Z.J., Yang B.B. (2013). Both mature miR-17-5p and passenger strand miR-17-3p target TIMP3 and induce prostate tumor growth and invasion. *Nucleic Acids Res.* 41 (21):9688-704. doi: 10.1093/nar/gkt680.
- Young K.M., Fogarty M., Kessar N., Richardson W.D. (2007). Subventricular zone stem cells are heterogeneous with respect to their embryonic origins and neurogenic fates in the adult olfactory bulb. *J Neurosci.* 27 (31):8286-96.

- Yuzwa S.A., Borrett M.J., Innes B.T., Voronova A., Ketela T., Kaplan D.R., Bader G.D.3, Miller F.D. (2017). Developmental Emergence of Adult Neural Stem Cells as Revealed by Single-Cell Transcriptional Profiling. *Cell Rep.* 21 (13):3970-3986. doi: 10.1016/j.celrep.2017.12.017.
- Zhang L., Zhang S., Yao J., Lowery F., Zhang Q., Huang. et al. (2015). Microenvironment-induced PTEN loss by exosomal microRNA primes brain metastasis outgrowth. *Nature.* 527 (7576):100-104. doi: 10.1038/nature15376.
- Zhang X., Zuo X., Yang B., Li Z., Xue Y., Zhou Y., et al. (2014). MicroRNA directly enhances mitochondrial translation during muscle differentiation. *Cell* 158:607–19. doi: 10.1016/j.cell.2014.05.047
- Zhao C., Sun G., Li S., Lang M.F., Yang S. Li, W. et al. (2010). MicroRNA let-7b regulates neural stem cell proliferation and differentiation by targeting nuclear receptor TLX signaling. *Proc. Natl. Acad. Sci. U. S. A.* 107, 1876-1881.
- Zhao C., Sun G., Li S., Shi Y. (2009). A feedback regulatory loop involving microRNA-9 and nuclear receptor TLX in neural stem cell fate determination. *Nat. Struct. Mol. Biol.* 16, 365-371.